1-1-2016

Insights into Mbd2 Function Revealed by a Novel Genetic Tagging Approach

Kathleen Wood
University of Pennsylvania, kathwood@mail.med.upenn.edu

Insights into Mbd2 Function Revealed by a Novel Genetic Tagging Approach

Abstract
Methylation of cytosine is an epigenetic mark essential for many cellular and developmental processes. How methylation is interpreted into transcriptional regulation is not fully understood, but previous studies have found that this process involves the methyl-CpG binding domain (MBD) family of proteins. Three MBD proteins, MeCP2, MBD1 and MBD2, specifically bind methylated cytosines and recruit different co-repressor complexes to regulate transcription and chromatin states. Genetic studies also linked MeCP2 and MBD1 to neurodevelopmental disorders in humans and mice. However, a role for MBD2 in the brain has not been described. In this work, we characterized the phenotypes of mice lacking MBD2. We found that, unlike MeCP2 and MBD1, Mbd2 null mice behave similarly to wildtype littermates, with the exception of mildly altered nesting and locomotor activity and reduced body weight. To investigate the underlying cause of different functional requirements for the MBDs, we generated knockin mice in which endogenous MBD2 and MBD1 are biotin-tagged. We systematically compared the spatiotemporal expression patterns of the MBDs and found that MeCP2, MBD1 and MBD3 are primarily expressed in the brain. In contrast, MBD2 is widely expressed throughout the body at young and adult ages. In addition, the expression of MBD2 is upregulated in adult spleen and small intestine compared to younger ages, while MBD1 and MBD3 are only enriched at early ages in the brain. We also determined that MBD2 interacts with the NuRD complex ubiquitously across tissues. We conclude that MBD2 is likely dispensable for brain function and instead may mediate NuRDrelated functions primarily in peripheral tissues. Our study provides novel genetic tools and reveals new directions to investigate MBD2 functions in vivo.

Degree Type
Dissertation

Degree Name
Doctor of Philosophy (PhD)

INSIGHTS INTO MBD2 FUNCTION REVEALED BY A NOVEL

GENETIC TAGGING APPROACH

Kathleen H. Wood

A DISSERTATION

in

Cell and Molecular Biology

Presented to the Faculties of the University of Pennsylvania

in

Partial Fulfillment of the Requirements for the

Degree of Doctor of Philosophy

2016

Supervisor of Dissertation

_____

Zhaolan Zhou, Ph.D.

Associate Professor of Genetics

Graduate Group Chairperson

_____

Daniel S. Kessler, Ph.D., Associate Professor of Cell and Developmental Biology

Dissertation Committee

Thomas A. Jongens, Ph.D., Associate Professor of Genetics

Marisa S. Bartolomei, Ph.D., Professor of Cell and Developmental Biology

Klaus H. Kaestner, Ph.D., Thomas and Evelyn Suor Butterworth Professor in Genetics

Christopher J. Lengner, Ph.D., Assistant Professor of Biomedical Sciences

INSIGHTS INTO MBD2 FUNCTION REVEALED BY A NOVEL GENETIC TAGGING APPROACH

ACKNOWLEDGEMENTS

I would like to thank all past and present members of the Zhou lab, and especially my advisor Joe, for their support throughout this project. Joe works very hard to ensure we as the members of his lab perform at our best and are well prepared for the next stages of our careers, and I sincerely appreciate all of his guidance. Everyone in this lab has offered me invaluable help and advice, both academic and personal, which allowed me to complete this project successfully. I would especially like to thank Brian Johnson for initiating this project and for our many helpful and encouraging talks in our bay. I also thank Sarah Welsh for her very significant contribution to the MBD1^{Tavi} project, without which this part of the project would not have been completed. Thank you to Dr. Jerry Zhao for his work to analyze high-throughput sequencing data and for helpful discussions. I would like to thank former lab members Drs. Darren Goffin and Judy Wang for their considerable help when I was new in the lab, and for teaching me how to perform behavioral and statistical analyses. I also thank Jun Lee for his assistance with maintaining my mouse colony, which allowed me to focus on completing my experiments. Finally, I especially thank Yolanda Cui for her very hard work to keep our lab running smoothly and maintain our mouse colonies.

I would like to acknowledge the help I received from many people outside the Zhou lab. First, I would like to thank the members of my thesis committee, Drs. Tom Jongens, Marisa Bartolomei, Chris Lengner, and Klaus Kaestner, for their invaluable help with this project. I also thank my earlier mentors Dr. Karen Hales and Dr. Tom Schwarz for their guidance before I started this program. Thank you to Dr. Meera Sundaram for her mentorship through the Genetics T32 training grant. Thank you to Dr. Marisa Bartolomei and Dr. Lara Abramowitz for providing *Mbd2* and *Mbd1* null mice and helping to initiate this project. The labs of Drs. Edward S. Brodkin, Tracy Bale, and Steve Siegel provided expertise and equipment for the behavioral assays. Elizabeth Krizman in Dr. Michael Robinson's lab performed HPLC experiments and both her and Dr. Robinson provided helpful discussion. I also thank members of Dr. Brian Gregory's lab, specifically Dr. Ian Silverman, Nate Berkowitz, and Sager Gosai, for their help with RNA

extraction, high-throughput sequencing library construction, data analysis, and for being very patient TAs for the Python Bootcamp course. Thank you to members of Dr. Klaus Kaestner's lab, particularly Dr. Karyn Sheaffer and Rinho Kim, for assistance with experimental techniques using the gastrointestinal tract. Finally, I thank all members of Dr. Doug Epstein's lab for help with staining and imaging techniques and for being great neighbors. I would also like to acknowledge the Neurobehavior Testing Core and Dr. Tim O'Brien for assistance with behavioral assays, the Next-Generation Sequencing Core, the Pathology Core Laboratory at CHOP, the Cell Center stockroom, the members of the Genetics Department, all staff members of the University Laboratory Animal Resources, and the administrative staff of the CAMB program for making this project possible.

I want to thank my friends and family for all of their support over these years. My fellow graduate students have encouraged me so much by reminding me that we all have similar struggles through this process. I also could not have completed this project without the support of my many friends both near and far outside of this program, who give me much-needed breaks from science and also remind me why I want to do it. I give a huge thank you to Ian Silverman, who has supported me in every aspect throughout this journey. I can't imagine how I would have gotten here without his help literally starting from day one. Finally, I am incredibly grateful to my family for their unwavering confidence in me. Thank you for all of your encouragement and guidance over the years.

ABSTRACT

INSIGHTS INTO MBD2 FUNCTION REVEALED BY A NOVEL

GENETIC TAGGING APPROACH

Kathleen H. Wood

Zhaolan Zhou, Ph.D.

Methylation of cytosine is an epigenetic mark essential for many cellular and developmental processes. How methylation is interpreted into transcriptional regulation is not fully understood, but previous studies have found that this process involves the methyl-CpG binding domain (MBD) family of proteins. Three MBD proteins, MeCP2, MBD1 and MBD2, specifically bind methylated cytosines and recruit different co-repressor complexes to regulate transcription and chromatin states. Genetic studies also linked MeCP2 and MBD1 to neurodevelopmental disorders in humans and mice. However, a role for MBD2 in the brain has not been described. In this work, we characterized the phenotypes of mice lacking MBD2. We found that, unlike MeCP2 and MBD1, *Mbd2* null mice behave similarly to wildtype littermates, with the exception of mildly altered nesting and locomotor activity and reduced body weight. To investigate the underlying cause of different functional requirements for the MBDs, we generated knockin mice in which endogenous MBD2 and MBD1 are biotin-tagged. We systematically compared the spatiotemporal expression patterns of the MBDs and found that MeCP2, MBD1 and MBD3 are primarily expressed in the brain. In contrast, MBD2 is widely expressed throughout the body at young and adult ages. In addition, the expression of MBD2 is upregulated in adult spleen and small intestine compared to younger ages, while MBD1 and MBD3 are only enriched at early ages in the brain. We also determined that MBD2 interacts with the NuRD complex ubiquitously across tissues. We conclude that MBD2 is likely dispensable for brain function and instead may mediate NuRD-related functions primarily in peripheral tissues. Our study provides novel genetic tools and reveals new directions to investigate MBD2 functions *in vivo.*

TABLE OF CONTENTS

ACKNOWLEDGEMENTS iii

ABSTRACT v

LIST OF TABLES viii

LIST OF FIGURES ix

CHAPTER 1: Introduction 1

- **DNA METHYLATION AND ITS READERS** 1
- **MOLECULAR FUNCTIONS OF MBD2** 6
- **BIOLOGICAL FUNCTIONS OF MBD2** 13
- **THE CHARACTERIZATION OF MBD2 FUNCTIONS *IN VIVO*** 21
- **CHAPTER 1 FIGURES** 23

CHAPTER 2: Phenotypic characterization of *Mbd2* Null Mice 30

- **ABSTRACT** 30
- **INTRODUCTION** 31
- **METHODS** 32
- **RESULTS** 38
- **DISCUSSION** 45
- **CHAPTER 2 FIGURES** 52

CHAPTER 3: Genetic tagging of MBD2 reveals different spatiotemporal expression and supports distinct functions from related MBD proteins 59

- **ABSTRACT** 59

INTRODUCTION **60**

METHODS **61**

RESULTS **67**

DISCUSSION **80**

CHAPTER 3 FIGURES **86**

CHAPTER 4: Discussion and Future Directions **101**

BIBLIOGRAPHY **114**

LIST OF TABLES

CHAPTER 2: Phenotypic characterization of *Mbd2* Null Mice 30

Table 2.1. *Mbd2* and *Mbd1* null mice genotyping primer sequences. 33

Table 2.2. Primers used for RT-qPCR. 37

Table 2.3. Total and uniquely mapped reads from wildtype and *Mbd2*$^{-/-}$ poly-A selected RNA-seq in the striatum. 45

Table 2.4. List of differentially expressed genes in the striatum of *Mbd2*$^{-/-}$ mice compared to wildtype littermates. 58

CHAPTER 3: Genetic tagging of MBD2 reveals different spatiotemporal expression and supports distinct functions from related MBD proteins 59

Table 3.1. Primers used to generate targeting constructs for *Tavi*-tagged alleles of *Mbd2* and *Mbd1*. 62

Table 3.2. Primers used to genotype *Mbd2*^{Tavi} and *Mbd1*^{Tavi} mice. 63

Table 3.3. Primers used for ChIP-qPCR. 66

LIST OF FIGURES

CHAPTER 1: Introduction 1

Figure 1.1. The cytosine modification cycle..... 23

Figure 1.2. Models of DNA methylation affecting transcription factor recruitment. 24

Figure 1.3. The methyl-CpG binding domain (MBD) family of proteins. 25

Figure 1.4. The isoforms of MBD2 contain different functional domains. 26

Figure 1.5. Simplified model of transcriptional regulation by MBD2 and NuRD. 27

Figure 1.6. DNA binding dynamics of MBD2 isoforms and NuRD. 28

Figure 1.7. DNA binding dynamics of MBD2 depend on post-translational modifications.... 29

CHAPTER 2: Phenotypic characterization of *Mbd2* Null Mice 30

Figure 2.1. Behavioral characterization of *Mbd2*$^{-/-}$ mice compared to wildtype and heterozygous littermates. 52

Figure 2.2. *Mbd2*$^{-/-}$ mice show decreased body and brain weight associated with reduced food intake..... 54

Figure 2.3. Hypothalamic neuropeptide expression in *Mbd2*$^{-/-}$ mice. 55

Figure 2.4. *Mbd2*$^{-/-}$ mice have equivalent biogenic amine content to wildtype littermates.. 56

Figure 2.5. RNA-seq from the striatum of *Mbd2*$^{-/-}$ mice confirms loss of *Mbd2* exon 2 and expression of full-length transcript. 57

Figure 2.6. Differentially expressed genes in the striatum of *Mbd2*$^{-/-}$ mice compared to wildtype littermates. 57

CHAPTER 3: Genetic tagging of MBD2 reveals different spatiotemporal expression and supports distinct functions from related MBD proteins 59

Figure 3.1. Schematic of biotin-affinity tagging approach. 86

Figure 3.2. Development of *Mbd2*^{Tavi} knockin mice. 87

Figure 3.3. Development of *Mbd1*^{Tavi} knockin mice. 88

Figure 3.4. Streptavidin-mediated pulldown of biotinylated MBD2^{Tavi} compared to detection of MBD2 with an antibody. 89

Figure 3.5. Different isoforms of biotinylated MBD2^{Tavi} can be detected with streptavidin in multiple tissues. 91

Figure 3.6. Distinct *in vivo* binding partners of MBD2 and MeCP2 in the brain and lung and ubiquitous MBD2-NuRD interactions across tissues. 93

Figure 3.7. MBD2 is depleted at genomic loci with activating histone marks. 94

Figure 3.8. Spatiotemporal expression of MBD2 at P7 and P42. 95

Figure 3.9. Spatiotemporal expression of MBD1 at P7 and P42. 96

Figure 3.10. MeCP2 is consistently highly expressed in the brain while MBD3 is downregulated in the adult brain. 96

Figure 3.11. Summary of MBD protein spatiotemporal expression patterns. 97

Figure 3.12. Quantification of MBD2a^{Tavi} and MBD1a^{Tavi} expression levels. 98

Figure 3.13. MBD2 expression throughout the adult brain is visualized with β-gal staining. 99

Figure 3.14. MBD2 is expressed specifically in epithelial crypt cells of the gastrointestinal tract. 100

CHAPTER 1: Introduction

Adapted from: Wood KH and Zhou Z. Emerging Molecular and Biological Functions of MBD2, a Reader of DNA Methylation. *Frontiers in Genetics.* Submitted.

DNA METHYLATION AND ITS READERS

Establishment of DNA methylation and oxidized forms

DNA methylation at the 5' position of cytosine (mC) is a chemical modification that is essential for mammalian viability and development (Smith and Meissner, 2013; Suzuki and Bird, 2008). DNA methylation at CpG dinucleotides (mCG) has historically been associated with gene repression; however, recent advances have revealed a complex role for DNA methylation in regards to its dynamic turnover, cell type specific distribution patterns and effect on transcriptional regulation (Suzuki and Bird, 2008). DNA is methylated by the de novo methyltransferases DNMT3A and DNMT3B (Okano et al., 1999), in association with DNMT3L (Bourc'his et al., 2001), and the mark is maintained through cell division by the maintenance methyltransferase DNMT1 (Yoder and Bestor, 1998). Passive demethylation occurs in the absence of DNMT activity as cells divide without maintenance methylation (Chen et al., 2003). Active demethylation also occurs through the conversion of mC to hydroxymethylcytosine (hmC) by the ten-eleven translocation (TET) family of proteins (Tahiliani et al., 2009). hmC can be further oxidized by the TET proteins to 5-formylcytosine (5fC) and 5-carboxylcytosine (5caC) (Ito et al., 2011), which is then modified by thymine-DNA glycosylase (TDG) and can be replaced with an unmodified cytosine through base excision repair (BER) mechanisms (He et al., 2011). Alternatively, hmC can lead to passive demethylation even in cells expressing the maintenance methyltransferase DNMT1, as it is a poor substrate for this enzyme (Hashimoto et al., 2012a).These processes together complete the cycle of cytosine modification (Figure 1.1).

Methylation and its oxidized forms are also found outside of the CpG context (mCH) in many cell types (Lister et al., 2009; Schultz et al., 2015). While mCG is the most abundant

modification, both mCH and hmC are also detected across tissues and are highly enriched in embryonic stem cells (ESCs) and the brain (Lister et al., 2009, 2013; Schultz et al., 2015). The distribution of these modifications is developmentally dynamic and cell-type specific, but the mechanisms that direct the precise establishment of these patterns have yet to be fully determined (Pastor et al., 2013; Schübeler, 2015). It is critical to gain further understanding of the mechanisms of DNA methylation because these findings will in turn aid in our elucidation of other biological processes, including the differentiation of pluripotent cells, neuronal development and function, and tumorigenesis, amongst many others.

DNA methylation and transcriptional regulation

It is well established that methylation affects transcriptional regulation differently depending on the genomic context. Most CpG sites in the mammalian genome are methylated, with the exception of CpG-dense, hypomethylated domains at putative regulatory elements or promoter regions called CpG islands (CGI) (Deaton and Bird, 2011). A subset of CGIs are highly methylated and induce transcriptional silencing of the associated gene with cell-type specificity (Deaton and Bird, 2011; Illingworth et al., 2008). Highly methylated CGIs also correspond to regions with long-term or constitutive silencing, such as imprinted genes (Li et al., 1993), the inactive X chromosome (Csankovszki et al., 2001), and endogenous retroviruses (Walsh et al., 1998). In contrast, increased mCG and particularly mCH density across the gene body is associated with transcriptional activation (Maunakea et al., 2010; Mo et al., 2015; Yang et al., 2014b). hmC is also associated with active regulatory and transcribed regions and is dynamically regulated throughout development (Lister et al., 2013; Pastor et al., 2011; Stroud et al., 2011).

DNA methylation is intimately linked to other epigenetic factors and together these mechanisms comprise the chromatin state and direct gene expression programs (reviewed in (Chen and Dent, 2014). However, it is not clear how or in what order histone modifications and DNA methylation are established and how they influence each other (Cedar and Bergman, 2009; Schübeler, 2015; Spruijt and Vermeulen, 2014; Suzuki and Bird, 2008). Different histone marks

correlate with different regions of chromatin, such as promoters, enhancers and coding regions (Kim and Shiekhattar, 2015). Different histone modifications also direct the binding of many factors to DNA and can affect DNA methylation deposition by the differential recruitment of DNMTs (Baubec et al., 2015; Eberl et al., 2013; Noh et al., 2015). Conversely, DNA methylation, or the absence of methylation at CGIs, can direct the establishment of different histone marks (Thomson et al., 2010).

DNA methylation can also directly determine how and where protein factors bind to DNA. Transcription factors can be repelled by methylation at promoters (Blattler and Farnham, 2013; Domcke et al., 2015), but can also bind to methylation without having repressive activity (Figure 1.2.A-C) (Spruijt and Vermeulen, 2014). Finally, mC and its oxidized forms are bound specifically by several classes of proteins referred to as 'readers' of methylation, which can in turn recruit other chromatin-modifying proteins to DNA amongst other diverse functions (Spruijt et al., 2013). These studies have made it apparent that DNA methylation is an integral and dynamic part of chromatin and transcriptional regulation, far from its originally presumed role as a simple transcriptional repressor.

Readers of DNA methylation

The readers of methylation are a key component of epigenetic regulation as they function at the intersection of several critical mechanisms that affect transcriptional regulation. The reader proteins include the methyl-CpG binding domain (MBD), Kaiso, and SET- and Ring finger-associated (SRA) domain and other protein families, some of which have cell-type specificity (Filion et al., 2006; Hendrich and Bird, 1998; Prokhortchouk et al., 2001; Spruijt et al., 2013; Unoki et al., 2004). The readers of methylation may induce transcriptional silencing by blocking transcription or other activating protein factors from binding to DNA (Figure 1.2.D), or by inducing chromatin remodeling through their binding partners (Du et al., 2015). However, there is evidence that readers of methylation, particularly certain MBD proteins, are also found at actively transcribed genes in promoters or intragenic sites, although the effect of this binding on

transcriptional regulation is not fully understood (Baubec et al., 2013; Günther et al., 2013) (Figure 1.2.E,F). These findings show that the readers of methylation and its derivatives are dynamic and developmentally regulated and therefore are essential to our understanding of epigenetic processes. Despite many biochemical studies on proteins that bind to methylation, the precise functions of these proteins *in vivo* remain unclear. In particular, the functions of the MBD family of proteins have been of great interest because these proteins have been genetically linked to disease in both humans and mouse models (Du et al., 2015).

The methyl-CpG binding domain family of proteins

Of the DNA methylation readers, the methyl-CpG binding domain (MBD) family represents a group of proteins that generally act as intermediates between methylation and other chromatin and histone modifying protein complexes. Members of the MBD protein family are essential for varied biological processes, such as embryogenesis and brain function and have been studied in human patients and animal models (Amir et al., 1999; Du et al., 2015; Hendrich et al., 2001). The first MBD protein identified was MeCP2 (Lewis et al., 1992), after which six additional proteins containing the conserved MBD were described to make up the canonical MBD family (Figure 1.3) (Baymaz et al., 2014; Hendrich and Bird, 1998). An additional four proteins, SETDB1/2 and BAZ2A/B, contain a phylogenetically distinct MBD and are therefore not included in the MBD family (Hendrich and Tweedie, 2003). The non-MBD readers of methylation recognize mCG through other protein domains, such as the SRA domain or zinc finger domains in Krüppel or Kaiso-related proteins (Filion et al., 2006; Prokhortchouk et al., 2001; Spruijt et al., 2013; Unoki et al., 2004).

Despite the name, in fact not all members of this family bind to mCG with exclusivity, or at all. Instead, the MBD proteins have distinct DNA-binding properties that may contribute to their respective functions. Early studies showed that only certain MBD proteins, including MeCP2, MBD1, MBD2 and MBD4, are localized to hypermethylated major satellite regions (Hendrich and Bird, 1998; Nan et al., 1997). More detailed biochemical analysis demonstrated that all the MBD

proteins, with the exception of MBD3, MBD5, and MBD6, bind with high affinity to mCG (Hashimoto et al., 2012a). It was later shown that MBD1 is the only MBD protein with demonstrated affinity for unmodified cytosines, which is mediated through two or three alternatively spliced CxxC-type zinc finger domains (Jørgensen et al., 2004). MBD4 binds to methylated DNA and has DNA glycosylase activity that is unique in the MBD family (Hashimoto et al., 2012b). The most recently described MBD proteins, MBD5 and MBD6, are localized at pericentric heterchromatin but do not specifically bind methylated DNA (Laget et al., 2010).

Whether or not any MBD proteins can specifically bind to hmC has been a source of controversy; however, it seems that none bind to hmC preferentially over mCG or unmodified cytosine (Hashimoto et al., 2012a; Spruijt et al., 2013). MeCP2 was reported to bind hmC (Mellén et al., 2012), but a closer examination showed that MeCP2 specifically binds hmC at CpA, but not CpG, dinucleotides in addition to binding to methylation in CpG and CpA contexts (Gabel et al., 2015; Guo et al., 2014). MBD3 has been linked to hmC and Tet protein function in ESCs, suggesting that MBD3 may be specifically targeted to hydroxymethylation (Yildirim et al., 2011). However, *in vitro* studies have not detected a specific interaction between MBD3 and hmC and instead show MBD3 binding to mC, hmC and unmodified C with relatively low, equal affinity (Hashimoto et al., 2012a; Spruijt et al., 2013).

The MBD proteins were first described as mediators of transcriptional repression that bind to methylated DNA and recruit various chromatin-modifying or co-repressor protein complexes (Feng and Zhang, 2001; Nan et al., 1998; Ng et al., 1999, 2000). However, only MeCP2, MBD1, and MBD2 fit this model precisely by recruiting co-repressor complexes through their transcriptional repression domains (TRDs) (Figure 1.3). Additionally, each of these proteins has distinct functions. Both MBD2 and MBD3 are part of the nucleosome remodeling and histone deacetylation (NuRD) protein complex (Feng and Zhang, 2001; Le Guezennec et al., 2006). However, MBD2 binds to mCG while MBD3 has a point mutation in the MBD that abolishes specific binding to methylated DNA (Saito and Ishikawa, 2002). MeCP2 associates with the Sin3A, coREST and NCoR co-repressor complexes, but has also been linked to heterochromatin

formation, long-range chromatin looping, and alternative splicing (Agarwal et al., 2007; Ballas et al., 2005; Ebert et al., 2013; Kernohan et al., 2014; Lyst et al., 2013; Maunakea et al., 2013; Nan et al., 1998). MBD1 functions in transcriptional repression and replication-dependent heterochromatin formation (Fujita et al., 2003b, 2003c; Ng et al., 2000). Therefore, although MeCP2, MBD1 and MBD2 are superficially similar, these proteins have distinctive DNA binding properties, protein associations, and functions, and should be considered separately but in context of each other. In this study, we have focused on MBD2 with the goal of characterizing MBD2 *in vivo* functions through phenotypic, molecular, and gene expression analyses.

MOLECULAR FUNCTIONS OF MBD2

Evolutionary origins of MBD proteins

MBD2 and MBD3 are the two most closely related mammalian MBD proteins, with identical genomic structure and over 70% identical amino acid sequences (Hendrich et al., 1999). These two MBD proteins presumably arose through a gene duplication event approximately concurrent with the separation of the ancestral vertebrate lineage. They also likely correspond to the ancestral MBD protein because the single MBD2/3 form found in invertebrates is the only MBD-containing protein identified in this lineage. The other MBD proteins are unique to vertebrates and either arose from further gene duplication events of the ancestral MBD2/3, or from an orphan MBD-like protein (Hendrich and Tweedie, 2003). The functions of MBD2/3 are highly conserved from invertebrates to vertebrates with some important distinctions. For example, the *Drosophila melanogaster* MBD2/3 orthologue interacts with components of the NuRD complex to mediate transcriptional repression (Ballestar et al., 2001), but binds preferentially to mCH instead of mCG (Marhold et al., 2004). There is also some variation amongst vertebrates in the number and structure of the MBD2/3 genes. The African clawed frog (*Xenopus laevis*) and zebrafish (*Danio rerio*) each have two forms of MBD3, one of which does bind mCG, and one form corresponding more closely to mammalian MBD2 (Hendrich and Tweedie, 2003; Wade et

al., 1999). In contrast, mammals have one MBD2 gene with methylation-specific binding capability and one MBD3 gene that does not bind to methylation, each with several alternatively spliced or translated isoforms (Hendrich et al., 1999; Hendrich and Bird, 1998).

MBD2 gene and protein structure

Mammalian MBD2 was identified in a search for proteins containing the conserved MBD (Hendrich and Bird, 1998). MBD2 and MBD3 are on different chromosomes in humans and mice, but have a highly similar genomic structure, further indicating the occurrence of an ancestral gene duplication event (Hendrich et al., 1999; Hendrich and Tweedie, 2003). Murine MBD2 is encoded by six coding and one non-coding exons, with the MBD spanning exons 2 and 3, and has three isoforms: MBD2a, MBD2b, and MBD2c (also known as MBD2t) (Figure 1.4.A) (Hendrich et al., 1999; Hendrich and Bird, 1998). The distinctions between the isoforms of MBD2 correspond to different functions, and are therefore critical for the understanding of MBD protein function *in vivo*. MBD2a and MBD2b arise from two alternative translation start sites and differ only in the inclusion of a GR-rich N-terminal domain in MBD2a (Figure 1.4.B). Both isoforms contain the full MBD and C-terminal TRD, which is essential for MBD2 interactions with co-repressor protein complexes, including the NuRD complex (Boeke et al., 2000).

The inclusion of the GR-rich domain in MBD2a may have important functional consequences, as post-translational methylation of this region affects interactions with DNA and NuRD (Tan and Nakielny, 2006). Furthermore, the GR-rich domain also mediates MBD2 interactions with RNA (Jeffery and Nakielny, 2004). MBD2a protein consistently appears as a doublet in western blot analyses, suggesting that a fourth alternatively spliced, translated, modified, or cleaved isoform may be present (Ng et al., 1999). The C-terminal TRD region of MBD2 includes two domains that interact with different members of the NuRD complex. The intrinsically disordered region immediately downstream of the MBD interacts directly with the NuRD components RBBP4/7, HDAC1/2 and MTA1/2/3 (Desai et al., 2015), while a coiled-coil domain mediates interactions with p66α and p66β (later renamed GATAD2a and GATAD2b)

(Feng and Zhang, 2001; Gnanapragasam et al., 2011). The third isoform, MBD2c or MBD2t, utilizes an alternative third exon and produces a truncated protein that includes the N-terminal GR-rich domain and the MBD, without the C-terminal TRD (Figure 1.4.B) (Hendrich and Bird, 1998). This isoform is expressed exclusively in the testes and ESCs and does not interact with the NuRD complex, with important functional consequences particularly for pluripotent stem cells (Baubec et al., 2013; Hendrich and Bird, 1998; Lu et al., 2014).

MBD2 and NuRD

MBD2 was first described as part of a methylation-binding protein named MeCP1 (Meehan et al., 1989), which was later resolved to be the components of the NuRD complex in addition to MBD2 (Ng et al., 1999; Zhang et al., 1999). The composition and functions of the NuRD complex are conserved from mammals to other vertebrates and insects (Marhold et al., 2004; Wade et al., 1999). NuRD consists of the ATP-dependent remodeling enzymes CHD3/4, histone deacetylases HDAC1/2, histone chaperones RBBP4/7, and DNA binding proteins GATAD2A/B and MTA1/2/3 in addition to MBD2 and MBD3 (Torchy et al., 2015). NuRD has both ATP-dependent nucleosome remodeling and histone deacetylase activity (Basta and Rauchman, 2015). Early studies of MBD protein function focused on the transcriptional repressive activities of NuRD. The first model of MBD2 function proposed that MBD2 recruits NuRD to methylated sites to induce histone-deacetylase-dependent transcriptional silencing and chromatin compaction (Figure 1.5.A) (Ng et al., 1999). In this simplified model, reduced DNA methylation density corresponds to less MBD2/NuRD binding activity, increased histone acetylation and more open chromatin allowing for active transcription (Figure 1.5.B). This activity was observed in numerous studies examining repression of methylated reporter constructs and endogenous methylated promoters of several genes, particularly those related to cancer (Auriol et al., 2005; Chatagnon et al., 2009; Feng and Zhang, 2001; Ng et al., 1999; Ramírez et al., 2012).

Despite the biochemical evidence for this model of MBD2/NuRD mediated transcriptional repression, many studies now suggest that this model does not constitute the full activity of

MBD2/NuRD. NuRD unexpectedly has both repressive and activating effects on transcription, and may be better described as a modulator of transcriptional activity (Reynolds et al., 2013). Furthermore, it has been challenging to identify specific methylated genes that are targeted for regulation by MBD2 when studying transcriptome changes on a genome-wide scale. Upon loss of MBD2, both upregulation and downregulation occurs and it is difficult to distinguish direct from indirect effects, implying that MBD2-mediated transcriptional regulation may be context-specific (Günther et al., 2013; Lopez-Serra et al., 2008; Stefanska et al., 2013). By correlating MBD2 binding sites determined by chromatin immunoprecipitation (ChIP) with differentially expressed genes upon knockdown of MBD2, several studies support the model that loss of MBD2 primarily results in derepression of lowly expressed genes (Devailly et al., 2015; Günther et al., 2013).

One possible explanation for the subtle gene regulation by MBD2 is that the interactions between MBD2 and NuRD are more complicated than originally realized. This may be due to different isoforms of MBD2, of which only two interact with NuRD, and post-translational modifications of MBD2 that can also affect NuRD interactions (Baubec et al., 2013; Tan and Nakielny, 2006). Recent findings are in opposition to the original model which proposed that MBD2 recruits NuRD to methylated sites (Ng et al., 1999). Surprisingly, NuRD shows less than expected co-occupancy with MBD2 at methylated regions (Figure 1.6.A). MBD2 is also found at unmethylated, active regions and requires interaction with the NuRD complex for this localization (Baubec et al., 2013). These findings suggest NuRD is recruiting MBD2 to unmethylated sites where it would otherwise not bind (Figure 1.6.B). It is plausible that MBD2b, which has the C-terminal TRD, interacts with NuRD and methylated and unmethylated DNA in a similar manner to MBD2a (Figure 1.6.C,D). In contrast, MBD2c, which does not interact with NuRD due to the absence of the TRD, may still bind methylated sites without NuRD but is absent from unmethylated sites (Figure 1.6.E,F) (Baubec et al., 2013). These findings support the view that MBD2, through its interactions with NuRD, may be involved in transcriptional activation as well as repression (Baubec et al., 2013; Reynolds et al., 2013).

The other critical factor that may be affecting MBD2 function is the role of MBD3 in complex with NuRD. MBD3 was identified as an essential member of the NuRD complex with transcriptional repressive activity, despite not binding to methylated DNA (Wade et al., 1999). Two further studies gave strong indication that MBD2 and MBD3 may have very different molecular functions *in vivo.* First, NuRD incorporates MBD2 or MBD3 into mutually exclusive complexes (Le Guezennec et al., 2006) and second, genetic studies of mice show distinctly different null phenotypes for each gene (Hendrich et al., 2001). MBD3 is considered to be a core NuRD component with repressive activity (Morey et al., 2008; Saito and Ishikawa, 2002; Wade et al., 1999), but its exact functions within NuRD and the functional mechanisms of NuRD assembly with either MBD2 or MBD3 are unknown.

It is clear that MBD2/NuRD and MBD3/NuRD have distinct genome-wide distributions (Baubec et al., 2013; Günther et al., 2013) and different functions, particularly in ESCs (Gu et al., 2011; Kaji et al., 2006; Lu et al., 2014). Together these findings suggest that transcriptional regulation by MBD2 is more dynamic and multifaceted than originally proposed, and this may help explain why direct targets of MBD2 regulation have been difficult to identify *in vivo*. Further work is required to determine the dynamics of MBD2, MBD3 and NuRD recruitment to chromatin and how MBD2 may function within and also independently of NuRD.

MBD2 and other protein complex interactions

Although MBD2 is usually associated with the NuRD co-repressor complex, there is increasing evidence that MBD2 functions may rely on interactions with several other diverse protein complexes. Several of these interactions directly affect MBD2 binding to NuRD, and it is possible that they also mediate NuRD-independent functions. The most well described example is the post-translational methylation of MBD2 by PRMT1 and PRMT5 (Le Guezennec et al., 2006; Tan and Nakielny, 2006). Methylation of the N-terminal RG-rich region of MBD2a (Figure 1.7.A,B), and presumably MBD2c although this has not been shown directly (Figure 1.7.C,D), reduces the affinity of MBD2 for the NuRD complex and for methylated DNA. Importantly, these

interactions are MBD2-specific because no PRMT proteins are associated with MBD3/NuRD (Le Guezennec et al., 2006). Methylation of histone H4 by PRMT1 or PRMT5 produces transcriptionally active or repressed chromatin, respectively (Nicholson et al., 2009). It is unknown if either PRMT protein modifies chromatin in addition to MBD2 where MBD2/NuRD is bound, or if these functions are independent from each other.

There is also evidence that MBD2 interacts with other chromatin- or transcription-regulating protein complexes besides NuRD. MBD2 can form a complex with TACC3 and the histone acetyltransferase pCAF to activate transcription (Angrisano et al., 2006). Another study showed that MBD2a, but not MBD2b, reactivates transcription of unmethylated, cAMP-responsive genes through interactions with RNA helicase A, part of the CREB transcriptional coactivator complex (Fujita et al., 2003a). Interestingly, when MBD2 is associated with either of these protein complexes it is not bound to histone deacetylases, which are key components of the NuRD complex. It is not clear if these interactions represent additional NuRD-independent functions of MBD2, or if they only serve to mediate MBD2-NuRD interactions.

Finally, there is evidence that MBD2 has a role in cell cycle progression. MBD2 was found to associate with the transcription factor histone nuclear factor P (HiNF-P, also known as MIZF), which regulates transcription of histone H4 genes at the G1/S phase transition (Mitra et al., 2003; Sekimata et al., 2001). Another group found that MBD2 immunoprecipitates with and co-localizes with DNMT1 at replication foci (Tatematsu et al., 2000). However, a more recent study demonstrated that MBD2 and other MBD proteins are delayed in their recruitment to chromatin after DNA replication, as opposed to binding concurrently or soon after replication (Alabert et al., 2014). Further work is necessary to resolve the many remaining questions surrounding the mechanisms of MBD2 function both in association with and independent of the NuRD complex. The majority of studies on MBD2 protein complex interactions have been performed in cell culture systems, and there is little information on these mechanisms in a relevant biological context.

DNA binding properties and genome-wide localization of MBD2

Several MBD proteins have different DNA-binding properties that may be related to their different functions *in vivo*, such as MeCP2 binding to non-CpG methylation, which is abundant in neurons (Gabel et al., 2015). MBD2 binds specifically to mCG, and there has been no demonstrated affinity for methylation in mCH contexts, hmC or unmodified cytosine (Hashimoto et al., 2012a; Spruijt et al., 2013). Interestingly, MBD2 also binds to mRNA and siRNA with high affinity in an MBD-independent manner through its basic N-terminal RG repeats *in vitro* (Jeffery and Nakielny, 2004). One candidate for regulation by MBD2 is the lncRNA *Xist*, which is de-repressed in the absence of MBD2, but not other MBD proteins (Barr et al., 2007). However, this repression is maintained through transcriptional silencing of the methylated *Xist* locus, and it is unknown if MBD2 also interacts with the *Xist* lncRNA directly.

The binding of MBD2 to methylated sites depends on the presence of an intact MBD and the methylating activities of the DNMT proteins (Baubec et al., 2013). Several studies have examined MBD2 binding to specific loci such as the methylated regulatory regions of *BRCA1* or *Foxp3* (Auriol et al., 2005; Wang et al., 2013), but only a few attempts have been made to determine the genome-wide distribution of MBD2. These experiments are complicated by the fact that DNA methylation patterns are dynamic and cell-type specific (Schultz et al., 2015) and antibodies to MBD2 are generally unreliable; therefore all ChIP data to date have been acquired using cell culture or biochemical tagging approaches (Baubec et al., 2013; Chatagnon et al., 2011; Devailly et al., 2015; Günther et al., 2013; Menafra et al., 2014).

Studies in HeLa cells (Chatagnon et al., 2011; Günther et al., 2013), mouse ESCs (Baubec et al., 2013), and breast cancer cell lines (Devailly et al., 2015; Menafra et al., 2014) all showed that MBD2 localization is highly correlated with methylation, as expected, with no detectable sequence specificity. MBD2 is enriched at transcription start sites, promoters, and exons that coincide with methylated CGIs (Baubec et al., 2013; Günther et al., 2013; Menafra et al., 2014). Highly methylated sites that have low mCG density, such as most repetitive regions

and low-CpG promoters, introns and intergenic regions, show low or no enrichment for MBD2 (Baubec et al., 2013; Günther et al., 2013).

Surprisingly, MBD2 was also detected at unmethylated sites including intermediate- and high-CpG promoters that correlate with the presence of activating histone marks. The MBD2c isoform, which lacks the C-terminal region that interacts with NuRD, was lost from these regions but retained at methylated sites, which suggests that MBD2 localization to unmethylated sites is NuRD-dependent. MBD2 binding to unmethylated promoters is also associated with tissue-specific regulatory regions and low levels of gene expression (Baubec et al., 2013; Günther et al., 2013; Menafra et al., 2014).

In contrast, MBD3 binding, similar to NuRD, is not correlated with methylation and instead is enriched at transcriptionally active, open chromatin (Baubec et al., 2013; Günther et al., 2013). Despite evidence from several studies that MBD2/NuRD and MBD3/NuRD are localized at active chromatin, biochemical evidence shows that NuRD is repelled by the activating histone mark H3K4me3 (Eberl et al., 2013). Therefore, the mechanisms of MBD2/NuRD recruitment and distribution on chromatin remain poorly understood. Additionally, the dynamics and biological consequences of NuRD formation with either MBD2 or MBD3 are unclear, particularly in the *in vivo* cellular context.

BIOLOGICAL FUNCTIONS OF MBD2

Neuronal functions of the MBD protein family

Epigenetic mechanisms in the brain are distinctive because DNA methylation changes dynamically throughout development and in learning and memory processes (Heyward and Sweatt, 2015; Lister et al., 2013; Szulwach et al., 2011). The highly complex network of diverse neuronal subtypes have distinct epigenomic and transcriptional profiles (Mo et al., 2015), further suggesting that epigenetic regulation is essential for the maintenance and function of the brain. Most MBD proteins are associated with neuronal functions in both humans and mice. The most

well studied example is *MECP2*, which when mutated, deleted, or duplicated causes the neurodevelopmental disorder Rett syndrome (Amir et al., 1999; Pohodich and Zoghbi, 2015). Loss of MBD5 is the causative factor in 2q23.1 microdeletion syndrome, characterized by intellectual disability, behavioral problems and seizures (Talkowski et al., 2011). Mutations in the other MBD proteins have not been definitively shown to cause specific disorders in humans, but have been correlatively linked to autism spectrum disorder (ASD) (Cukier et al., 2010, 2012; Li et al., 2005).

Mouse models with deletion of *Mecp2* or *Mbd5* closely recapitulate the symptoms of the respective human disorders, reflecting the conserved functions of these proteins (Camarena et al., 2014; Guy et al., 2001). Mice with mutation, deletion or duplication of *Mecp2* show changes in many phenotypes associated with the human disorder, including decreased anxiety-related phenotypes, impaired motor ability, reduced sociability, deficits in learning and memory, seizures, respiratory abnormalities, and premature lethality (Bissonnette et al., 2014; Goffin et al., 2012). Mice with loss of *Mbd1* show many of the same phenotypes as *Mecp2* mice that are commonly associated with ASDs in humans, including changes in anxiety-related phenotypes, decreased sociability and impaired learning and memory (Allan et al., 2008; Zhao et al., 2003).

Furthermore, the NuRD complex and MBD3 also have important neuronal functions. *Mbd3* constitutive null mice are embryonic lethal (Hendrich et al., 2001), but a *Mbd3* brain-specific conditional null mouse has defects in cortical thickness and neuronal differentiation and is neonatal lethal (Knock et al., 2015). In addition, a recent study identified a brain-specific isoform of the NuRD component CHD5 which interacts with MBD3, but not MBD2, which suggests that MBD3 has brain-specific functions distinct from MBD2 (Potts et al., 2011). The NuRD complex is also essential in the brain. Genetic deletion of NuRD complex component CHD4, which disrupts the NuRD complex, affects gene expression programs in the cerebellum that regulate synaptic differentiation (Yamada et al., 2014).

In contrast to the relatively severe phenotypes of the other MBD protein null mice, *Mbd2* null mice are viable and fertile and the only reported behavioral phenotype is a maternal nurturing

deficit (Hendrich et al., 2001). It has been speculated that MBD2 may also have brain-specific functions judging by the essential role of the other closely-related MBD proteins in the brain (Du et al., 2015). A role for MBD2 in several other peripheral cell types have reported, including embryonic stem cells and various cells of the immune system, but the effect of these functions on any phenotypes of *Mbd2* mice have not been fully characterized (Cook et al., 2015; Lu et al., 2014; Wang et al., 2013).

Isoform-specific roles of MBD2 in pluripotent cells

The maintenance, proliferation and differentiation of pluripotent cells is highly dependent on epigenetic mechanisms (Meissner, 2010). It is clear that MBD3 has an essential role in pluripotent ESCs because *Mbd3* null mice are early embryonic lethal (Hendrich et al., 2001). In contrast, mice with loss of each other MBD protein are viable, albeit with a range of phenotypic severity (Du et al., 2015). Recent work has revealed an important role for MBD2 in pluripotent cells. MBD2 is more lowly expressed in ESCs compared to MBD3 (Lu et al., 2014) and was initially thought to repress reprogramming of somatic to induced pluripotent stem (iPS) cells (Lee et al., 2013). However, further efforts found that differentially spliced isoforms of MBD2 actually have a role in both repression and promotion of reprogramming to pluripotency in human pluripotent stem cells (hPSCs) (Lu et al., 2014). *MBD2a*, the longest isoform that includes both the N-terminal GR-rich domain and C-terminal TRD, is specifically enriched in differentiated fibroblasts (DFs) while alternatively spliced *MBD2c,* which lacks the TRD, is enriched in hPSCs. Overexpression of *MBD2a* in hPSCs disrupts pluripotency presumably by mediating NuRD targeting to the *OCT4* and *NANOG* promoter regions and downregulating their expression. In contrast, *MBD2c* is also bound at these promoters but does not interact with NuRD. Overexpression of *MBD2c* together with other reprogramming factors in DFs actually enhances reprogramming efficiency. The authors conclude that *MBD2a* and *MBD2c* mediate the balance between proliferation and differentiation of hPSCs (Lu et al., 2014).

It is unclear why *Mbd2* constitutive null mice are viable and fertile when there is a role for MBD2 and NuRD in pluripotent cells (Hendrich et al., 2001; Lu et al., 2014; Reynolds et al., 2012). Similarly to the brain, it is possible that MBD3 may be sufficient to mediate NuRD-related functions during embryogenesis. However, a genetic interaction between *Mbd2* and *Mbd3* argues that MBD3 cannot fully compensate for loss of MBD2 (Hendrich et al., 2001). The role of MBD3 in pluripotent cells has been better studied but is not fully understood. MBD3-deficent blastocysts fail to develop mature epiblast after implantation, accompanied by significant gene expression changes, suggesting that MBD3 is required for differentiation (Kaji et al., 2006, 2007). These findings were supported by a study that showed that NuRD, with MBD3, is required to dynamically regulate expression of pluripotency genes in ESCs in order to transition to differentiation (Reynolds et al., 2012). The function of MBD3 in reprogramming of differentiated somatic cells to iPS cells has been controversial. Two studies found that removal of NuRD increased reprogramming efficiency (Luo et al., 2013; Rais et al., 2013), while another study supports that NuRD is essential for reprogramming (Dos Santos et al., 2014). These conflicting results suggest that MBD3/NuRD may have different context-specific effects on differentiation, but further studies are needed to resolve this question.

Emerging roles for MBD2 in immunity

There is strong evidence that DNA methylation and other epigenetic mechanisms are essential in hematopoiesis and differentiation of myeloid and lymphoid cell lineages (Álvarez-Errico et al., 2014; Shih et al., 2014). For example, CD4+ T cells undergo extensive transcriptional, chromatin remodeling and DNA methylation changes during maturation (Komori et al., 2015). NuRD, MBD2 and MBD3 have roles in multiple lymphoid cell populations (Dege and Hagman, 2014a). The core NuRD component CHD4 is required for the maintenance and differentiation of hematopoietic stem cells (Yoshida et al., 2008). However, a specific role for MBD2 in these cells and other early progenitors has not been described. *Mbd2* null mice have unaltered lymphoid organs and major lymphocyte subsets, suggesting that MBD2 may not be

required at early stages of hematopoiesis (Hutchins et al., 2002). In B cells, the NuRD complex interacts with various transcription factors to mediate temporal changes in development and differentiation (Gao et al., 2009; Musselman et al., 2012). Transcriptional regulation of the B-cell specific *Cd79a* gene involves MBD2-dependent CHD4/NuRD recruitment, but whether B cells are broadly affected in *Mbd2* null mice is unknown (Ramírez et al., 2012).

The functions of NuRD and MBD2 in several T cell populations have been studied more extensively. Loss of MBD2 has been linked to changes in proliferation or maturation of multiple T cell populations. These changes may arise from altered expression of several critical factors, some of which are controlled by differentially methylated regulatory regions. For example, loss of MBD2 or NuRD components CHD4 or MTA2 skews CD4+ T cell polarization towards Th2 populations, with implications for pathogen resistance (Hosokawa et al., 2013; Hutchins et al., 2002, 2005; Lu et al., 2008). One study proposed that these changes may occur because MBD2/NuRD regulates expression from the Th2 cytokine locus, which is demethylated during Th2 cell differentiation (Aoki et al., 2009).

Interestingly, MBD2 also indirectly affects CD4+ T cell maturation by regulating gene expression programs in dendritic cells, which are required to direct T helper cell maturation (Cook et al., 2015). The maturation of CD8+ T cell populations into effector and memory cells after acute viral infection is also directly affected by loss of MBD2, consistent with MBD2 regulating expression of surface markers and cytokines (Kersh, 2006). Finally, MBD2 regulates the expression of the master T regulatory (Treg) cell transcription factor Foxp3 (Lal et al., 2009; Wang et al., 2013). MBD2 binds to a Treg-specific demethylation region (TSDR) upstream of *Foxp3* that becomes demethylated in thymus-derived natural Tregs. MBD2 promotes the Tet2-mediated demethylation of the TSDR in Treg cells. Consequently, *Mbd2* null mice show decreased Treg numbers and impaired Treg suppressive function in addition to retaining methylation at the TSDR (Wang et al., 2013).

Disruptions to the NuRD complex are detrimental to immunity, as evidenced by a study that showed mice with loss of MTA2 develop a severe lupus-like autoimmune disease (Lu et al.,

2008). Although loss of MBD2 results in reduced numbers of Treg cells, *Mbd2* null mice surprisingly do not develop autoimmunity possibly because their T effector cells are less responsive to stimulation and more susceptible to Treg suppression (Wang et al., 2013). In fact, loss of MBD2 is protective against experimental autoimmune encephalomyelitis, a model of T cell mediated autoimmunity and demyelinating diseases of the central nervous system (Zhong et al., 2014). In human patients, increased levels of MBD2 and global demethylation in CD4+ T cells has been observed in several autoimmune disorders, including systemic lupus erythematosus (Balada et al., 2007; Liu et al., 2011), systemic sclerosis, dermatomyositis (Lei et al., 2009) and *MBD2* was determined to be a susceptibility locus for psoriasis (Tsoi et al., 2012). These human and mouse studies point to MBD2/NuRD being an essential regulator of immune function with therapeutic potential. However, considerable effort is required to fully understand the complexities of MBD2 function in immunity at the cellular and systemic levels.

Implications for MBD2 function in cancer

Factors that shape the epigenome have been studied extensively in regards to cancer initiation, progression and treatments (Baylin and Jones, 2011). The NuRD complex is thought to mediate tumorigenesis by modifying expression or activities of transcription factors linked to cancer, targeting hypermethylated tumor suppressor genes for transcriptional silencing, and maintaining genomic stability (Lai and Wade, 2011). Many studies have attempted to link loss of MBD2 or MBD3 to significantly increased cancer predisposition in human patients, but evidence for this is limited. Studies of MBD2 and MBD3 in cancer have therefore focused on their potential as therapeutic targets. However, concerns have been raised regarding the feasibility of directly targeting these proteins and possible off-target effects (Parry and Clarke, 2011).

MBD2 has been studied particularly in the context of colorectal cancer, but questions remain as to the specific role of MBD2 in tumor initiation or progression. MBD2 is required for regulation of gene expression in the gastrointestinal tract, as *Mbd2* null mice show altered spatial expression of several genes in the small intestine and colon (Berger et al., 2007). Loss of MBD2

is protective against tumorigenesis specifically in $Apc^{Min/+}$ mice, a mouse model of sporadic colorectal tumorigenesis (Sansom et al., 2003). The $Apc^{Min/+}$mouse develops tumors due to significantly upregulated Wnt signaling (Sansom, 2004), which is downregulated in the absence of MBD2 (Phesse et al., 2008). While these results suggest targeting MBD2 may have therapeutic potential for colorectal cancer, further investigations show that the downregulation of Wnt signaling may not be related to MBD2-specific functions. First, *Mbd2* null mice in a wildtype background do not show any changes in intestinal histology or Wnt signaling (Phesse et al., 2008). More importantly, similar downregulation of Wnt signaling and reduced tumorigenesis occurs when perturbing several other chromatin binding or modifying factors, including the DNMTs (Cai et al., 2014), the methylation-binding protein Kaiso (Prokhortchouk et al., 2006), and the chromatin remodeling factor Brg1 (Holik et al., 2014). In contrast, MBD3 is more likely to have a direct function in the gastrointestinal tract. Loss of MBD3 specifically in the gut results in increased tumorigenesis induced by inflammation through the upregulation of targets of the AP-1 transcription factor (Aguilera et al., 2011). It is currently unknown if these pathways are also affected by loss of MBD2.

MBD2 may directly affect tumorigenesis because reduced expression of MBD2 inhibits tumor growth in cultured cell lines and in human cancer cell xenografts in mice (Campbell et al., 2004). One way this could occur is through the de-repression of tumor suppressor genes. MBD2 binds to hypermethylated promoters of tumor suppressor genes and contributes to their transcriptional silencing, which has been shown to occur in multiple human cancer cell lines (Lopez-Serra et al., 2008). Therefore, loss of MBD2 may be protective against tumorigenesis by relieving transcriptional repression of hypermethylated tumor suppressor genes such as *p14(ARF)* and *p16(INK4A)* that commonly show aberrant methylation in colon cancer cells (Magdinier and Wolffe, 2001; Martin et al., 2008). Similar mechanisms have been observed in glioma cells (Zhu et al., 2011) and breast cancer cells (Mian et al., 2011).

Interestingly, MBD2 has been shown to directly repress human telomerase reverse transcriptase (*hTERT*) in several cancer cell types (Chatagnon et al., 2009). *hTERT* is usually

hypermethylated and silenced, but is expressed in most cancer cells and therefore, in regards to this mechanism, loss of MBD2 may encourage tumor growth. However, loss of MBD2 has complex effects on gene expression with both upregulation and downregulation of many genes in breast cancer and liver cancer cell lines (Devailly et al., 2015; Stefanska et al., 2013). Downregulation of certain genes in the absence of MBD2 may be protective against tumorigenesis. In prostate cancer cells, loss of MBD2 suppresses tumor growth through hypermethylation and silencing of pro-metastatic genes (Shukeir et al., 2006). These complexities indicate that identification and manipulation of specific therapeutic pathways targeted via MBD2 will be challenging. Furthermore, the majority of these studies have identified misregulation of a single locus in cultured cells and do not fully address the role of MBD2 in a biological, cellular context.

Studies of MBD2 in human cancer patients also point to MBD2 as a potential regulator of tumorigenesis. The finding that the 18q21 locus that includes Mbd2 is deleted in 70% of human colorectal cancers (Fearon et al., 1990) led to speculation that Mbd2 could be a candidate tumor suppressor gene itself. However, further investigation showed that only the deleted in colon cancer (DCC) gene at this locus is likely to be directly linked to cancer progression. All other neighboring genes, including *Mbd2,* are rarely affected by hypermethylation or point mutations in colorectal cancer (Bader et al., 2003; Derks et al., 2009). *Mbd3* is also generally unaffected by mutations or epigenetic changes in colon cancer (Zhu et al., 2004).

Despite the absence of mutations in MBD2 or MBD3 in cancer patients, there is evidence that these genes show altered regulation in tumors. Both MBD2 and MBD3 are downregulated in multiple human tumor types, but it is not clear what effect this has on tumor progression (Kanai et al., 1999; Müller-Tidow et al., 2001; Pontes et al., 2014). Studies of MBD2 in breast cancer have produced conflicting results. One study found that MBD2 is upregulated in breast tumors (Billard et al., 2002), while another found no difference (Müller et al., 2003). Analysis of single nucleotide polymorphisms in *Mbd2* and breast cancer were similarly difficult to interpret, although some weak associations were detected (Sapkota et al., 2014; Zhu et al., 2005). Because MBD2

appears to have variable or context specific effects on tumorigenesis, significant further investigations into the molecular mechanisms of MBD2 function must be undertaken to identify potential therapeutic targets associated with these functions.

THE CHARACTERIZATION OF MBD2 FUNCTIONS *IN VIVO*

Of the MBD family proteins, considerable efforts have been made to understand the functions of MeCP2 because mutations in this protein are genetically linked to neurological disease (Pohodich and Zoghbi, 2015). MBD1, MBD3 and MBD5 have also been the subject of many mouse model studies with implications for brain development and embryogenesis (Camarena et al., 2014; Yildirim et al., 2011, 3; Zhao et al., 2003). In contrast, MBD2 functions have been examined almost exclusively using cultured cells (Feng and Zhang, 2001; Ng et al., 1999). These studies have shed light on important biochemical attributes of MBD2, but the functions of MBD2 *in vivo* remain largely unexplored.

Previous work has shown that *Mbd2* null mice are viable and fertile with only a reported nurturing deficit (Hendrich et al., 2001). This scenario raises significant questions about MBD2 function *in vivo*. It is surprising that MBD2 is the most highly conserved MBD protein in mammals with reported functions in immune and ESCs, yet in contrast to the other MBD proteins, loss of MBD2 does not result in overt or specific phenotypes (Cook et al., 2015; Lu et al., 2014; Wang et al., 2013). The most common explanation put forth for this observation is that the other MBD proteins are compensating for the loss of MBD2 functions. However, the fact that the MBD proteins have distinct DNA binding properties and protein associations does not support this hypothesis (Du et al., 2015). Even MBD3, arguably the best candidate for MBD2 compensation due to their common association with NuRD, has distinctly different DNA-binding properties and is unlikely to recapitulate the role of MBD2 (Baubec et al., 2013; Hendrich et al., 2001). Therefore, there likely remain many unrealized functions for MBD2 *in vivo*. Previous studies have pointed to

a role for MBD2 in immunity (Wang et al., 2013), the gastrointestinal system (Berger et al., 2007), and in tumorigenesis (Sansom et al., 2003), all with significant implications for human disease.

In this study, we sought to expand our understanding of MBD2 *in vivo* functions with two parallel genetic approaches. First, we characterized multiple aspects of the *Mbd2* null mouse phenotype, beginning with phenotypes that have been observed in other MBD protein null mice (Chapter 2) (Guy et al., 2001; Zhao et al., 2003). Second, in order to analyze MBD2 *in vivo* functions, we developed a novel transgenic mouse lines expressing biotin-tagged alleles of endogenous MBD2 and systematically compared the spatiotemporal expression of MBD2 in context of the other MBD proteins (Chapter 3). Together, this work identifies previously uncharacterized *in vivo* aspects of MBD2 function and new directions for further studies.

CHAPTER 1 FIGURES

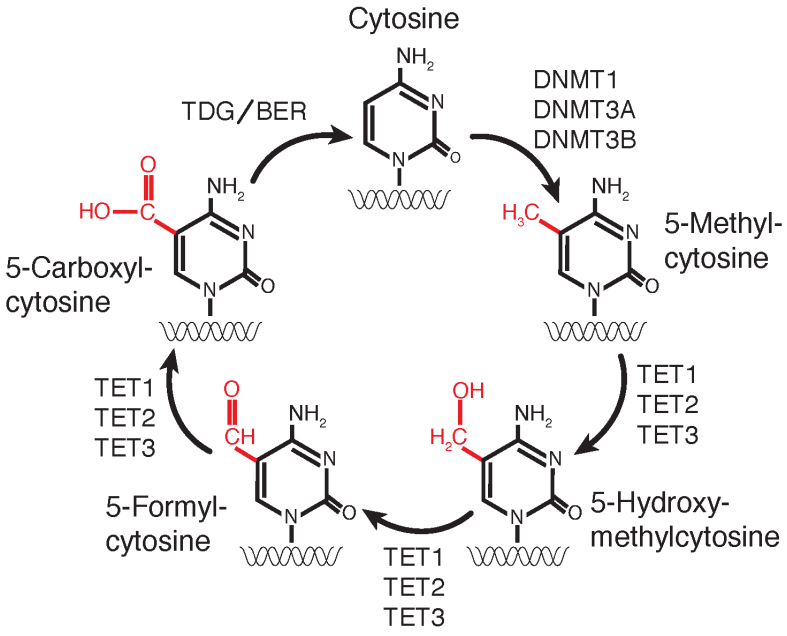

Figure 1.1. The cytosine modification cycle.
Unmodified cytosine is methylated by the DNA methyltransferase proteins DNMT1, DNMT3A and DNMT3B. 5-methyl cytosine is oxidized by TET1, TET2, or TET3 to 5-hydroxymethylcytosine. Further oxidation of hydroxymethylcytosine by the TET proteins yields 5-formylcytosine and 5-carboxylcytosine. 5-carboxylcytosine is converted to an unmodified cytosine by thymine-DNA glycosylases (TDG) and base excision repair (BER) pathways.

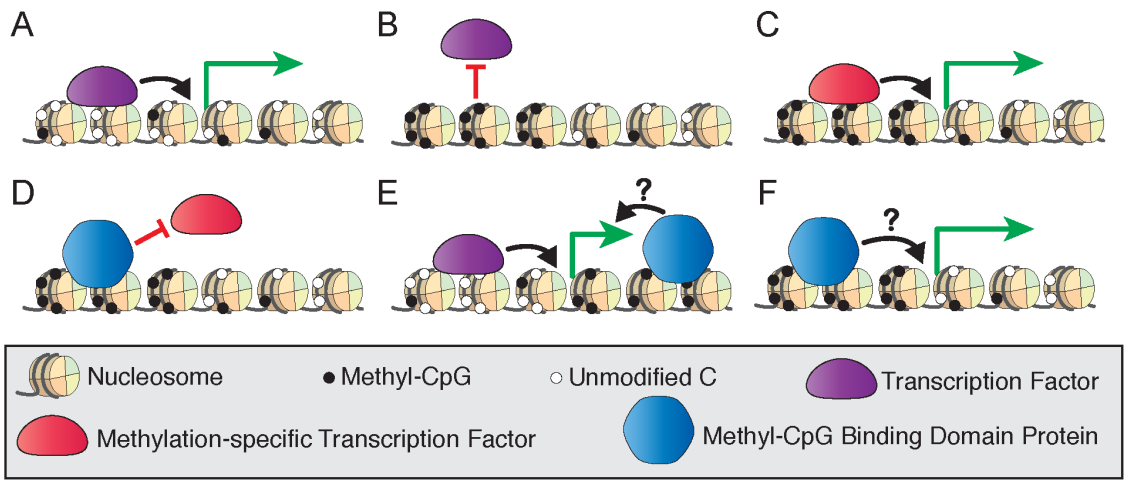

Figure 1.2. Models of DNA methylation affecting transcription factor recruitment.
(A) The binding of transcription factors at hypomethylated regulatory regions drives transcriptional activation. **(B)** Activating transcription factors are blocked from binding to hypermethylated regulatory regions, resulting in transcriptional silencing. **(C)** Methylation-specific transcription factors may bind hypermethylated regulatory regions to activate transcription. **(D)** Methyl-CpG binding domain (MBD) proteins can bind mCG-dense regions and block transcription factor binding, leading to transcriptional silencing. MBD proteins may bind to actively transcribed genes at intragenic **(E)** or promoter **(F)** sites, but the effect of this binding on transcriptional regulation is unclear.

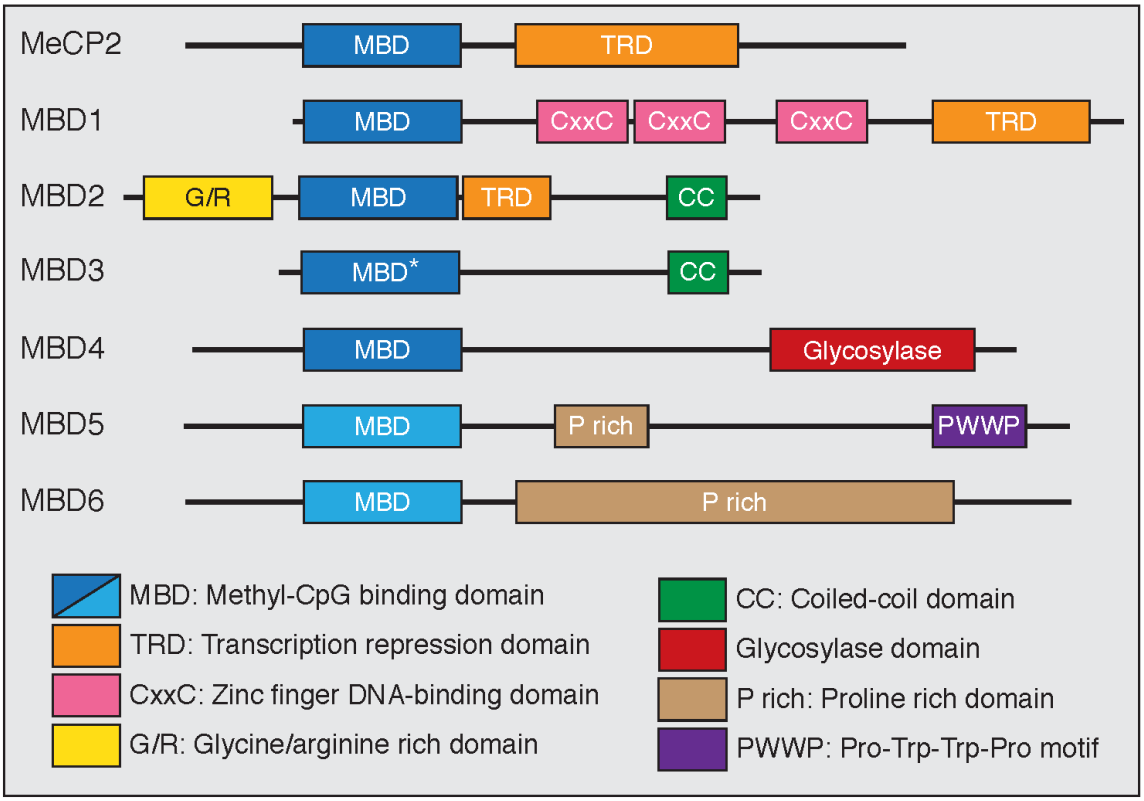

Figure 1.3. The methyl-CpG binding domain (MBD) family of proteins.
All MBD family proteins contain a highly conserved methyl-CpG binding domain (blue box) in addition to other functional domains. The MBD of MBD3 has a point mutation (*) that abolishes methyl-CpG binding. MBD5 and MBD6 do not specifically bind methyl-CpG (lighter blue box). MeCP2, MBD1 and MBD2 contain C-terminal transcriptional repression domains (TRD) that interact with co-repressor protein complexes (orange box). MBD1 has CxxC-type zinc finger domains which mediate DNA binding. MBD2 has an N-terminal glycine/arginine rich domain (yellow box) and a C-terminal coiled-coil domain, which is also found in MBD3 (green box). The functions of MBD4 are mediated through a C-terminal glycosylase domain (red box). Both MBD5 and MBD6 contain proline rich domains (tan box) while MBD5 has a PWWP motif (purple box) that binds methylated histones.

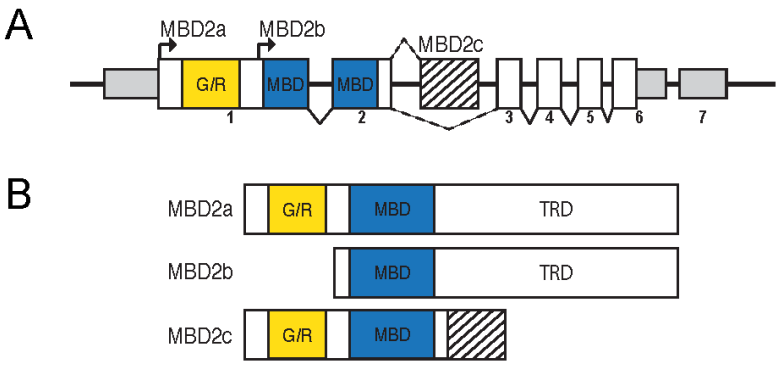

Figure 1.4. The isoforms of MBD2 contain different functional domains.
(A) The *Mbd2* transcript has seven exons, with non-coding regions (smaller gray box) in exons 1, 6 and 7. Coding regions are contained in exons 1-6 (white and filled boxes). The methyl-CpG binding domain (MBD, blue box) is split between exons 2 and 3 with the glycine/arginine rich region (yellow box) in exon 1. There are two translation start sites corresponding to MBD2a and MBD2b, respectively. MBD2c includes an alternatively spliced exon (striped box) between exons 2 and 3. **(B)** MBD2a utilizes the first translation start site and includes the G/R rich domain, MBD and C-terminal transcriptional repression domain (TRD). Translation of MBD2b excludes the N-terminal G/R rich domain. MBD2c includes the alternatively spliced exon and does not contain the C-terminal TRD.

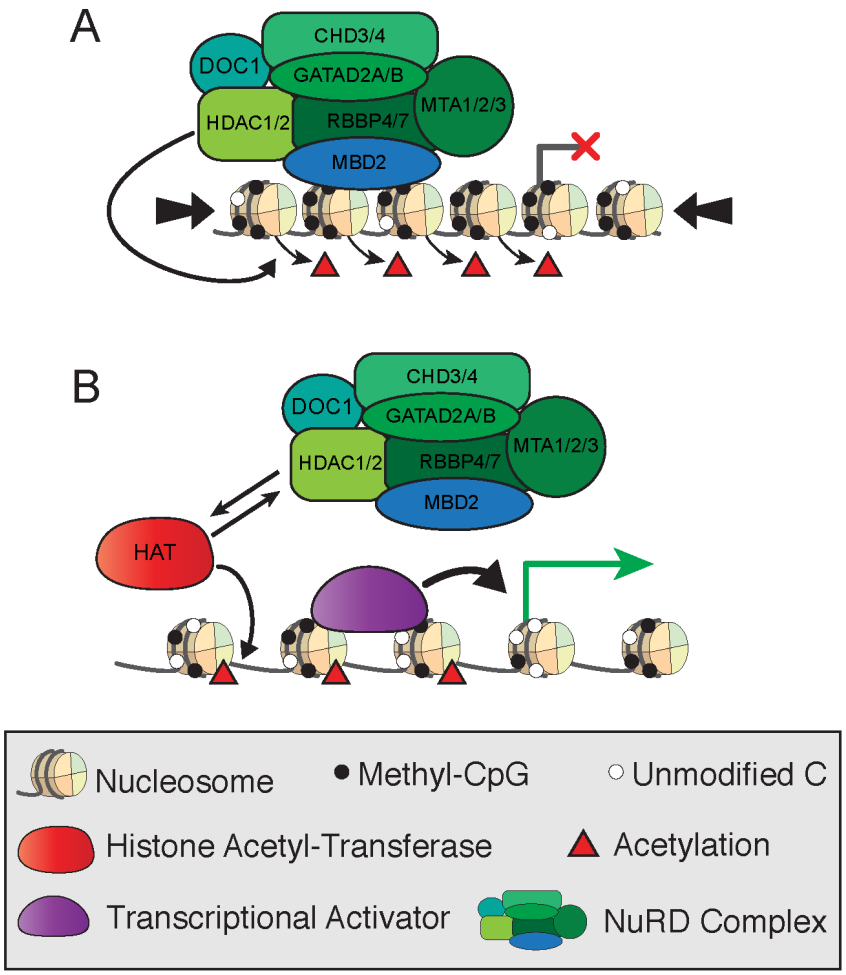

Figure 1.5. Simplified model of transcriptional regulation by MBD2 and NuRD.
(A) MBD2 binds to mCG-dense regions as a component of the NuRD complex, which induces histone deacetylation and chromatin compaction (large arrows) leading to transcriptional silencing. **(B)** At transcriptionally active sites, MBD2/NuRD is replaced by histone acetyltransferases and activating transcription factors to induce histone acetylation and open, active chromatin.

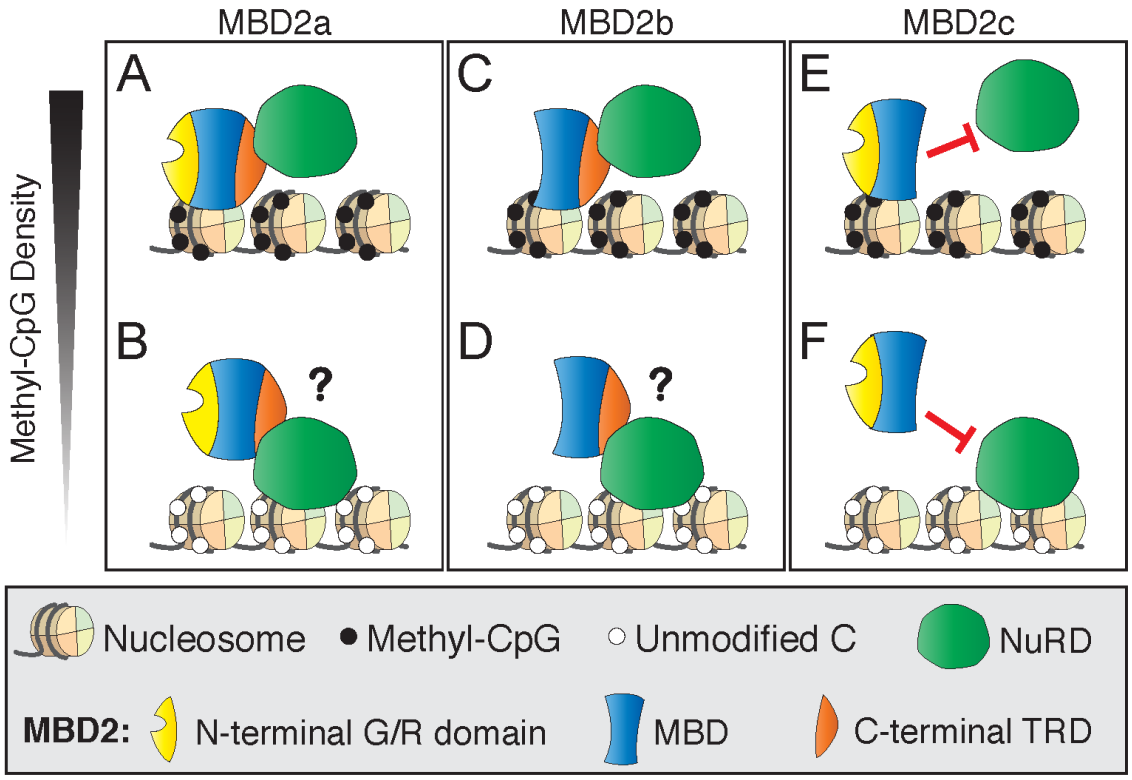

Figure 1.6. DNA binding dynamics of MBD2 isoforms and NuRD.
(A) MBD2a binds to methyl-CpG dense sites with the NuRD complex. **(B)** At unmethylated sites, MBD2 recruitment to DNA is dependent on interactions with NuRD through the C-terminal transcriptional repression domain (TRD). **(C)** Similarly to MBD2a, MBD2b binds to methyl-CpG dense sites with NuRD and may be recruited to unmethylated sites via interaction with NuRD **(D)** MBD2c lacks the C-terminal TRD and does not interact with NuRD. Therefore, MBD2c may bind methylated sites without NuRD **(E)** and, in this model, would not be recruited to unmethylated sites by NuRD **(F).**

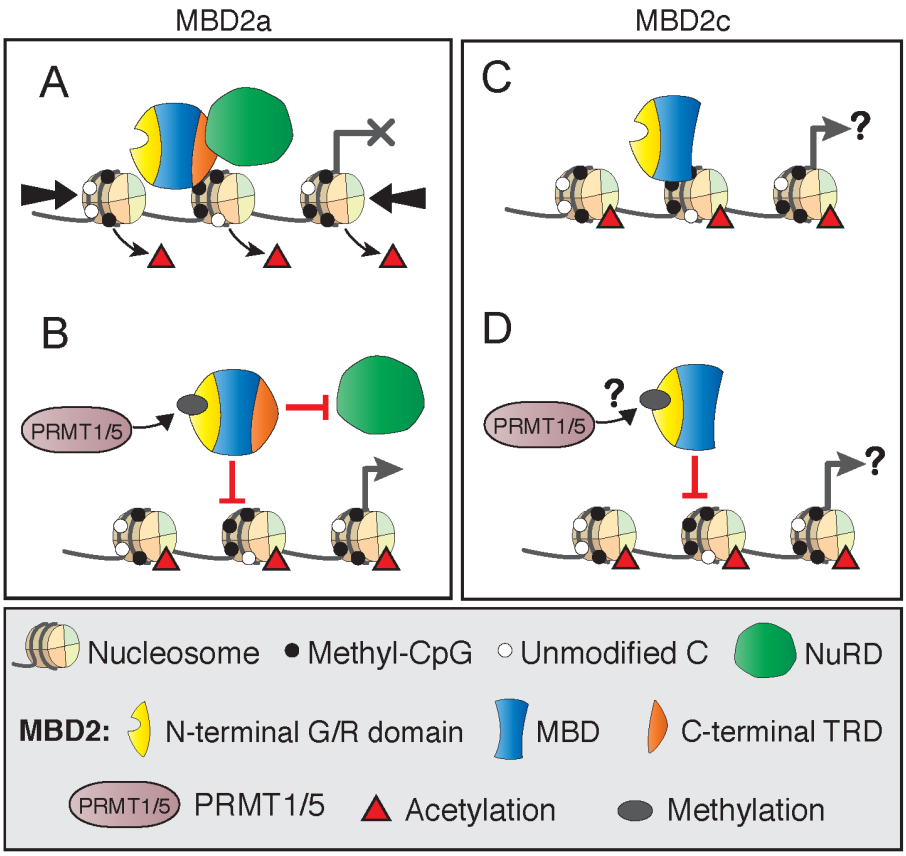

Figure 1.7. DNA binding dynamics of MBD2 depend on post-translational modifications. **(A)** MBD2a and NuRD binding to methylated sites results in nucleosome remodeling (large arrows) and deacetylation, producing transcriptional silencing. **(B)** Post-translational methylation of the N-terminal glycine/arginine rich region of MBD2a by PRMT1/5 reduces the affinity of MBD2a for NuRD and methylated DNA and may not produce transcriptional repression. **(C)** MBD2c does not interact with the NuRD complex but does bind methylated DNA. It is not fully understood how this binding may affect transcriptional regulation. **(D)** MBD2c has the N-terminal G/R rich domain, but it is not clear if it is also methylated by PRMT1/5 and if this modification would affect DNA binding similarly to MBD2a.

CHAPTER 2: Phenotypic characterization of *Mbd2* Null Mice

Adapted from: Wood, K. H., Johnson, B. S., Welsh, S. A., Lee, J. Y., Cui, Y., Krizman, E., Brodkin, E. S., Blendy, J. A., Robinson, M. B., Bartolomei, M. S., Zhou, Z. Tagging methyl-CpG binding domain proteins reveals different spatiotemporal expression and supports distinct functions. *Epigenomics*. In Press.

ABSTRACT

Methylation of cytosine is an epigenetic mark that is essential for many biological processes, including brain development and function. The methyl-CpG binding domain (MBD) family of proteins specifically bind methylated cytosines and recruit different co-repressor complexes to regulate transcription and chromatin state. Genetic studies have linked the MBD proteins MeCP2 and MBD1 to neurodevelopmental disorders related to autism spectrum disorder (ASD) in humans and mice. However, a role for MBD2 in the brain has not been described. In this study, we characterized the behavioral phenotypes of mice lacking MBD2. We found that, in contrast to MeCP2 and MBD1, *Mbd2* null mice are largely similar to control littermates, with mildly altered home-cage activity, nesting and body weight. To further investigate these phenotypes, we examined gene expression changes in the striatum and hypothalamus of *Mbd2* null mice and also quantified the levels of biogenic amines in the cortex and striatum. Our results show that a small number of genes show altered expression in the striatum and hypothalamus and that biogenic amine levels are equivalent to wildtype littermates. We conclude that, in contrast to the closely related proteins MeCP2 and MBD1, MBD2 appears to be dispensable for brain functions at the age that we examined.

INTRODUCTION

Epigenetic mechanisms, including DNA methylation, are essential for proper brain function. DNA methylation at CpG and CpH sites and hydroxymethylation change dynamically in the brain throughout development concurrently with maturation of synapses (Lister et al., 2013). In the mature brain, synaptic plasticity and learning and memory processes are dependent on epigenetic mechanisms (Feng et al., 2010; Heyward and Sweatt, 2015). Furthermore, epigenetic mechanisms are linked to the vast diversity of neuronal cell types, each with unique transcriptional programs and functional properties (Mo et al., 2015).

Genetic studies of MBD proteins in humans and animal models have demonstrated a critical role for this protein family in the brain (Allan et al., 2008; Amir et al., 1999; Cukier et al., 2010, 2012; Guy et al., 2001; Zhao et al., 2003). Mutations in several MBD proteins have been identified in individuals with autism spectrum disorder (ASD), although further work is needed to determine if these mutations are causative (Cukier et al., 2010, 2012). MeCP2 and MBD5 are linked to the specific neurological diseases Rett syndrome and 2q23.1 microdeletion syndrome, respectively (Amir et al., 1999; Talkowski et al., 2011), both of which are closely recapitulated in mouse models with deletion or mutation of each gene (Camarena et al., 2014; Goffin et al., 2012). *Mbd1* null mice also exhibit behavioral phenotypes that mimic features of ASD such as learning and memory deficits, reduced sociability, and changes in anxiety-related phenotypes (Allan et al., 2008; Zhao et al., 2003). Furthermore, MBD3 and multiple components of the MBD-associated co-repressor complexes, such as NuRD, Sin3A, and NCoR/SMRT, also have critical roles in the brain (Knock et al., 2015; McQuown et al., 2011; Potts et al., 2011; Schoch and Abel, 2014; Yamada et al., 2014).

Given the similarities between the MBD proteins and the link between MBD proteins and neurodevelopmental disorders, we hypothesized that MBD2 may also have a role in brain function. Although a nurturing deficit has been reported in *Mbd2* null ($Mbd2^{-/-}$) mice (Hendrich et al., 2001), the extent to which loss of MBD2 leads to other behavioral phenotypes related to brain

function has yet to be determined. We carried out behavioral characterization of *Mbd2*$^{-/-}$ mice similar to studies of *Mecp2* and *Mbd1* null mice (Allan et al., 2008; Goffin et al., 2012). Many of the phenotypes we found in *Mbd2*$^{-/-}$ mice are seen in mice with genetic or pharmacological disruption to striatal dopamine (Palmiter, 2008). In order to determine if these systems are affected by loss of MBD2, we asked if loss of MBD2 affects biogenic amine levels or gene expression in the striatum. We also assessed hypothalamic neuropeptide expression to investigate if the low body weight observed in *Mbd2*$^{-/-}$ mice has neurological etiologies. We found that *Mbd2*$^{-/-}$ mice are equivalent to wildtype and heterozygous littermates on most measures, including behavioral assays, differentially expressed genes, and levels of biogenic amines. Therefore, our results indicate that MBD2, unlike the closely related proteins MeCP2 and MBD1, is largely dispensable for brain functions and behaviors examined in this study.

METHODS

Animal Husbandry

All experiments were conducted in accordance with the ethical guidelines of the US National Institutes of Health and with the approval of the Institutional Animal Care and Use Committee of the University of Pennsylvania. All mice were housed in a standard 12 h light/12 h dark cycle with access to ample amounts of food and water. All experiments were performed on mice on a congenic sv129:C57BL/6J background unless otherwise stated. All assays were performed on male littermates aged 2-3 months. Mice deficient in MBD2 (*Mbd2*$^{-/-}$) are previously described (Hendrich et al., 2001). All *Mbd2*$^{-/-}$ mice, wildtype and heterozygous littermates were bred from heterozygous parents to avoid any confounding effects from nurturing deficits reported in *Mbd2*$^{-/-}$ dams (Hendrich et al., 2001). Male and female mice were weighed weekly beginning at postnatal day 14. Mice deficient in MBD1 (*Mbd1*$^{-/-}$) are previously described (Zhao et al., 2003). Mice were genotyped using a PCR-based strategy to detect mutant and wildtype alleles of *Mbd2* and *Mbd1*. The genotyping primer sequences are listed in Table 2.1.

Table 2.1. *Mbd2* and *Mbd1* null mice genotyping primer sequences.

Primers	Sequences	Product size
Mbd2 knockout allele genotyping	5'-ACGCTGGCCTAGTGCCGTGC-3' 5'-TTGTGGTTGTGCTCAGTTC-3' 5'-TCCGCAAACTTCTATTTCTG-3'	Wildtype*:* 631bp *Mbd2* knockout: 200bp
Mbd1 knockout allele genotyping	5'-TCTTCTCAGACTGAGAAGGGTGA-3' 5'-CACTGAACATTGCCCAGAGCACA-3' 5'-AAACGGCGGATTGACCGTAATGG-3'	Wildtype*:* 300bp *Mbd2* knockout: 500bp

Behavioral Assays

All animal behavioral studies and video analysis were performed blinded to genotype. Mice were allowed to habituate to the testing room for a minimum of 30 minutes before testing began for all assays. Each test was performed at the same time of day. All equipment was thoroughly cleaned between trials. Tests were performed in the following order with less stressful assays performed first: zero maze, social approach, locomotor, Barnes maze, accelerating rotarod, fear conditioning.

Locomotor

Locomotor activity was measured by the number of infrared beam breaks in a photobeam frame (Med Associates). Mice were individually placed into a home cage-like environment with clean bedding surrounded by the infrared photobeam frame. Activity was quantified as the total number of beam breaks over one sixty-minute trial.

Accelerating Rotarod

Mice were place on an accelerating rotarod apparatus (Med Associates) for 16 trials (4 trials a day for 4 consecutive days). Each trial lasted a maximum of 5 minutes while the rod accelerated from 4 to 40 rpm. Mice were allowed to rest for at least 15 minutes between trials. The time and

rpm at which the mouse fell off the apparatus or completed a full rotation while gripping the rod was recorded.

Zero Maze

The elevated Zero Maze (Stoelting) consists of a circular platform with two open quadrants and two walled (closed) quadrants. Mice were placed in the center of one closed quadrant and allowed to freely explore for 5 minutes. Video recordings of each trial were hand-scored for time spent in open and closed quadrants.

Social Approach Test

The social approach test was performed in a three-chambered apparatus as previously described (Fairless et al., 2011). Mice were tested in a box with walls partially dividing the chamber into three areas: center, left and right. Two identical clear Plexiglas cylinders with holes were placed in the left and right sides. During the first habituation phase, the test mouse was placed into the center of the box and allowed to freely explore the three chambers with empty cylinders for 10 minutes. During the second social test phase, an unfamiliar stimulus mouse (adult male gonadectomized A/J mouse; The Jackson Laboratory) was placed into one cylinder in the designated social chamber. A novel plastic object (paperweight) was simultaneously placed into the other cylinder in the designated non-social chamber. The test mouse was then allowed to explore freely for 10 minutes. Left and right chambers were designated as social or non-social chambers alternately for each trial before the trial began. Video recordings of each trial were analyzed with TopScan software (Clever Systems) for the time the mouse spent in each chamber and the time spent directly sniffing the cylinders during each test phase.

Olfaction

Mice were tested for their ability to distinguish between neutral and social odors using a previously described protocol with modification (Yang and Crawley, 2009). Mice were placed

individually into a clean cage with bedding and presented with cotton-tipped wooden applicators dipped in water, almond extract, or bedding of an unfamiliar cage. Each stimulus scent was presented for 1 minute with a 1-minute inter-trial interval. Time spent sniffing was defined as time the animal spent oriented with its nose 2 cm or closer to the cotton tip with scent.

Buried food retrieval

Mice were tested for their ability to find a small piece of hidden food using a previously described protocol with modifications (Yang and Crawley, 2009). For two consecutive days before testing, single-housed mice were presented with a piece of novel palatable food (one piece of sweetened cereal). Mice that did not consume the cereal by the next day were excluded from the study. To test the mice, a piece of cereal was buried under clean bedding in a new cage in a randomly determined corner. Mice were placed in the new cage and the amount of time needed to find and begin eating the buried food was recorded.

Nesting

Nesting behavior was assessed using the scoring system previously described (Deacon, 2006). Mice were single housed with clean bedding and provided with a pressed square of cotton. Twenty-four hours later, nests were assigned a score of 0 (no nest building behavior observed) to 5 (cup shaped nest with high walls, all material used).

Barnes Maze

Mice were tested for spatial learning and memory using a Barnes maze (Sunyer et al., 2007) (San Diego Instruments), which consists of a white circular platform (36 inch diameter) with 20 holes (2 inch diameter) around the perimeter. An escape box was located under the target hole. Entry into off-target holes was blocked by a piece of black Plexiglas. The platform was 36 inches above the floor and four distinct visual cues were placed on the walls surrounding the platform. During each trial, the test mouse was allowed to explore the maze until the mouse found and

entered the escape box or for a maximum of 150 seconds. If the mouse did not enter the escape box at the completion of the trial, it was gently guided into the box by the experimenter and allowed to remain there for 1 minute before returning to its home cage. Mice were trained in one trial per day for four consecutive days. Trials were video recorded and analyzed with TopScan software (Clever Systems). Measures quantified included primary latency (time to initially reach the target hole) and total latency (time to enter escape box through target hole), and number of errors (visits to non-target holes).

Fear conditioning

On the training day, mice were placed in individual chambers (Med Associates) for two minutes followed by a loud tone (85 dB, 2 kHz) for 20 seconds, co-terminating with a two second, 0.75-mA foot shock. Mice were left undisturbed for two minutes, after which a second tone-shock pairing was delivered. Mice were returned to their home cage 90 seconds after the second shock. Twenty-four hours later, mice were tested for context-dependent memory by being placed into the same testing chambers without a tone or shock for 5 minutes. One hour later, mice were tested for cued memory by being placed into a novel chamber for two minutes and playing the same loud tone without shock for one minute. Freezing behavior, defined as no movement except for respiration, was analyzed with FreezeScan NI version 2.0.

Food Intake

Single-housed male mice were each given 150g of standard chow in their home cages. Mice had unrestricted access to food and water during testing. For two consecutive days, food was removed, weighed, and carefully replaced to habituate mice to this process. Measurements from the first two days were not included in the analysis. Food was removed, weighed, and replaced for five consecutive days following habituation and mice were weighed on the final testing day.

Quantitative reverse transcription PCR

Total RNA was isolated using Trizol reagent (Invitrogen) and treated with TURBO DNase (Ambion). cDNA was generated from 1 µg of total RNA by random hexamer priming using SuperScriptIII reverse transcriptase (Invitrogen). Quantitative PCR (qPCR) was performed on 10 ng of the resulting cDNA using SYBR Green detection (Applied Biosystems). All qPCR primer pairs are exon-spanning and listed in Table 2.2. *Gapdh* was used as an internal normalization control.

Table 2.2. Primers used for RT-qPCR.

Gene	Forward Primer	Reverse Primer
Agrp	5'-TAGATCCACAGAACCGCGAGT-3'	5'-GAAGCGGCAGTAGCACGTA-3'
Npy	5'-CTCCGCTCTGCGACACTAC-3'	5'-AGGGTCTTCAAGCCTTGTTCT-3'
Pomc	5'-CTGGAGACGCCCGTGTTTC-3'	5'-TGGACTCGGCTCTGGACTG-3'
Mbd2	5'- AACTGGAGGAGGCACTGATG-3'	5'- GGGGAAGGTCAGTCGAAAGT-3'
Mecp2	5'-CATACATAGGTCCCCGGTCA-3'	5'-CAGGCAAAGCAGAAACATCA-3'
Gapdh	5'-GATGCCCCCATGTTTGTGAT-3'	5'-GGTCATGAGCCCTTCCACAAT-3'

HPLC analysis of monoamine levels

Brain tissues were resected on ice, weighed, and immediately frozen in liquid nitrogen. Samples were sonicated on ice for 10 sec in homogenizing buffer containing 250nM 3,4-dihydroxybenzylamine as an internal standard, followed by centrifugation at 14,000 rpm at 0°C for 20 min. Levels of monoamines were determined using HPLC with standard methods as described previously (Howerton et al., 2014). The standard curve was from 0-10 pmol for each monoamine. Data acquisition and analysis was performed by blinded to genotype.

RNA-seq

Total RNA was isolated using Trizol reagent (Invitrogen) and treated with TURBO DNase (Ambion). 2µg of total RNA was used as input with the TruSeq Stranded mRNA Library Prep Kit (Illumina) according to the manufacturer's instructions. Samples were sequenced to an

approximate depth of 50 million reads per sample at 100 nucleotides using the HiSeq 2000 (Illumina). The raw FASTQ files of the RNA-seq were mapped using STAR program (Dobin et al., 2013) under the parameters of "--outFilterMultimapNmax 1 --outFilterMismatchNmax 3". Number of reads for each gene was counted using in house Perl programs. Differentially expressed genes were identified by edgeR (Robinson et al., 2010) with a false discovery rate (FDR) < 0.05.

Statistics

Statistical analysis was performed using Prism 6.0 (GraphPad Software). Individual statistical tests are stated in the figure legends.

RESULTS

Behavioral characterization of *Mbd2* null mice

Given that genetic studies of humans and mice have linked several MBD proteins to ASD and neurodevelopmental disorders, we hypothesized that MBD2 may also have a critical role in brain function and that loss of MBD2 would result in behavioral phenotypes similar to those observed in *Mecp2* or *Mbd1* null mice (Allan et al., 2008; Camarena et al., 2014, 5; Du et al., 2015; Guy et al., 2001). Although an *Mbd2* null mouse (*Mbd2*$^{-/-}$) has been generated, the only reported phenotype is a pup nurturing and retrieval deficit (Hendrich et al., 2001) and a full phenotypic characterization has not been reported. In this mouse, exon 2 of *Mbd2* is replaced with a promoterless 7kb β-*Geo LacZ* cassette, removing most of the conserved MBD (Hendrich et al., 2001). Small amounts of read-through transcript are present, but no full-length protein of either MBD2 isoform (MBD2a and MBD2b) is detectable, indicating this is a null allele (Hendrich et al., 2001). We focused our analysis on behavioral phenotypes that are affected in mouse models of ASDs, such as *Mecp2* or *Mbd1* null mice, and assessed motor function, anxiety-related behaviors, sociability, and learning and memory (Allan et al., 2008; Goffin et al., 2012; Pasciuto et al., 2015).

Changes in locomotor activity have been observed in *Mecp2* null mice (Goffin et al., 2012) so we quantified the locomotor activity of *Mbd2*$^{-/-}$ mice in a home-cage like environment. We found that *Mbd2*$^{-/-}$ mice show significantly reduced locomotor activity compared to wildtype (*Mbd2*$^{+/+}$) and heterozygous (*Mbd2*$^{+/-}$) littermates (Figure 2.1.A). We then asked if the observed hypoactivity could be attributed to motor impairments, as motor function is also affected in *Mecp2* null mice (Goffin et al., 2012). We tested motor coordination and learning in a rotarod task, in which mice were challenged to stay on an accelerating rod for 16 total trials over four days. All genotypes showed comparable improvement in this task over each trial and testing day, indicating that motor coordination and learning is not impaired in *Mbd2*$^{-/-}$ mice (Figure 2.1.B). Anxiety-related phenotypes are altered in both *Mecp2* and *Mbd1* null mice (Allan et al., 2008; Goffin et al., 2012). Therefore, we used a zero maze to assess anxiety, a task that takes advantage of a mouse's innate preference for enclosed spaces. Mice that spend increased time in the open arm of the maze are inferred to have decreased anxiety-related behavior (Crawley, 2007). We found *Mbd2*$^{-/-}$ mice displayed a preference for the closed arm that was equivalent to control littermates, indicating that anxiety-related behavior is not affected by the loss of MBD2 (Figure 2.1.C).

We next assessed whether *Mbd2*$^{-/-}$ mice exhibited several autistic-like phenotypes that have been shown to be affected in mice lacking MeCP2 or MBD1 (Allan et al., 2008; Goffin et al., 2012). Impaired social interaction is a common feature of ASDs and is recapitulated in numerous mouse models (Fairless et al., 2011; Pasciuto et al., 2015). Mice are inherently social animals and most mice prefer to interact with other mice (Fairless et al., 2011). We tested sociability of *Mbd2*$^{-/-}$ mice using the social approach test in a three-chambered apparatus (Figure 2.1.D). This assay tests the preference of the test mouse to interact with a novel social stimulus (unfamiliar mouse) or novel object. In the first habituation phase of the test, *Mbd2*$^{+/+}$, *Mbd2*$^{+/-}$ and *Mbd2*$^{-/-}$ mice showed no significant difference in time spent sniffing two empty cylinders. At the start of the second phase of the test, a novel stimulus mouse and novel object were introduced to the cylinders. We found no significant difference between *Mbd2*$^{+/+}$, *Mbd2*$^{+/-}$, and *Mbd2*$^{-/-}$ littermates in

the amount of time spent sniffing the social stimulus mouse, suggesting sociability is not affected by the loss of MBD2.

Detection of olfactory cues is essential for many murine behaviors including social interactions. MBD2 and MeCP2 deficient mice have impairments in differentiation or proliferation of olfactory receptor neurons, but it is unknown if olfaction is affected (Macdonald et al., 2010). Impairment in olfactory ability may affect outcomes in the sociability assay and other behavior tests. Therefore, we evaluated olfaction by testing whether *Mbd2*$^{-/-}$ mice can distinguish between scent cues in a swab-sniff test (Figure 2.1.E). We found that all genotypes spent more time sniffing a social scent versus neutral water or almond scents as expected, indicating these mice have the olfactory ability to distinguish between scents. However, *Mbd2*$^{-/-}$ mice spent significantly less time sniffing a social scent than wildtype littermates. This result may be due to decreased home-cage activity (Figure 2.1.A) because there is a trend for *Mbd2*$^{-/-}$ mice to spend less time sniffing the neutral scent swabs as well. Alternatively, this result may indicate olfactory impairment. To distinguish between these possibilities, we performed a secondary olfaction test in which we quantified the time needed for mice to find and retrieve a buried piece of food in a clean home cage (Figure 2.1.F). *Mbd2*$^{-/-}$ mice found and retrieved the hidden food as quickly as littermates, indicating these mice can detect and respond to olfactory cues similarly to littermates.

We next assayed nest building as test that is commonly used to assess home cage behaviors. Nesting is a spontaneous, complex behavior and is considered to be an indicator of home-cage social behavior and general welfare in mice (Deacon, 2006). Nesting is affected by neurological and as well as external factors affecting behavior. Several mouse models of ASD and neurodegenerative disease and mice experiencing social defeat have impaired nesting activity (Jirkof, 2014; Otabi et al., 2015; Pasciuto et al., 2015). We found that *Mbd2*$^{-/-}$ mice show impaired nest building activity in contrast to wildtype and heterozygous littermates (Figure 2.1.G). Together with the reduced home-cage locomotor activity (Figure 2.1.A), these findings indicate that *Mbd2*$^{-/-}$ mice have altered home-cage behaviors but the exact etiologies of these changes in behavior are difficult to determine.

Deficits in learning and memory have been found in numerous mouse models of ASDs and have also been observed in mice lacking MeCP2 or MBD1 (Allan et al., 2008; Goffin et al., 2012; Pasciuto et al., 2015). To determine if *Mbd2*$^{-/-}$ mice have a similar phenotype, we tested spatial learning and memory using the Barnes maze paradigm over four consecutive training days. *Mbd2*$^{-/-}$ mice showed a slight but significant increase in the time needed to initially reach the target hole on the second training day (primary latency, Figure 2.1.H), but equal time to enter the target hole and complete the trial on all testing days (total latency, Figure 2.1.I) compared to wildtype and heterozygous littermates. The increase in primary latency time on the second training day is unlikely to reflect significant changes in learning and memory because *Mbd2*$^{-/-}$ mice are comparable to control littermates on all other measures in this assay, including the number of errors made on all days (total number of visits to non-target holes, Figure 2.1.J).

As the Barnes maze paradigm primarily tests hippocampal-dependent spatial memory, we also sought to determine if other aspects of learning and memory are affected in *Mbd2*$^{-/-}$ mice. The fear conditioning test assesses amygdala-dependent cued memory in addition to amygdala- and hippocampus-dependent contextual memory (Crawley, 2007). During training, there were no significant differences between genotypes in freezing behavior before or after the foot shock (Figure 2.1.K). On the testing day, *Mbd2*$^{-/-}$ mice showed significantly less cue-dependent freezing behavior than wildtype and heterozygous littermates, but equivalent context-dependent freezing behavior. Although these findings may be indicative of a mild learning and memory phenotype, the altered home-cage activity levels (Figure 2.1.A) may confound the results obtained here. Furthermore, the absence of a significant phenotype in the Barnes maze analysis (Figure 2.1.H-J) support that these findings may be attributed to differences in activity rather than learning and memory phenotypes.

In summary, we found that *Mbd2*$^{-/-}$ mice are equivalent to wildtype and heterozygous littermates on most measures tested, with the notable exception of homecage locomotor activity and nest building. These results are in contrast to mice lacking MeCP2 or MBD1, which show significant alterations in locomotor activity, sociability, anxiety-related behaviors and deficits in

learning and memory (Allan et al., 2008; Goffin et al., 2012). Therefore we conclude that unlike most MBD proteins, MBD2 does not have a major impact on brain functions that underlie many key behavioral phenotypes relevant to ASD.

Mbd2$^{-/-}$ mice have reduced body weight and decreased food intake associated with altered hypothalamic neuropeptide expression

Although *Mbd2*$^{-/-}$ mice are viable and fertile as previously reported (Hendrich et al., 2001), we noticed that these mice have reduced reproductive ability. We also weighed *Mbd2*$^{+/+}$, *Mbd2*$^{+/-}$, and *Mbd2*$^{-/-}$ male and female littermates and found that *Mbd2*$^{-/-}$ males and females have subtle but significantly lower body weights beginning at 4 and 6 weeks of age, respectively (Figure 2.2.A,B). Loss of MeCP2 and MBD1 both affect brain weight, as well (Goffin et al., 2012; Zhao et al., 2003). Therefore, we tested if brain weight is affected in *Mbd2*$^{-/-}$ mice and compared these values to total body weight. We observed that *Mbd2*$^{-/-}$ male mice have slightly but significantly decreased brain weight, but have increased brain weight as a percentage of body weight compared to littermates (Figure 2.2.C,D). This finding suggests that the low brain weight of *Mbd2*$^{-/-}$ mice is likely due to loss of overall body mass.

To further explore the low body weight observed in *Mbd2*$^{-/-}$ mice, we next measured daily food intake for each genotype. We found that male *Mbd2*$^{-/-}$ mice consume less food per day compared to wildtype and heterozygous littermates (Figure 2.2.E). However, when food consumption is normalized to body weight, *Mbd2*$^{-/-}$ mice consume comparable amounts of food for their body size as littermates (Figure 2.2.F). These findings are in contrast to mice with *Mecp2* mutations, which show increasing phenotypic severity with age in addition to significantly reduced body and brain weight (Goffin et al., 2012).

We then asked if the low body weight observed in *Mbd2*$^{-/-}$ mice has a neuronal origin. Neuronal systems sense levels of circulating hormones such as leptin and insulin and nutrient signals in order to regulate body energy stores and feeding activity (Schwartz, 2005). The arcuate nucleus of the hypothalamus contains several populations of neurons including the orexigenic

agouti-related peptide (AgRP)–neuropeptide Y (NPY) neurons that stimulate food intake and reduce energy expenditure and the anorxegenic proopiomelanocortin (POMC) neurons that reduce appetite and stimulate energy expenditure. Lower levels of body fat and caloric intake are associated with reduced levels of leptin, which in turn increases expression of *Agrp* and *Npy* and downregulates expression of *Pomc* (Yi and Tschop, 2012) (Figure 2.3.A). Changes in expression of these peptides are therefore indicative of hypothalamic sensing of an energy imbalance. However, this does not reveal the etiology of the imbalance, which may be affected by neuronal factors such as reduced dopamine signaling (Yang et al., 2014a) or extrinsic factors such as a high fat diet (Schwartz, 2005).

We examined the expression levels of the orexigenic peptides *Agrp* and *Npy* and anorexigenic peptide *Pomc* and in the hypothalamus of three-month old wildtype and *Mbd2*$^{-/-}$ mice using RT-qPCR (Figure 2.3.B). As a control, we also determined that *Mbd2* expression is significantly reduced and *Mecp2* expression is unchanged in *Mbd2*$^{-/-}$ mice, as expected. In *Mbd2*$^{-/-}$ mice, *Pomc* is significantly downregulated, which indicates hypothalamic sensing of a energy or nutrient deficit. Unexpectedly, *Agrp* and *Npy* expression show no statistically significant differences between wildtype and *Mbd2*$^{-/-}$ mice and in fact show a trend towards down regulation. Together, these results signify that *Mbd2*$^{-/-}$ mice are sensing a nutrient deficit but are not motivated neurochemically to increase their food consumption.

Mbd2$^{-/-}$ mice have equivalent biogenic amine content and few differentially expressed genes in the striatum compared to wildtype littermates

Although *Mbd2*$^{-/-}$ mice are comparable to control littermates on most measures, we next sought to determine if the observed changes in locomotor activity, body weight, and impaired nesting behavior are linked to any alterations in biogenic amine levels. Genetic or pharmacological disruption of biogenic amine levels, particularly striatal dopamine, is associated with many of these phenotypes, including low body weight, hypophagia, hypoactivity, and impairments in nesting and pup nurturing (Henschen et al., 2013; Palmiter, 2008; Yang et al.,

2014a). We performed HPLC analysis to measure the abundance of essential monoamines and their metabolites in the cortex and striatum of wildtype and *Mbd2*$^{-/-}$ littermates (Figure 2.4.A,B). These include norepinephrine (NE), dopamine (DA) and its metabolites 3,4-dihydroxyphenylacetic acid (DOPAC) and homovanillic acid (HVA), serotonin (5-HT) and its metabolite 5-hydroxyindoleacetic acid (5-HIAA). We found that none of the measured biogenic amine levels in the cortex and striatum are altered in *Mbd2*$^{-/-}$ mice compared to wildtype littermates. Therefore, the loss of MBD2 is unlikely to affect monoamine signaling in the brain, in contrast to the essential role of MeCP2 in regulating these systems (Panayotis et al., 2011).

In addition to examining biogenic amines particularly in the striatum, we also sought to determine if loss of MBD2 is associated with significant changes in gene expression in the brain. We assessed differentially expressed genes (DEGs) in the striatum of adult wildtype and *Mbd2*$^{-/-}$ littermates, as disruption to striatal signaling and particularly dopamine is associated with many of the phenotypes observed in *Mbd2*$^{-/-}$ mice (Henschen et al., 2013; Palmiter, 2008; Yang et al., 2014a). We performed poly-A selected mRNA-seq and first analyzed the total number of reads and mapped reads (Table 2.3). As an additional experimental verification, we determined that there are no reads mapped to exon 2 of *Mbd2* in *Mbd2*$^{-/-}$ mice, as this exon is deleted (Hendrich et al., 2001) (Figure 2.5).

We found a total of 38 DEGs using an FDR value of <0.05, including 21 genes upregulated and 17, including *Mbd2*, downregulated. Of these DEGs, 18 genes showed greater than 2-fold change in expression comparing wildtype to *Mbd2*$^{-/-}$ mice (Figure 2.6). The DEGs have diverse functions with no significant enrichment for any gene ontology terms (data not shown, Figure 2.7). Although several genes have been linked to ASDs, it is not clear if MBD2 is directly regulating expression of these genes or if the DEGs are secondary effects of MBD2 function in other cell types or systems. In either scenario, further work is required to determine the biological implications of altered expression of these genes and whether they contribute to the phenotypes observed in *Mbd2*$^{-/-}$ mice.

Table 2.3. Total and uniquely mapped reads from wildtype and *Mbd2*$^{-/-}$ poly-A selected RNA-seq in the striatum.

Sample	Total Reads	Uniquely Mapped Reads
Wildtype Replicate 1	57,648,692	49,232,956 (85.40%)
Wildtype Replicate 2	51,110,555	43,509,724 (85.13%)
Mbd2$^{-/-}$ Replicate 1	66,516,889	56,179,825 (84.46%)
Mbd2$^{-/-}$ Replicate 2	44,545,090	37,886,828 (85.05%)

DISCUSSION

In this study, we show that loss of MBD2, relative to MeCP2 and MBD1, surprisingly has only a minor impact on brain function. We present the first behavioral characterization of *Mbd2*$^{-/-}$ mice, with emphasis on phenotypes affected by loss of related proteins MeCP2 or MBD1 (Allan et al., 2008; Goffin et al., 2012). In addition to behavior, we also assessed whether loss of MBD2 affects hypothalamic and striatal gene expression and biogenic amine levels in the striatum.

Unexpectedly, we found that loss of MBD2 results in few subtle behavioral phenotypes. Most behavioral measures were generally unaffected in *Mbd2*$^{-/-}$ mice compared to wildtype and heterozygous littermates, including motor coordination and learning, anxiety-related behaviors, sociability, olfaction, and spatial and contextual learning and memory (Figure 2.1). In contrast, mice with loss of MeCP2 or MBD1 show significant deficits on the majority of these measures (Allan et al., 2008; Goffin et al., 2012). We found that *Mbd2*$^{-/-}$ mice are hypoactive in a home-cage environment (Figure 2.1.A) and show significant differences to littermates in measures of nest building and olfaction (Figure 2.1.E,G). Specifically, we observed that *Mbd2*$^{-/-}$ mice spend significantly less time engaged in sniffing behavior of a social scent during a test of olfactory discrimination (Figure 2.1.E). Finally, *Mbd2*$^{-/-}$ mice show reduced cue-dependent freezing behavior in a fear conditioning assay (Figure 2.1.K).

Despite finding statistically significant differences between *Mbd2*$^{-/-}$ mice and control littermates on several tests, the results of all tests as a whole must be considered before

interpreting results of individual tests as discrete behavioral phenotypes. Most importantly, the hypoactivity phenotype (Figure 2.1.A) complicates the interpretation of several tests that depend on activity levels, in particular nesting, the swab sniff olfaction test, and fear conditioning. Phenotypes such as hypoactivity, nesting, and low body weight are multigenic and complex in nature and therefore it is challenging to determine the precise etiologies of these phenotypes (Gaskill et al., 2013; Reed et al., 2008; Tou and Wade, 2002). Furthermore, low body weight (Figure 2.2.A,B) is inexorably linked to activity levels, and therefore must also be considered in interpretation of these phenotypes (Tou and Wade, 2002).

Changes in body weight have been observed in over 30% of viable, single-gene null mice, which illustrates the sensitivity of this phenotype to genetic perturbations in multiple cellular processes (Reed et al., 2008). While hypoactivity has been observed in several mouse models of ASD including *Mecp2* null mice, in these mice hypoactivity is accompanied by significant deficits in other behavioral measures such as learning and memory deficits or seizures, supporting a neuronal etiology (Goffin et al., 2012; Pasciuto et al., 2015). The origins of changes in nesting behavior are similarly challenging to classify in this scenario. Nesting can be affected by a range of experimental factors, such as genetic models of neurodegenerative disease, pharmacological treatments, or external factors such as stress arising from social defeat (Jirkof, 2014; Otabi et al., 2015; Pasciuto et al., 2015). Therefore, we conclude that the nesting deficits observed in *Mbd2*$^{-/-}$ mice are likely related to the overall reduced home cage activity levels (Figure 2.1.A), but we cannot precisely determine the cause of impaired nesting in *Mbd2*$^{-/-}$ mice without further additional experiments.

We found that *Mbd2*$^{-/-}$ mice spend significantly less time sniffing a social scent during a test of olfaction than control littermates (Figure 2.1.E). However, we expect that this finding does not indicate that olfactory ability is impaired in *Mbd2*$^{-/-}$ mice to the extent that it would affect behaviors for the following reasons. First, *Mbd2*$^{-/-}$ mice show a trend of spending less time sniffing overall during the water and almond phases of this test, indicating that the decreased sniffing of the social scent may be more indicative of lower overall home cage activity levels (Figure 2.1.A)

rather than a true olfactory deficit. This conjecture is supported by our findings that there is no significant difference between genotypes in time spent sniffing a cylinder containing a novel stimulus animal in a sociability assay (Figure 2.1.D) or the buried food retrieval assay, an independent olfaction test (Figure 2.1.F).

Similarly, we found subtle changes between *Mbd2*$^{-/-}$ mice and control littermates in the Barnes maze assay and cued fear conditioning (Figure 2.1.H-K), but we hypothesize that these results may be linked to reduced overall activity levels rather than representing specific deficits in learning and memory. In the Barnes maze assay, if spatial memory were directly affected in *Mbd2*$^{-/-}$ mice, we would expect to see increased primary and total latency on additional training days (Figure 2.1.H,I) or increased errors (Figure 2.1.J). However, *Mbd2*$^{-/-}$ mice are equivalent to control littermates on all measures with the exception of primary latency on the second training day (Figure 2.1.H), indicating that spatial memory is likely unaffected. In a fear-conditioning assay, we found that *Mbd2*$^{-/-}$ mice show significantly more time freezing in response to cue, but not a context, associated with an aversive foot shock (Figure 2.1.K). The results on this assay are difficult to interpret because *Mbd2*$^{-/-}$ mice show a trend of reduced freezing behavior during the training phase after the foot shock, although this difference is not statistically significant. The readout for this assay, freezing behavior, is also activity-dependent and the overall decreased activity levels in *Mbd2*$^{-/-}$ mice may confound the results. Therefore, this assay must be repeated to ensure that *Mbd2*$^{-/-}$ mice have an equivalent pain threshold and freezing response to control littermates.

In summary, *Mbd2*$^{-/-}$ mice show subtle phenotypes on several measures but several of these results may be indicative of overall reduced activity levels rather than additional, specific phenotypes related to brain function. The phenotypes that are clearly affected, including home-cage activity, nesting and body weight, are complex and multigenic in nature and may have non-neuronal etiologies. Therefore, in the absence of additional changes in behavior, striatal gene expression changes, or biogenic amine levels, we expect that the observed subtle behavioral

phenotypes are likely not neuronal in origin. We conclude that, unlike most MBD proteins, MBD2 is largely not required for brain functions that affect behavioral outcomes examined here.

We also found that loss of MBD2 results in subtle, but significantly decreased body weight (Figure 2.2A,B). Although *Mbd2*$^{-/-}$ mice eat less food per day, they consume equivalent food normalized to body weight as wildtype littermates (Figure 2.2.E,F). These findings support the conclusion that low body weight is established early in *Mbd2*$^{-/-}$ mice after weaning, after which *Mbd2*$^{-/-}$ mice stabilize and continue to eat a sufficient amount of calories to maintain their body weight at steady state (Figure 2.2.A,B). Although *Mbd2*$^{-/-}$ mice maintain their body weights, they do show altered expression levels of the hypothalamic peptide *Pomc* (Figure 2.3.B). Reduced *Pomc* expression is generally caused by reduced levels of serum leptin associated with reduced adipose tissue. Downregulation of *Pomc* expression is usually accompanied by increased expression of the orexigenic peptides *Npy* and *Agrp*, which together stimulate increased food intake and reduced energy expenditure (Myers et al., 2008). Paradoxically, Mbd2$^{-/-}$ mice show a trend, although not statistically significant, for downregulation of hypothalamic *Agrp* and *Npy* (Figure 2.3.B). This finding may indicate that loss of MBD2 is directly affecting hypothalamic gene expression. Alternatively, energy homeostasis pathways may be affected in *Mbd2*$^{-/-}$ mice at one or multiple different areas, including the liver or levels of circulating hormones, for example. Due to the absence of significant behavioral phenotypes, striatal gene expression changes, or biogenic amine levels in *Mbd2*$^{-/-}$ mice, we hypothesize that the reduced *Pomc* expression is likely due to changes in peripheral tissues and pathways and does not reflect a specific hypothalamic function for MBD2.

To determine if loss of MBD2 affects brain function at the molecular or cellular level, we assessed biogenic amine levels in the striatum and cortex and also looked for gene expression changes in the striatum. We choose to examine the striatum because genetic or pharmacological disruptions to this system, and particularly striatal dopamine signaling, produce phenotypes similar to those seen in *Mbd2*$^{-/-}$ mice, including hypoactivity, low body weight, hypophagia, and altered nurturing behavior (Bromberg-Martin et al., 2010; Henschen et al., 2013; Palmiter, 2008).

We did not find any significant alterations in the levels of biogenic amines and their metabolites in the striatum or cortex of *Mbd2*$^{-/-}$ mice, unlike what has been observed in *Mecp2* or *Mbd1* null mice (Figure 2.4.A,B) (Allan et al., 2008; Panayotis et al., 2011). These results indicate that the phenotypes of *Mbd2*$^{-/-}$ mice are likely not related to changes in biogenic amine signaling pathways such as striatal dopamine, and instead may have more complex or non-neuronal origins.

In addition to assessing levels of biogenic amines in the striatum, we also sought to determine if gene expression is altered in the striatum upon loss of MBD2. The striatal DEGs in *Mbd2*$^{-/-}$ mice have diverse functions (Figure 2.7). Several of the DEGs have been linked to brain-specific functions related to ASD. Mutations in *Grin2b,* an NMDA receptor subunit, are associated with intellectual disability, ASD and seizures (Endele et al., 2010). Engrailed homeobox factor 2 (*En2*) is upregulated during CNS development and is also linked to neurological phenotypes in mouse models and human patients (Benayed et al., 2005; Cheh et al., 2006). Several DEGs point to increased inflammatory stress in *Mbd2*$^{-/-}$ mice. For example, lipocalin2 (*Lcn2*) is upregulated in the prefrontal cortex and hippocampus in response to stress or neural injury such as stroke and elevated transthyretin (*Ttr*), the primary transporter of thyroid hormone and retinol in the cerebral spinal fluid, is used clinically as a marker of inflammatory stress (Buxbaum and Reixach, 2009; Lee et al., 2009). While these findings indicate directions for future investigations, it is unclear if expression levels of the DEGs are directly affected by MBD2-mediated transcriptional mechanisms or if these are secondary effects of loss of MBD2 in other cell types or systems. Due to the absence of notable behavioral phenotypes and unchanged biogenic amine levels in the striatum of *Mbd2*$^{-/-}$ mice, the DEGs observed are likely to be secondary effects of loss of MBD2 rather than an indication of brain-specific MBD2 functions.

Although these phenotypes of *Mbd2*$^{-/-}$ mice are complex, additional experiments would clarify these findings. First, despite the absence of robust behavioral phenotypes, a subtler neuronal cellular phenotype may be present in *Mbd2*$^{-/-}$ mice. One study found that olfactory receptor neurons in *Mbd2*$^{-/-}$ mice show enhanced proliferation but reduced lifespan and differentiation capability (Macdonald et al., 2010). However, it is unclear how or if this cellular

phenotype may affect olfactory function as we did not detect a notable difference in odor-induced behaviors in these mice on several independent tests (Figure 2.1.D-F). It is therefore possible that additional cellular phenotypes may be present without significantly affecting the behaviors examined in this study in adult mice.

Because *Mbd2*$^{-/-}$ mice have significantly decreased home-cage activity and reduced body weight (Figure 2.1.A, Figure 2.2.A,B), these phenotypes may confound the interpretation of several other behavior tests performed in this study that rely on mobility and activity. Therefore, to better understand the phenotype of *Mbd2*$^{-/-}$ mice it would be beneficial to perform additional tests that do not directly or indirectly measure activity levels as an output. For example, prepulse inhibition can be used to assess deficits in sensorimotor gating and is affected by loss of MBD1 in mice (Allan et al., 2008). Alternatively, the Y-maze spontaneous alteration test assesses spatial cognition but does not depend on the subject mouse's speed to reach a target, as does the Barnes maze (Crawley, 2007).

Another approach to study the effects of loss of MBD2 would be to perform the tests described here on mice with conditional loss or rescue of MBD2. It is likely that several of the phenotypes of *Mbd2*$^{-/-}$ mice such as low body weight and hypoactivity are interrelated and may even have a synergistic effect. By genetically isolating MBD2 functions to a specific cell type or tissue, it may be possible to determine which phenotypes are direct consequences of loss of MBD2 and which may be secondary effects. For example, an *Mbd2* conditional null and/or rescue mouse would be beneficial to study the low body weight phenotype of *Mbd2*$^{-/-}$ mice. If a brain-specific *Mbd2* null mouse also had low body weight, this would be strong evidence that this phenotype is neuronal in origin and may be primarily attributed to misregulation in the hypothalamus, for example. Alternatively, this phenotype could be due to a gastrointestinal-related MBD2 function that could be explored through an intestine epithelial cell-specific loss of MBD2.

In summary, we found that loss of MBD2 results in subtle phenotypes including low body weight, hypoactivity, and deficits in nesting behavior. We also determined that loss of MBD2

reduces expression of the anorexigenic hypothalamic peptide *Pomc* and affects expression of a limited number of genes in the striatum. However, additional experiments are required to assess if expression of these differentially expressed genes is directly regulated by MBD2-dependent mechanisms, or if these findings represent secondary effects of loss of MBD2. The limited number of genes affected and the equivalent levels of biogenic amines in the brain of *Mbd2*$^{-/-}$ mice support the hypothesis that these are likely to be indirect effects. We conclude that, in contrast to MeCP2 or MBD1, MBD2 is generally not required for the behavioral outcomes and brain functions examined in this study.

CHAPTER 2 FIGURES

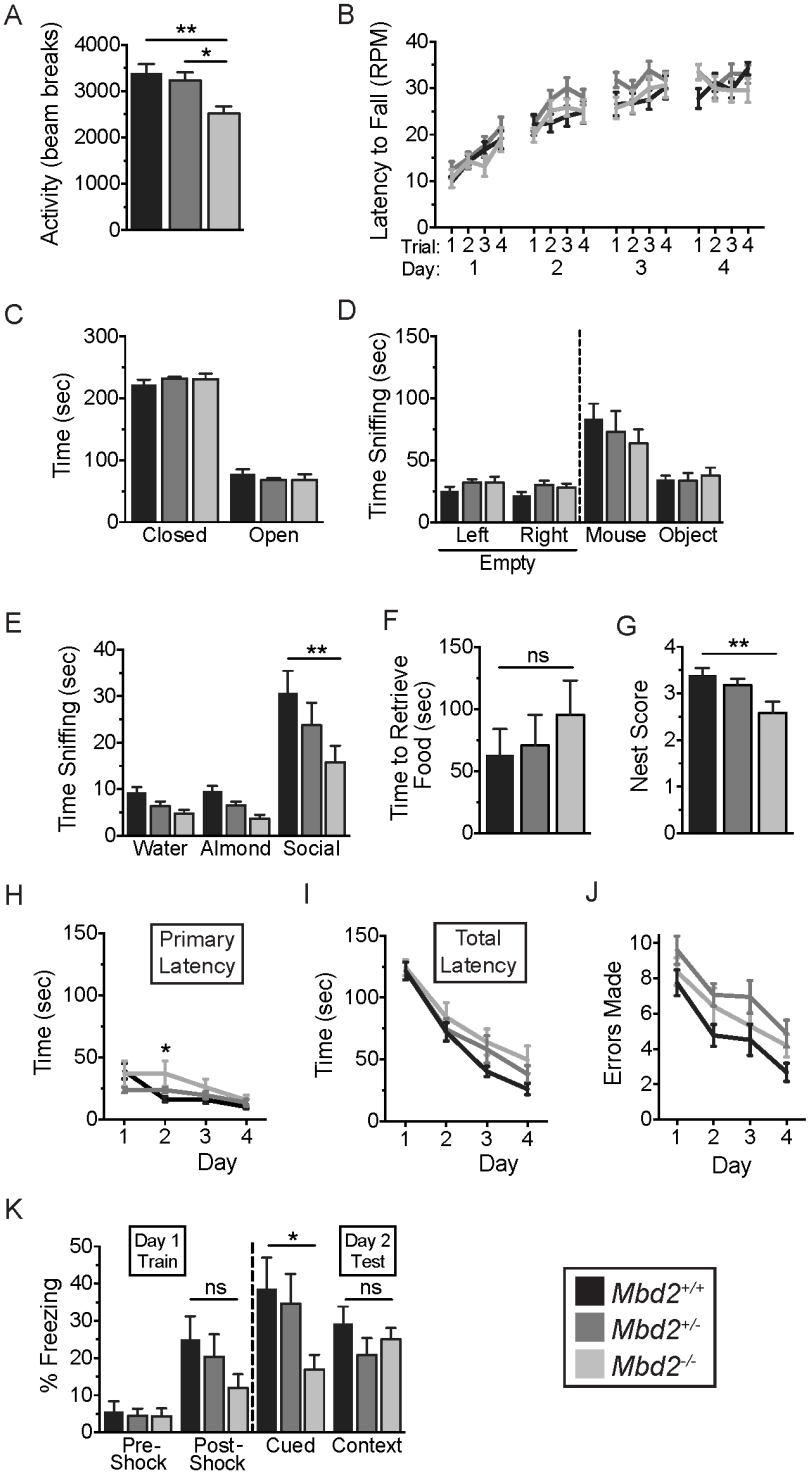

Figure 2.1. Behavioral characterization of *Mbd2*$^{-/-}$ mice compared to wildtype and heterozygous littermates.

Figure 2.1 Behavioral characterization of *Mbd2*$^{-/-}$ mice compared to wildtype and heterozygous littermates.

(A) *Mbd2*$^{-/-}$ mice are hypoactive as measured by the number of infrared beam breaks in a home-cage like environment over sixty minutes (n = 14 per genotype, $^{**}P < 0.01$, $^{*}P < 0.05$, one-way ANOVA with Tukey's test). **(B)** *Mbd2*$^{-/-}$ mice perform similarly to littermates in the rotarod task indicating unaffected motor coordination or learning (n = 14 per genotype, two-way ANOVA). **(C)** *Mbd2*$^{-/-}$ mice have unaltered anxiety-related behavior in a zero maze assay (n = 14 per genotype, one-way ANOVA of time in open arm). **(D)** Sociability of *Mbd2*$^{-/-}$ mice was assessed in the social approach test in a three-chambered apparatus. All genotypes show equal preference between two empty cylinders (left and right) during the habituation phase. All genotypes show equivalent increased preference for a social stimulus (mouse) versus a non-social stimulus (object) (*Mbd2*$^{+/+}$ and *Mbd2*$^{+/-}$ n = 13, *Mbd2*$^{-/-}$ n = 14, two-way ANOVA). **(E)** The ability to distinguish between neutral (water and almond) and social scents was determined by assessing time spent sniffing a swab with each scent. All genotypes have increased interaction (sniffing) with a social scent compared to neutral scents, but *Mbd2*$^{-/-}$ show significantly less time sniffing a social scent (n = 12 per genotype, $P < 0.0001$ effect of scent, $P < 0.001$ effect of genotype, $^{**}P < 0.01$, two-way ANOVA with Tukey's test). **(F)** *Mbd2*$^{-/-}$ mice take equivalent time to littermates to find and retrieve a buried piece of food in a home-cage like environment (*Mbd2*$^{+/+}$ and *Mbd2*$^{-/-}$ n = 13, *Mbd2*$^{+/-}$ n = 11, ns not significant, one-way ANOVA). **(G)** Mbd2$^{-/-}$ mice have significantly impaired nest-building behavior (*Mbd2*$^{+/+}$ n = 22, *Mbd2*$^{+/-}$ n = 19, *Mbd2*$^{-/-}$ n = 18, $^{**}P < 0.01$, one-way ANOVA with Tukey's test). **(H-J)** Spatial learning and memory were assessed using a Barnes maze paradigm. *Mbd2*$^{-/-}$ mice show a slight but significant delay to initially reach a target escape hole on the second training day (primary latency, **H**), but equivalent time to enter the escape hole (total latency, **I**) during four days of training. *Mbd2*$^{-/-}$ mice made comparable numbers of errors to control littermates (visits to non-target hole, **J**) during all training days (*Mbd2*$^{+/+}$ n = 22, *Mbd2*$^{+/-}$ n = 19, *Mbd2*$^{-/-}$ n = 18, $^{*}P$ <0.05, two-way ANOVA with Tukey's test). **(K)** In a fear conditioning learning and memory assay, all genotypes responded with equivalent freezing behavior to a paired tone-footshock. *Mbd2*$^{-/-}$ mice showed significantly less freezing behavior in response to a cued stimulus, but equivalent freezing behavior to a contextual stimulus compared to control littermates (*Mbd2*$^{+/+}$ and *Mbd2*$^{-/-}$ n = 14, *Mbd2*$^{+/-}$ n = 12, $^{*}P$ <0.05, two-way ANOVA with Tukey's test). All data are presented as mean ±SEM.

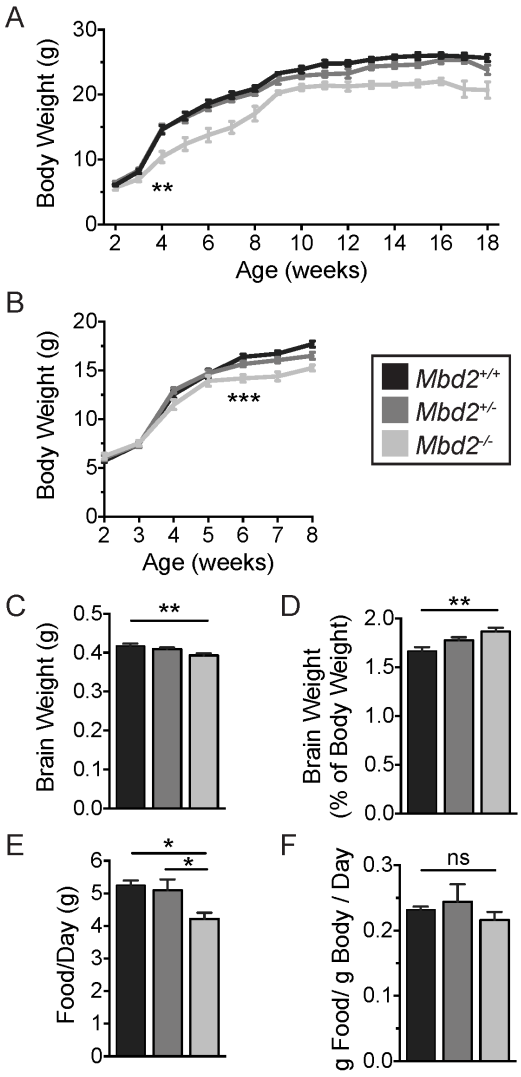

Figure 2.2. *Mbd2*$^{-/-}$ mice show decreased body and brain weight associated with reduced food intake.

(A) Male *Mbd2*$^{-/-}$ mice have decreased body weight compared to *Mbd2*$^{+/+}$ and *Mbd2*$^{+/-}$ littermates (n = 10 per genotype, $P < 0.01$, interaction, two-way ANOVA). *Mbd2*$^{-/-}$ weight was significantly decreased at 4 weeks continuing to 18 weeks postnatal (**$P < 0.01$, two-way ANOVA with Tukey's test). **(B)** Female *Mbd2*$^{-/-}$ mice have decreased body weight (n = 10 per genotype, $P <$ 0.001, interaction, two-way ANOVA). *Mbd2*$^{-/-}$ weight was significantly decreased at 6 weeks continuing to 8 weeks postnatal (***$P < 0.001$, two-way ANOVA with Tukey's test). **(C)** 13-week old male *Mbd2*$^{-/-}$ mice have significantly decreased brain weight (*Mbd2*$^{+/+}$ and *Mbd2*$^{+/-}$ n = 11, *Mbd2*$^{-/-}$ n = 12, **$P < 0.01$, one-way ANOVA with Tukey's test). **(D)** 13-week old male *Mbd2*$^{-/-}$ mice have significantly increased brain weight as a percentage of body weight (*Mbd2*$^{+/+}$ and *Mbd2*$^{+/-}$ n = 11, *Mbd2*$^{-/-}$ n = 12, **$P < 0.01$, one-way ANOVA with Tukey's test)**. (E)** 8 week old male *Mbd2*$^{-/-}$ mice consume significantly less food per day on an unrestricted diet of standard chow, but **(F)** consume equivalent food normalized to body weight (*Mbd2*$^{+/+}$ and *Mbd2*$^{+/-}$, n = 5, *Mbd2*$^{-/-}$ n = 8, * P <0.05, ns not significant, one-way ANOVA with Tukey's test). All data are presented as mean ±SEM.

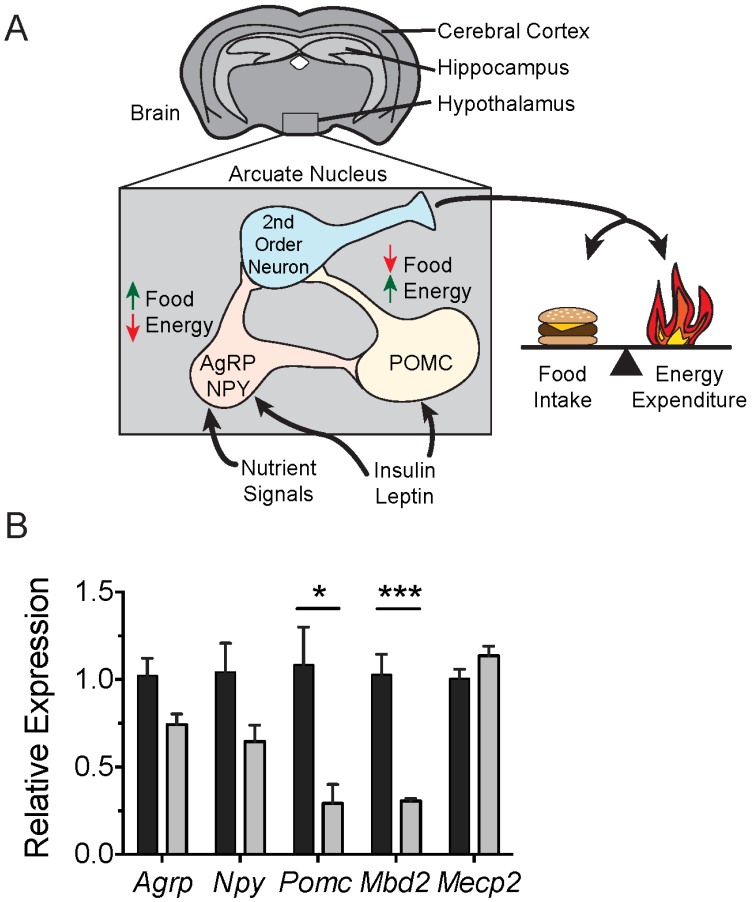

Figure 2.3. Hypothalamic neuropeptide expression in *Mbd2*$^{-/-}$ mice.
(A) Simplified diagram of the orexigenic AgRP-NPY and anorexigenic POMC neurons in the arcuate nucleus of the hypothalamus, which contribute to the regulation of food intake and energy expenditure. **(B)** The relative expression levels of *Agrp* and *Npy* in the hypothalamus are equivalent between wildtype and *Mbd2*$^{-/-}$ mice, but *Pomc* is significantly downregulated. *Mbd2* is significantly downregulated and *Mecp2* expression is unaffected in *Mbd2*$^{-/-}$ mice, as expected (*Mbd2*$^{+/+}$ and *Mbd2*$^{-/-}$ n = 5, unpaired two-tailed t test with Holm-Sidak multiple comparison correction). All data are presented as mean ±SEM.

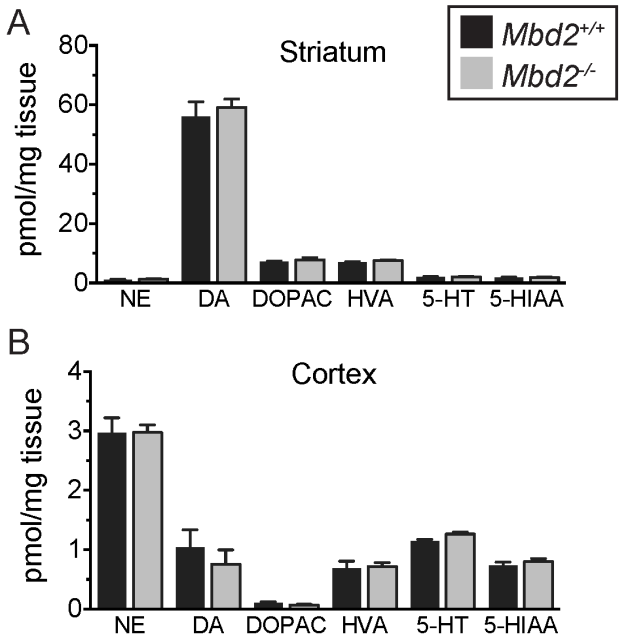

Figure 2.4. *Mbd2*$^{-/-}$ mice have equivalent biogenic amine content to wildtype littermates. HPLC analysis showed equivalent levels of biogenic amines and their metabolites in the cortex **(A)** and striatum **(B)** between 12 week old male *Mbd2*$^{+/+}$ and *Mbd2*$^{-/-}$ mice (*Mbd2*$^{+/+}$ *n* = 6, *Mbd2*$^{-/-}$ *n* = 8, unpaired two-tailed *t* test with Holm-Sidak multiple comparison correction). All data are presented as mean ±SEM.

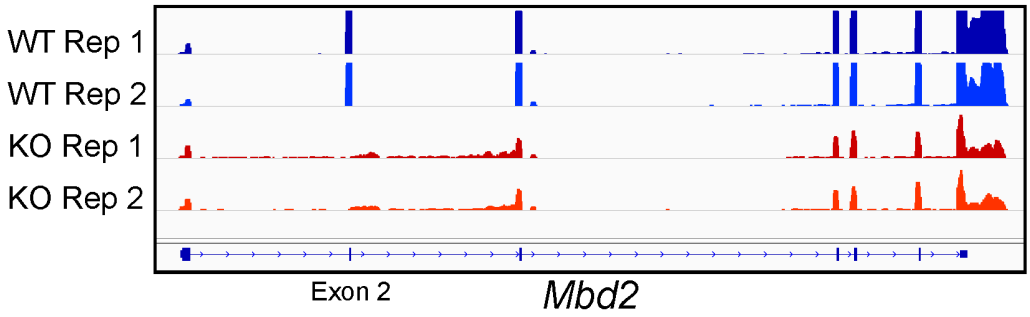

Figure 2.5. RNA-seq from the striatum of *Mbd2*$^{-/-}$ mice confirms loss of *Mbd2* exon 2 and expression of full-length transcript.
RNA-seq tracks from two wildtype replicates (blue) and two *Mbd2*$^{-/-}$ (KO) replicates shows a loss of reads corresponding to exon 2, which is deleted in *Mbd2*$^{-/-}$ mice. Small amounts of read-through transcript are detectable in the KO samples, as reported (Hendrich et al., 2001).

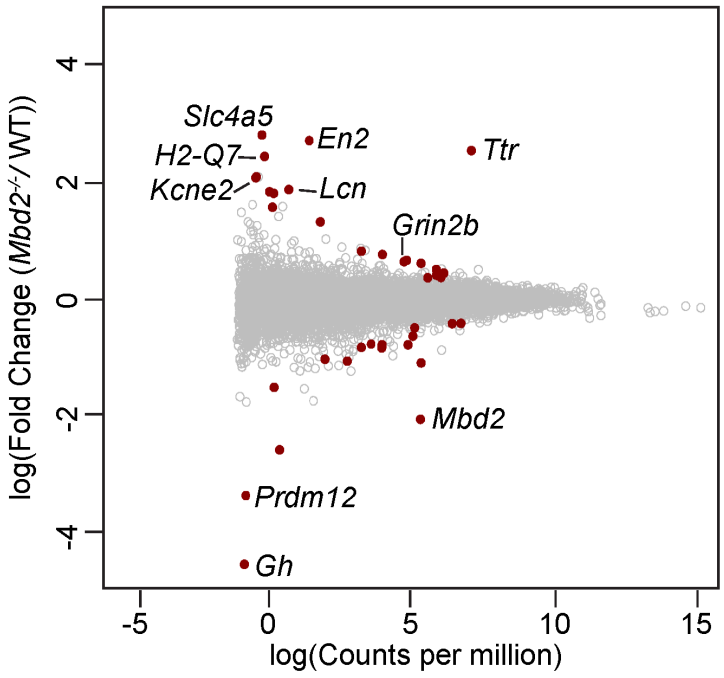

Figure 2.6. Differentially expressed genes in the striatum of *Mbd2*$^{-/-}$ mice compared to wildtype littermates.
MA plot showing differential gene expression and abundance from RNA-seq analysis of *Mbd2*$^{-/-}$ versus wildtype striatal tissue. Genes that are significantly differentially expressed (FDR < 0.05) are labeled in red. Selected and discussed genes are labeled.

Gene Name	Predicted Function	logFC	logCPM	FDR (<0.05)
Slc4a5	sodium bicarbonate cotransporter	2.720	-0.180	0.001
En2	homeobox transcription factor	2.627	1.466	0.000
Ttr	retinol and thyroxine transport	2.461	7.124	0.000
H2-Q7	Histocompatibility 2, Q region locus 7	2.365	-0.090	0.000
Kcne2	Potassium voltage-gated channel	2.028	-0.372	0.014
H2-Q6	Histocompatibility 2, Q region locus 6	2.012	-0.396	0.004
Lcn2	Lipocalin 2	1.817	0.750	0.001
Lrg1	Leucine-Rich Alpha-2-Glycoprotein 1	1.780	0.081	0.005
Aqp1	Aquaporin 1	1.755	0.226	0.043
Tgtp2	T cell specific GTPase 2	1.526	0.184	0.023
Gbp4	Guanylate Binding Protein 4	1.283	1.857	0.020
Parp3	Poly(ADP-ribosyl) transferase 3	0.798	3.280	0.033
Grin2b	Glutamate Receptor	0.743	4.026	0.000
H2-K1	Histocompatibility 2, K region locus 1	0.647	4.863	0.002
Xdh	Xanthine dehydrogenase	0.626	4.775	0.014
H2-D1	Histocompatibility 2, D region locus 1	0.598	5.364	0.001
Kcng1	Potassium Voltage-Gated Channel	0.496	5.908	0.000
Scrt2	Scratch homolog 2, zinc finger protein	0.435	6.167	0.003
Hdhd2	Haloacid Dehalogenase-Like Hydrolase	0.401	5.915	0.008
Nt5e	5'-Nucleotidase, Ecto (CD73)	0.364	6.069	0.042
Fabp5	Fatty Acid Binding Protein 5	0.359	5.598	0.049
Lars2	Leucyl-TRNA Synthetase 2	-0.394	6.765	0.010
Il33	Interleukin 33	-0.400	6.460	0.022
Slc7a11	anionic amino acid transport	-0.470	5.142	0.009
Akap12	A Kinase (PRKA) Anchor Protein 12	-0.607	5.082	0.001
4930503L19Rik	predicted protein coding gene	-0.737	3.624	0.009
St8sia5	membrane bound glycosyltransferase	-0.749	4.016	0.007
Fosl2	JUN/AP-1 signal transduction pathway	-0.750	4.912	0.003
Fos	JUN/AP-1 signal transduction pathway	-0.792	3.280	0.046
Cd59a	complement-mediated cell lysis	-0.801	4.004	0.001
Sec14l3	SEC14-Like 3	-0.988	2.019	0.014
Gpx6	Glutathione Peroxidase 6	-1.020	2.791	0.009
Apold1	Apolipoprotein L Domain Containing 1	-1.049	5.367	0.010
Met	Met Proto-Oncogene	-1.454	0.239	0.018
Mbd2	Methyl-DNA binding domain protein 2	-1.982	5.345	0.000
A230065H16Rik	predicted protein coding gene	-2.486	0.430	0.013
Prdm12	PR Domain Containing 12	-3.243	-0.750	0.014
Gh	Growth hormone	-4.379	-0.808	0.006

Table 2.4. List of differentially expressed genes in the striatum of *Mbd2*$^{-/-}$ mice compared to wildtype littermates.

All significantly DEGs (FDR < 0.05) and predicted functions are listed. Significantly differentially expressed genes with FC > log(1) are labeled in red.

CHAPTER 3: Genetic tagging of MBD2 reveals different spatiotemporal expression and supports distinct functions from related MBD proteins

Adapted from: Wood, K. H., Johnson, B. S., Welsh, S. A., Lee, J. Y., Cui, Y., Krizman, E., Brodkin, E. S., Blendy, J. A., Robinson, M. B., Bartolomei, M. S., Zhou, Z. Tagging methyl-CpG binding domain proteins reveals different spatiotemporal expression and supports distinct functions. *Epigenomics*. In Press.

ABSTRACT

DNA methylation and other epigenetic mechanisms are necessary to maintain cell-type specific gene expression programs and the chromatin state. However, it is not understood how DNA methylation is linked to the regulation of transcription and histone modifications. Previous biochemical studies have shown the methyl-DNA binding domain (MBD) family of proteins can bind to methylated DNA and recruit various co-repressor complexes to mediate transcriptional regulation. However, the *in vivo* roles of these proteins in a cellular context and their spatiotemporal expression patterns have not been fully determined. The study of the MBD proteins *in vivo*, and especially MBD2, has been limited by the lack of reliable antibodies. To overcome this limitation, we generated novel transgenic mice with endogenous MBD2 or MBD1 tagged with biotin. This approach allowed us to isolate biotin-tagged MBD2 for multiple applications to characterize MBD2 *in vivo* functions in the context of the MBD protein family. We were also able to reliably distinguish multiple isoforms of tagged MBD2, which may have distinct biological properties. We determined that MBD2 interacts with the NuRD complex in multiple tissues *in vivo*. We also found that MBD2 is broadly expressed throughout multiple tissues at young and adult ages, in contrast to related proteins MBD1, MeCP2, and MBD3, which are primarily expressed in the brain. Our findings support a critical role for MBD2 in peripheral tissues and reveal new directions and genetic tools for the study of MBD protein *in vivo* functions.

INTRODUCTION

Epigenetic mechanisms, including DNA methylation, are essential for the maintenance of chromatin state and gene expression programs (Smith and Meissner, 2013; Suzuki and Bird, 2008). The mechanism by which DNA methylation is interpreted into transcriptional output is not fully understood, but involves protein 'readers' that bind to methylated sites (Du et al., 2015). These readers include the methyl-CpG binding domain (MBD) family of proteins, comprised of methyl-CpG binding protein 2 (MeCP2) and MBDs 1-6 (Du et al., 2015; Hendrich and Bird, 1998). The MBD is a highly conserved domain originally identified for its ability to specifically bind mCG sites (Meehan et al., 1989). Most MBD proteins, with the exception of MBD3, MBD5 and MBD6, bind to DNA in a methylation density-dependent manner when expressed in ESCs (Baubec et al., 2013).

Biochemical studies support the role of MBD proteins in mediating transcriptional repression through the recruitment of various co-repressor complexes (Feng and Zhang, 2001; Nan et al., 1998; Ng et al., 2000). MBD2 or MBD3 are incorporated into mutually exclusive complexes with the Mi2/nucleosome remodeling and deacetylase (NuRD) complex, while MeCP2 associates with the repressive Sin3A and NCoR/SMRT complexes (Ebert et al., 2013; Le Guezennec et al., 2006; Lyst et al., 2013; Nan et al., 1998; Ng et al., 1999). MBD1 interacts with several heterochromatin-associated proteins, including repressive histone methyltransferases (Fujita et al., 2003c; Ichimura et al., 2005; Reese et al., 2003; Sarraf and Stancheva, 2004). However, the functional outcomes of these interactions in a cellular context have not yet been fully characterized.

The study of MBD protein functions *in vivo* has been severely limited by the lack of appropriate antibodies. Consequentially, the majority of studies on MBD proteins, and especially MBD2, have relied on the use of tagged alleles overexpressed in cultured cells to perform various experiments such as chromatin immunoprecipitation and sequencing (ChIP-seq), amongst other applications (Baubec et al., 2013). While these studies provide insight into molecular mechanisms

of MBD protein function, they do not fully address MBD protein function in a complex, differentiated cellular context *in vivo*.

In order to examine MBD functions *in vivo*, it is also necessary to identify the specific tissues or cell types where the MBD proteins are expressed. MBD expression at the transcriptional level has been assessed in several tissues for MeCP2, MBD1 and MBD2 (Hendrich and Bird, 1998; Roloff et al., 2003). However, a closer analysis of MeCP2 expression showed that MeCP2 protein levels do not correlate with transcript abundance in mouse or human tissues, indicating that significant post-transcriptional regulation may be occurring (Shahbazian et al., 2002). Phenotypic data must also be carefully evaluated to determine the cell-type specific functions of MBD proteins. For example, MeCP2 loss-of-function phenotypes in non-neuronal tissues may be occurring due to non-cell-autonomous effects that are neuronal in origin, as was recently shown in a study of muscle (Conti et al., 2015). However, a comprehensive analysis of MBD protein expression in tissues of interest has not been possible due to limitations of currently available antibodies, especially for MBD2.

In this study, we sought to explore the functions of MBD2 *in vivo* in the context of the other MBD family proteins. To investigate the underlying causes of the distinct behavioral and physiological outcomes of *Mecp2, Mbd1*, and *Mbd2* null mice, we generated mouse lines with gene replacement alleles expressing endogenous MBD2 or MBD1 tagged with biotin. We used these mice to systematically identify the *in vivo* binding partners, genomic localization, and spatiotemporal expression patterns of MBD2 in the context of the MBD protein family. Our findings reveal new insights and directions and provide novel genetic tools for the study of MBD2 function *in vivo.*

METHODS

Animal Husbandry

All experiments were conducted in accordance with the ethical guidelines of the US National Institutes of Health and with the approval of the Institutional Animal Care and Use Committee of the University of Pennsylvania. All mice were housed in a standard 12 h light/12 h dark cycle with access to ample amounts of food and water. All experiments were performed on mice on a congenic sv129:C57BL/6J background unless otherwise stated. All assays were performed on male littermates aged 2-3 months. Mice deficient in MBD2 (*Mbd2*$^{-/-}$) or MBD1 (*Mbd1*$^{-/-}$) are previously described (Hendrich et al., 2001; Zhao et al., 2003) and were genotyped using a PCR-based strategy (Chapter 2 Methods).

Generation of Tavi-tagged mice

The targeting constructs used for homologous recombination in ESCs were cloned in two arms by PCR amplification of sv129 genomic DNA. The primer sequences used to PCR amplify the 5' and 3' arms of *Mbd2* and *Mbd1*, respectively, and the Tavi oligo are listed in Table 3.1.

Table 3.1. Primers used to generate targeting constructs for *Tavi*-tagged alleles of *Mbd2* and *Mbd1*.

Primer	Forward Primer	Reverse Primer
Mbd2 5' arm	5'-GTTTGGCTTAACACATCTCAACC-3'	5'-GGATGAGTCAGGACAGAGGAGTA-3'
Mbd2 3' arm	5'-GAAGCTCAGGGTATGGTCTCAC-3'	5'-AAAGTATCACGCTCTGGTCCAT-3'
Mbd1 5' arm	5'-GCTGCAGATCCAGACCTTTC-3'	5'-TCCCTCATCCGAGTGTTCTC-3'
Mbd1 3' arm	5'-AAAAGCTGGTCCCACTCTCC-3'	5'-ATTTGGGCAGGCAACACAAG-3'
Tavi oligo	5'-GGGAAAACCTGTATTTTCAGGGCGCC GGCCTGAACGACATCTTCGAGCTCAGAA AATCGAATGGCACGAATAGGTT-3'	5'-AACCTATTCGTGCCATTCGATTTTCTG AGCCTCGAAGATGTCGTTCAGGCCGGC GCCCTGAAAATACAGGTTTTCCCGC-3'

The Tavi oligo contained a 5' SacII restriction site overhang and a 3' HpaI restriction site overhang and a stop codon directly upstream of the 3' HpaI site overhang. Insertional mutagenesis was then used to introduce SacII and HpaI restriction sites into exon 6 of *Mbd2* and exon 15 of *Mbd1* in the respective targeting constructs. These sites were immediately upstream of the stop codon in order to ligate the Tavi tag oligo in the correct orientation at the C terminus of

each gene. After ligation of the Tavi oligo into the 3'arm of each construct, each arm was cloned into a vector containing a loxP-flanked neomycin cassette (Neo) and a diphtheria toxin A negative-selection cassette. Each targeting construct was confirmed by sequencing, linearized using NotI and subsequently electroporated into sv129 mouse ESCs. Two ESC clones each of *Mbd2*^{Tavi} and *Mbd1*^{Tavi} were independently injected into C57BL/6 blastocysts and subsequently transferred to pseudopregnant females. The resulting chimeric offspring were mated with C57BL/6J EIIa-Cre mice (The Jackson Laboratory) for embryonic deletion of the Neo cassette, and the agouti offspring were screened by PCR genotyping to confirm germ line transmission of the *Mbd2*^{Tavi} or *Mbd1*^{Tavi}. Germline transmitted *Mbd2*^{Tavi} or *Mbd1*^{Tavi} mice were backcrossed to C57BL/6J for at least 5 generations. Mice were genotyped using a PCR-based strategy to detect wildtype and Tavi-tagged alleles of *Mbd2* and *Mbd1*. The genotyping primers sequences are listed in Table 3.2.

Table 3.2. Primers used to genotype *Mbd2*^{Tavi} and *Mbd1*^{Tavi} mice.

Primers	Sequences	Product Size
Mbd2^{Tavi}	5'- AAAGGCAAACAGGTCAGCCATTCC-3' 5'- ACAGGAAGAGCGAGTCCAACAAGT-3'	*Wildtype:* 473bp *Mbd2*^{Tavi}: 557bp
Mbd1^{Tavi}	5'-TTCCCACAGAGAACACTCGGATGA-3' 5'-TAGCAGGTCTTCAGCACACTTGGA-3'	*Wildtype:* 535bp *Mbd1*^{Tavi}: 619bp

Nuclear extract preparation

Tissues were minced on ice and homogenized in ice-cold lysis buffer (10mM HEPES pH 7.9, 1.5mM $MgCl_2$, 10mM KCl, 0.5% NP-40, 0.2mM EDTA, protease inhibitors). Nuclei were pelleted, washed and resuspended in nuclear extract (NE) buffer (20mM HEPES pH7.9, 1.5mM $MgCl_2$, 500mM KCl, 0.2mM EDTA, 10% glycerol, protease inhibitors). Nuclei were incubated in NE buffer at 4°C for two hours with rotation. Samples were cleared by ultracentrifugation with TLA 100.3 rotor (Beckman Optima TL) at 4°C for 30 minutes and the supernatant taken for nuclear extract. Protein concentration was quantified using a modified Bradford assay (Bio-Rad).

Western blot

Western blots were carried out and imaged with the LI-COR Odyssey Clx Infrared Imaging System following manufacturer's protocols. 50ug of nuclear extract was loaded per lane. Antibodies and dilutions used in this study are as follows: Avi tag, Abcam ab106159, 1:5000 (listed as anti-BirA, detects the minimal peptide substrate of biotin ligase BirA regardless of biotinylation status); Sin3A, Thermo Scientific PA1-870, 1:500; HDAC1, Abcam Ab7028, 1:2000; HDAC2, Cell Signaling 5113, 1:2000; HDAC3, Santa Cruz sc-11417, 1:1000; LaminB1, Santa Cruz sc-30264, 1:1000; TBLR1, Bethyl A300-408A, 1:1000; Chd4, Abcam ab70469, 1:1000; MTA2, Santa Cruz sc-9447, 1:200; H3, Abcam ab1791, 1:2000; MBD2, Diagenode CS-098-100, 1:500; MBD1, Santa Cruz sc-10751, 1:200; MBD3, Santa Cruz sc-9402, 1:200; MeCP2, rabbit polyclonal antibody directed to the C-terminus of MeCP2, 1:1,000 (Zhou et al., 2006). Secondary antibodies are as follows: Streptavidin DyLight 800 conjugated, Thermo Scientific, 1:1000; donkey anti-rabbit IRDye 680RD, donkey anti-mouse IRDye 800CW, donkey anti-goat IRDye 800CW, all from LI-COR Biosciences, 1:10,000.

Immunoprecipitation

1mg of nuclear extract was adjusted to 300µl total volume with NE buffer to perform IP in duplicate. Protein G Dynabeads or Streptavidin M-280 Dynabeads (Life Technologies) were washed three times in PBS with 0.1% Tween-20 and 0.1% BSA. Nuclear extracts were cleared for 30 minutes at 4°C with 25µl Protein G Dynabeads. For streptavidin pulldown, 50µl of streptavidin Dynabeads were added to the nuclear extract and incubated at 4°C for two hours with rotation. For antibody immunoprecipitation, 5µg of antibody was added to nuclear extract and incubated overnight at 4°C with rotation. 50µl of Protein G beads were blocked in wash buffer overnight at 4°C with rotation. Blocked beads were incubated with antibody-conjugated nuclear extract in the morning for two hours at 4°C with rotation. Beads were washed four times in PBS with 0.1% Tween-20 and split into two equal volumes. Each sample was resuspended in 25µl loading buffer with 50mM DTT and boiled for 10 minutes at 95°C prior to loading on gel.

Chromatin immunoprecipitation and qPCR

Tissue was suspended in 10ml ice-cold crosslinking buffer (10mM HEPES pH 7.5, 100mM NaCl, 1mM EDTA, 1mM EGTA, 1% formaldehyde) and homogenized with a Polytron tissue homogenizer (VWR). Homogenized tissue was rotated at room temperature for 5 minutes after which glycine was immediately added to a final concentration of 0.125M. Tissue was washed twice with ice-cold PBS, resuspended in lysis buffer 1 (50mM HEPES pH 7.5, 140mM NaCl, 1mM EDTA, 1mM EGTA, 0.25% Triton X-100, 0.5% NP-40, 10% glycerol, protease inhibitors) and dounced to lyse cells. Pelleted nuclei were washed and resuspended in lysis buffer 2 (10mM Tris pH 8.0, 1mM EDTA, 1mM EGTA, 0.25% SDS, protease inhibitors) and incubated on ice for 20 minutes to lyse nuclei. Chromatin was sheared using a Covaris S220 to approximately 200-500bp. Chromatin shearing efficiency was analyzed using agarose gel electrophoresis. 100µg of chromatin was diluted with lysis buffer without SDS to a final SDS concentration of 0.1% and 5µg was reserved as input. Chromatin was precleared with Protein A Dynabeads (Life Technologies) for 30 minutes with rotation at 4°C. For TEV protease pre-treatment, chromatin was incubated at this point with 20 units of TEV protease (Sigma-Aldrich) for 3 hours at 16°C before proceeding.

Chromatin was incubated with 5µg of antibody or IgG control, or with 50µl of streptavidin Dynabeads overnight at 4°C with rotation. For antibody ChIP, 30µl of Protein A Dynabeads were washed and blocked overnight at 4°C with rotation in blocking buffer (1% BSA in TBST). For antibody ChIP, chromatin was incubated for 3 hours at 4°C with blocked Protein A beads. The antibodies used for ChIP are anti-histone H3 (acetyl K27) (Abcam ab4729), anti-histone H3 (tri-methyl K4) (Abcam ab8580) and normal rabbit IgG (Cell Signaling 2729). Beads were washed as follows: once with low salt buffer (50mM HEPES pH 7.5, 150mM NaCl, 1mM EDTA, 1% Triton X-100, 0.1% DOC), once with high salt buffer (50mM HEPES pH 7.5, 500mM NaCl, 1mM EDTA, 1% Triton X-100, 0.1% DOC), once with LiCl buffer (10mM Tris-HCl pH 8.0, 1mM EDTA, 0.5% DOC, 0.5% NP-40, 250mM LiCl), and twice with TE buffer (10mM Tris pH 8.0, 1mM EDTA). Input and IP chromatin was eluted in 100µl elution buffer (50mM Tris pH 8.0, 10mM EDTA, 1% SDS)

overnight at 65°C to reverse crosslinks. DNA was treated with RNase A and proteinase K before phenol-chloroform purification following standard methods. DNA was quantified by Qubit Fluorometric Quantitation (Thermo Fisher Scientific). ChIP DNA was analyzed by qPCR using SYBR Green detection (Applied Biosystems) with the primers listed in Table 3.3.

Table 3.3. Primers used for ChIP-qPCR.

Locus	Forward Primer	Reverse Primer
Gapdh Promoter	5'- CCATCACGTCCTCCATCATC -3'	5'- CAGTCGGAAACTGGGAAGG-3'
Actb Promoter	5'- AGTGTCTACACCGCGGGAAT-3'	5'- CTGGCACAGCCAACTTTACG-3'
IAP element	5'- GCTTTCGTTTTTGGGGCTTGG -3'	5'- CTTACTCCGCGTTCTCACGAC-3'
Chr6 Gene Desert	5'- GGGAGAGAGTGATAGTCCAAGA -3'	5'- CTTTGGTAGAAGAGAATGGTGTTTG-3'

Fractionation of small intestine and colon crypts and protein lysate preparation

The gastrointestinal tract was dissected on ice, cut longitudinally and washed in cold PBS. The villi of the small intestine were gently scraped off using a glass coverslip. Remaining tissue was minced and incubated in ice-cold 5mM EDTA/PBS for 30 minutes with pipetting every 5 minutes to release crypt cells. After letting tissue settle to bottom of tube, the supernatant was filtered through a 70μm filter and transferred to a new tube. This was repeated with additional PBS until 100μl of supernatant was collected and cells were pelleted. Whole cell protein lysates were prepared by incubating cells in RIPA buffer (10mM Tris-HCl pH 8.0, 1mM EDTA, 0.5mM EGTA, 1% Triton X-100, 0.1% DOC, 0.1% SDS, 140mM NaCl) with dounce homogenization. Samples were cleared by centrifugation and quantified using a modified Bradford Assay (Bio-Rad).

Brain histology

Mice were anesthetized with 1.25% Avertin (wt/vol), transcardially perfused with 4% paraformaldehyde (wt/vol), and brains were post-fixed for 2 hours at 4°C. Brains were washed in PBS, cryoprotected in 30% sucrose/PBS at 4°C overnight, and snap frozen in OCT mounting medium (Sakura Finetek). Frozen tissue was cryosectioned at 20μm and mounted on glass slides for staining. For β-galactosidase (β-gal) staining, sections were incubated in X-gal staining solution (5mM $K_3Fe(CN)_6$, 5mM $K_4Fe(CN)_6$, 2mM $MgCl_2$, 0.01% DOC, 0.02% NP-40, 1mg/ml X-gal in PBS) overnight at 37°C. Slides were rinsed five times in PBS and coverslipped. For Nissl staining, mounted frozen sections were dehydrated in ethanol and xylene, rehydrated, incubated in cresyl violet acetate solution (0.1% cresyl violet, 0.25% glacial acetic acid (v/v)) for 10 minutes at room temperature, rinsed, dehydrated and coverslipped.

Gastrointestinal tract histology

Small intestine and colon was cut longitudinally and washed in ice-cold PBS. Fresh tissue was snap-frozen in OCT mounting medium (Sakura Finetek), cryosectioned at 20μm and mounted on slides for staining. β-gal staining was performed as described for brain tissue. Sections were counter-stained with nuclear fast red (Sigma-Aldrich) following manufacturer's protocols.

RESULTS

Generation of gene replacement alleles expressing biotin-tagged MBD2 or MBD1

Given that previous studies linked MeCP2 and MBD1 to brain function in both humans and mice (Allan et al., 2008; Cukier et al., 2010; Goffin et al., 2012; Guy et al., 2001), it is surprising that mice lacking MBD2 are equivalent to control littermates on most measures, including behavior, gene expression, and biogenic amine levels (Chapter 2). MBD2 likely has critical functions in other tissues and systems, such as the gastrointestinal and immune systems (Cook et al., 2015; Sansom et al., 2003; Wang et al., 2013), that may contribute to the hypoactivity, impaired nesting and nurturing (Hendrich et al., 2001), and low body weight

phenotypes observed in Mbd2 null mice. However, the study of MBD2 functions *in vivo* has been impeded by the lack of reliable antibodies that specifically recognize MBD2.

To overcome these limitations, we took a genetic approach and developed gene replacement alleles tagging MBD2 with a biotinylation consensus sequence derived from the *E. coli* biotin ligase, BirA (Figure 3.1). The tag was introduced to the C-terminus of MBD2 and consists of two parts: a tobacco etch virus (TEV) protease cleavage site and an avidin biotinylation consensus sequence that can be selectively biotinylated (Figure 3.1.A,B). We labeled this tag as the "Tavi" tag and the tagged allele as $Mbd2^{Tavi}$. We also generated a separate transgenic mouse line with BirA constitutively expressed from the Rosa26 locus ($R26^{BirA/+}$) (Johnson et al., manuscript in preparation). Therefore, $MBD2^{Tavi}$ protein can be specifically biotinylated in the presence of BirA (Figure 3.1.A,B). We can detect and pull down biotinylated endogenous MBD2 proteins using streptavidin-conjugated beads (Figure 3.1.C). Treatment with TEV protease cleaves off the biotinylated tag from the MBD2 protein (Figure 3.1.D). This set of transgenic mice allows us to detect and experimentally manipulate endogenous MBD2 with high specificity and reproducibility.

Two previously described isoforms of MBD2, MBD2a and MBD2b (Hendrich and Bird, 1998), carry the Tavi tag (Figure 3.2.A). These isoforms arise from alternative translation start sites from the same transcript that is expressed in adult somatic tissues (Hendrich and Bird, 1998). MBD2a, but not MBD2b, includes a N-terminal GR repeat region. Post-translational methylation of the GR repeat has been shown to affect MBD2a function by reducing its affinity for DNA and the NuRD complex (Tan and Nakielny, 2006). $MBD2^{Tavi}$ also includes a transcriptional repression domain (TRD) that interacts with the NuRD complex (Boeke et al., 2000). Another isoform, MBD2c, is expressed exclusively in the testes and ESCs (Hendrich and Bird, 1998; Lu et al., 2014). MBD2c has an alternatively spliced C terminus that does not include the Tavi tag and is not depicted in Figure 3.2.A. Mice heterozygous or homozygous for $Mbd2^{Tavi}$ are viable and fertile similar to littermate controls. In contrast to $Mbd2^{-/-}$ mice that have reduced body weight (Figure 2.2.A), $Mbd2^{Tavi/Tavi}$ mice with or without BirA expression show equivalent body weight to

wildtype and *R26*$^{BirA/+}$ littermates (Figure 3.2.B) and we have not observed any gross phenotypic abnormalities during routine handling. Therefore, biotinylation of MBD2^{Tavi} does not appear to impair MBD2 function.

We then used fluorophore-conjugated streptavidin to examine MBD2^{Tavi} expression by western blot (Figure 3.2.C). A representative commercial antibody to MBD2 (and others, data not shown) recognizes several unknown proteins that do not differ between wildtype (WT) and *Mbd2*$^{-/-}$ (KO) adult brain lysate (denoted by *), demonstrating invalidity of the stated antibody. In contrast, streptavidin detects three biotinylated MBD2^{Tavi} isoforms with high specificity in *Mbd2*$^{Tavi/Tavi}$*; R26*$^{BirA/+}$ mice, but not in mice expressing BirA without MBD2^{Tavi} (*R26*$^{BirA/+}$). In addition to the predicted MBD2a^{Tavi} and MBD2b^{Tavi} isoforms, we observed a third MBD2 isoform slightly smaller than MBD2a^{Tavi} that has been previously detected but not described in detail (Ng et al., 1999). This isoform has the C-terminal Tavi tag and is biotinylated in the presence of BirA. Given the consistency and reproducibility of this isoform in different tissues and time points (Figure 3.9), it is unlikely to be a degradation product of MBD2a^{Tavi}. Therefore, we designated this novel isoform as MBD2d. It includes exon 6 where the Tavi tag is inserted and may occur through alternative splicing or translation start site usage (Figure 3.2.A). Direct comparison of proteins detected by the MBD2 antibody versus streptavidin (Figure 3.2.C, merged image) demonstrates the specificity and robustness of this biotin-tagging approach to identify MBD2 isoforms.

In order to directly compare MBD2 to MBD1 *in vivo*, we employed the same approach and generated mice expressing gene replacement alleles for MBD1^{Tavi} (Figure 3.3.A) and also for MeCP2 (Johnson *et al.*, in preparation). Murine *Mbd1* has three reported alternatively spliced isoforms that have two or three CxxC zinc finger DNA-binding domains in addition to a transcriptional repression domain (TRD) (Jørgensen et al., 2004). MBD1a and MBD1b both carry the Tavi tag, but MBD1c has an alternatively spliced C-terminus that does not include the Tavi tag (Fig. 5A). *Mbd1*$^{Tavi/Tavi}$*; R26*$^{BirA/+}$ mice are viable and fertile with no gross phenotypic abnormalities observed during routine handling. Using western blots, we found that an antibody against MBD1 detects several cross-reacting proteins in postnatal day 7 (P7) brain lysate, comparing *Mbd1* null

(KO) to WT mice (Figure 3.3.B, denoted by *) (Zhao et al., 2003). All three isoforms of MBD1, MBD1a^{Tavi}, MBD1b^{Tavi} and untagged MBD1d, are visible in *R26$^{BirA/+}$* and *Mbd1$^{Tavi/Tavi}$; R26$^{BirA/+}$* mice when compared to *Mbd1* null mice using this antibody. In contrast to *R26$^{BirA/+}$* mice and *Mbd1* null mice, streptavidin detects two specific proteins corresponding to biotinylated MBD1a^{Tavi} and MBD1b^{Tavi} in lysate from *Mbd1$^{Tavi/Tavi}$; R26$^{BirA/+}$* mice. Streptavidin also detects a 75kDa endogenously biotinylated protein that is close in size to untagged MBD1d (denoted by *). The merged image demonstrates that streptavidin specifically detects the two biotin-tagged MBD1^{Tavi} isoforms that are also recognized by the MBD1 antibody (yellow bands) (Figure 3.3.B). In summary, this biotin-tagging approach represents a powerful tool to study multiple isoforms of endogenous MBD proteins, overcoming antibody limitations.

Streptavidin-mediated pulldown of biotinylated MBD2^{Tavi} detects multiple isoforms of MBD2 in several tissues

We first sought to compare our streptavidin-mediated approach to antibodies in the detection of biotinylated MBD2^{Tavi}. We examined protein lysate from two tissues, brain and lung, from adult *Mbd2$^{Tavi/Tavi}$; R26$^{BirA/+}$, R26$^{BirA/+}$*, and *MeCP2$^{Tavi/y}$; R26$^{BirA/+}$* mice in order to compare biotinylated MBD2^{Tavi} and MeCP2^{Tavi} to mice that do not express any Tavi-tagged proteins. We should detect only endogenously biotinylated proteins in lysate from *R26$^{BirA/+}$* mice and therefore can reliably distinguish biotinylated Tavi-tag proteins from background. We used streptavidin pulldown to enrich for biotinylated proteins and detected each protein with streptavidin and antibodies raised against MBD2 or MeCP2, respectively (Figure 3.4).

We observed that a commercial antibody to MBD2 detects multiple non-specific protein species in the brain and one notable non-specific protein in the lung that is close in size to MBD2 (Figure 3.4.A,C; denoted by *). However, streptavidin-mediated pulldown of biotinylated MBD2^{Tavi} reveals that this antibody detects only MBD2a^{Tavi}, and, furthermore, that this band is only detectable upon streptavidin-mediated enrichment of MBD2^{Tavi} in both brain and lung (Figure 3.4.A,C; note yellow band in merged image). The cross-reacting bands that are visible in the input

samples are depleted upon streptavidin-mediated enrichment of MBD2^{Tavi}. In contrast, streptavidin reveals the three biotinylated isoforms of MBD2 described above in addition to a constitutively expressed endogenous biotinylated protein of 75kDa (denoted by *). Therefore, we conclude that our approach to detect biotinylated MBD2^{Tavi} *in vivo* is significantly more robust and reliable than detection with antibodies alone.

In contrast, an antibody raised against MeCP2 detects endogenous MeCP2 and biotinylated MeCP2^{Tavi} with high specificity in protein lysate from both brain and lung (Figure 3.4.B,D). We found that streptavidin detects a constitutively expressed, endogenously biotinylated protein of approximately 75kDa that is close is size to MeCP2 which is also enriched after streptavidin pulldown (Figure 3.4.B,D; denoted by *). By examining the merged image, it is apparent that both biotinylated MeCP2^{Tavi} and MBD2^{Tavi} are enriched by streptavidin pulldown, but only MeCP2^{Tavi} is detected by the MeCP2 antibody (Figure 3.4.B,D; note yellow band in merged image).

We also validated the specific enrichment of biotinylated MBD2^{Tavi} and MeCP2^{Tavi} by streptavidin pulldown using an additional reagent. We used an antibody raised against the biotinylation consensus sequence for BirA (labeled Avi) to detect the Tavi tag of MBD2^{Tavi} and MeCP2^{Tavi} in addition to streptavidin to detect biotinylated proteins. This approach allowed us to simultaneously detect MBD2^{Tavi} and MeCP2^{Tavi} using the same reagents for a direct comparison of enrichment and expression levels. We performed streptavidin pulldown using protein lysate from four tissues, brain, lung, small intestine, and colon, from adult *Mbd2$^{Tavi/Tavi}$; R26$^{BirA/+}$*, *R26$^{BirA/+}$*, and *MeCP2$^{Tavi/y}$; R26$^{BirA/+}$* mice in order to compare biotinylated MBD2^{Tavi} and MeCP2^{Tavi} to mice that do not express any Tavi-tagged proteins (Figure 3.5). This comparison allowed us to assess the presence of multiple isoforms of MBD2 in different tissues, and also served as a preliminary analysis of MBD protein spatial expression.

We found that streptavidin and the Avi antibody detect three isoforms of MBD2^{Tavi} in all tissues examined here. The Avi antibody also detects several cross-reacting proteins that vary between tissues, must notably a band at 50kDa in the brain and colon that partially obscures

MBD2a^{Tavi} and MBD2d^{Tavi} (Figure 3.5.A,D). Streptavidin also detects several endogenously biotinylated proteins, including one at 75kDa that partially obscures MeCP2^{Tavi} in blots with brain, lung, and colon lysate (Figure 3.5.A,B,D). Despite these complications, it is apparent that MBD2 and MeCP2 carry the Tavi-tag and are biotinylated, as demonstrated by the merged signals using two methods of detection, the Avi antibody and streptavidin (yellow bands, merged images). We also observed that MeCP2 expression is not detectable in the small intestine, even after enrichment for MeCP2^{Tavi} with streptavidin pulldown (Figure 3.5.C). Additionally, we found that all three isoforms of MBD2^{Tavi} appear to be equivalently expressed in these four tissues, which we later re-evaluated with further experiments (Figure 3.9). These additional verifications demonstrate the necessity for a novel affinity-tagging approach in order to study MBD2 functions *in vivo*. This approach also allows for the enrichment and detection of biotinylated MBD2^{Tavi} and MeCP2^{Tavi} in parallel.

Streptavidin-mediated pulldown of biotinylated MBD2^{Tavi} reveals distinct binding partners for MBD2 and MeCP2 *in vivo* and ubiquitous MBD2-NuRD interactions

Our initial analysis of MBD2^{Tavi} and MeCP2^{Tavi} expression while verifying the biotinylation of each protein showed that these proteins are co-expressed in several tissues, including the brain, lung and colon (Figure 3.5). Despite being co-expressed and having similar DNA-binding properties, the MBD proteins have distinct functions that may be conferred through interactions with distinct protein complexes *in vivo* (Baubec et al., 2013; Nan et al., 1998; Zhang et al., 1999). However, for MBD2 these interactions have only been verified using cell culture systems and the dynamics of these interactions *in vivo* have not been fully explored. Therefore, in order to verify MBD2 and co-repressor interactions *in vivo*, we performed streptavidin-mediated co-pulldown experiments with MBD2^{Tavi} and MeCP2^{Tavi} using brain and lung lysate from *Mbd2$^{Tavi/Tavi}$; R26$^{BirA/+}$* and *MeCP2$^{Tavi/y}$; R26$^{BirA/+}$*, respectively, and *R26$^{BirA/+}$* adult mice. We assessed interactions between MBD2 and the NuRD that have been studied in cultured cells and interactions between

MeCP2 and the NCoR and SIN3A co-repressor complexes (Boeke et al., 2000; Ebert et al., 2013; Lyst et al., 2013; Nan et al., 1998; Zhang et al., 1999).

We detected interaction between MeCP2^{Tavi} and two core components of the NCoR complex, TBLR1 and HDAC3. We also detected interaction between MeCP2^{Tavi} and HDAC1, which associates with NCoR and SIN3A, and SIN3A itself in both brain and lung (Figure 3.6.A,B). We found that MBD2^{Tavi} had a strong association with components of the NuRD complex, including HDAC1, HDAC2 and MTA2 in both tissues. Interestingly, we found that MBD2 shows stronger association with HDAC1 compared to MeCP2 under these pulldown conditions. We also observed a weak interaction between MBD2^{Tavi} and SIN3A, as has been reported (Boeke et al., 2000). Neither MeCP2^{Tavi} nor MBD2^{Tavi} interacted with LaminB1, as expected (Baubec et al., 2013).

This approach also allowed us to determine if there are tissue-specific interactions between the MBD2, MeCP2 and co-repressor complexes. To analyze this question more closely, we also examined MBD2 interactions with NuRD in the colon in addition to the brain and lung of adult mice (Figure 3.6.C). These tissues are representative of cell types with MBD2 and MBD3 co-expression (brain), MBD2 expression but not MBD3, or MBD2 expression with lowly detectable MBD3 expression (Figures 3.8 and 3.9). We found essentially identical patterns of interaction for MeCP2^{Tavi} and MBD2^{Tavi} in the brain and lung. Furthermore, we observed similar interactions between MBD2^{Tavi} and components of the NuRD complex in the brain, lung and colon. This evidence suggests that these interactions are ubiquitous and may not have tissue or cell type specificity. These findings also raise important questions for the interactions between MBD2 and NuRD in tissues where MBD3 is not expressed, specifically the lung and colon.

Because all isoforms of MBD2 carry the Tavi tag, we were unable to distinguish which isoforms were interacting with NuRD by streptavidin pulldown of MBD2^{Tavi}. It has been reported that modifications to the N terminus of MBD2a can affect NuRD association (Tan and Nakielny, 2006).Therefore, we wanted to test which isoforms of MBD2 interact with NuRD *in vivo*. We performed co-immunoprecipitation with antibodies against two NuRD components, CHD4 (also

known as Mi2-β) and HDAC1 with brain lysate from adult *Mbd2*$^{Tavi/Tavi}$*; R26*$^{BirA/+}$ mice (Figure 3.6.D). Unexpectedly, we found that all three isoforms of MBD2^{Tavi} are co-immunoprecipitated with CHD4 and HDAC1. MBD2d^{Tavi} showed weaker interaction with CHD4 and HDAC1 compared to MBD2a^{Tavi} and MBD2b^{Tavi}, but the lower expression of this isoform makes quantitative interpretation difficult. In addition, all three MBD2^{Tavi} isoforms have significantly weaker interaction with CHD4 than HDAC1 under these conditions. We determined that we were not disrupting endogenous protein complex interactions by detecting CHD4 and HDAC1 interactions with other NuRD complex proteins, including HDAC2 and MTA2, and HDAC1 interaction with SIN3A. We conclude that *in vivo* MBD2 is associated with the NuRD complex in the brain. Additional experiments may reveal whether or under what circumstances MBD2a may have reduced interactions with NuRD *in vivo*, as has been reported (Tan and Nakielny, 2006).

MBD2^{Tavi} is depleted at genomic loci with chromatin marks associated with transcriptional silencing

Due to the limitations of antibodies for MBD2, previous attempts to perform chromatin immunoprecipitation (ChIP) for MBD2 have mainly relied on tagged alleles over expressed in cultured cells (Baubec et al., 2013; Günther et al., 2013; Menafra et al., 2014). These previous studies generally showed that MBD2 is localized at methylated CpG islands at transcription start sites, promoters, and exons. Interestingly, MBD2 binding is highly dependent on mCG density and is consequentially not enriched at highly methylated, low-density sites such as introns and intergenic regions. MBD2 and NuRD are also found at some actively transcribed loci, suggesting that more complex transcriptional regulation may be occurring beyond simple transcriptional repression associated with DNA methylation.

We wanted to determine if MBD2 shows similar patterns of localization *in vivo* by using streptavidin to perform ChIP for MBD2^{Tavi} in adult cortex tissue. Using ChIP followed by quantitative PCR analysis, we examined MBD2 enrichment at two constitutively expressed loci, the promoters of *Gapdh* and *Actb*. We also assessed two transcriptionally repressed or gene poor

regions, including intra-cisternal A-type particle (IAP) elements and a gene desert region on chromosome 6. IAP elements are high-copy number long terminal repeat (LTR) transposons that are found throughout the genome and transcriptionally silenced by methylation (Walsh et al., 1998). Although these sites are methylated, the mCG density is low and therefore MBD2 is not strongly enriched at IAP elements or other repetitive elements (Baubec et al., 2013).

In order to assess the chromatin state at each site, we first performed ChIP-qPCR for histone H3 lysine 4 trimethylation (H3K4me3) and histone H3 lysine 27 acetylation (H3K27ac), both of which are associated with transcriptional activation and open chromatin (Shlyueva et al., 2014). As expected, we determined that H3K4me3 and H3K27ac are enriched at the promoters of *Gapdh* and *Actb* relative to the transcriptionally repressed IAP elements and gene desert loci (Figure 3.7.A). We then used streptavidin to perform ChIP-qPCR for MBD2^{Tavi} at the same loci (Figure 3.7.B). We determined that MBD2^{Tavi} is enriched at the transcriptionally silent or gene-poor regions at IAP elements and in the gene desert region of chromosome 6 and is relatively depleted at the promoters of *Gapdh* and *Actb*. Streptavidin also binds to endogenously biotinylated proteins, although these proteins are not predicted to be chromatin-binding proteins and therefore are unlikely to interfere with MBD2^{Tavi} ChIP (de Boer et al., 2003).

In order to verify the specificity or the streptavidin ChIP approach for MBD2^{Tavi}, we repeated the ChIP experiment with an additional pre-treatment with TEV protease before performing the ChIP. This pre-treatment cleaves the C-terminal biotinylation consensus sequence from the coding sequence of MBD2^{Tavi}, and therefore should give no ChIP signal after streptavidin ChIP. We determined that pre-treatment with TEV protease effectively abolishes the ChIP signal for MBD2^{Tavi} at all loci (Figure 3.7.B), thereby demonstrating the specificity of this approach.

Distinct spatiotemporal expression patterns of endogenous MBD2 in contrast to MBD1, MeCP2 and MBD3

Together with published studies (Cook et al., 2015; Sansom et al., 2003; Wang et al., 2013), our results support a role for MBD2 in tissues or organs outside the brain, in notable

contrast to MeCP2 and MBD1 (Chapter 2). In order to better understand MBD2 functions *in vivo*, we sought to characterize where and when MBD2 is expressed in comparison to other MBD proteins. This has previously been challenging because, even with reliable antibodies, the variable immunoreactivity of each antibody makes comparison of the expression levels for different MBD proteins difficult. In contrast, our biotin-affinity tag approach allows for direct, quantitative comparison of expression levels of MBD2 and MBD1. To better understand where and when MBD2 functions in vivo, we analyzed the expression patterns of MBD2, MBD1, MeCP2, and MBD3 across eight different tissues and two developmental time points, P7 and P42. We took advantage of the Tavi-tagged alleles of MBD2 and MBD1 to reliably determine the expression level of each protein and compared their expression side-by-side using quantitative western blots. This approach allowed us to obtain a comprehensive view of endogenous MBD spatiotemporal expression patterns at the protein level.

Using MBD2^{Tavi} mice with constitutively expressed BirA (*Mbd2*$^{Tavi/Tavi}$*; R26*$^{BirA/+}$), we analyzed the expression of three Tavi-tagged isoforms of MBD2 (MBD2a, MBD2b, and MBD2d) using two complementary reagents. First, we used an antibody raised against the biotinylation consensus sequence for BirA (labeled Avi) to detect the Tavi tag of MBD2^{Tavi}. We also used streptavidin to detect biotinylated MBD2^{Tavi}. In order to exclude cross-reacting proteins recognized by the Avi antibody and also exclude endogenously biotinylated proteins, we first used these reagents with protein lysate from *R26*$^{BirA/+}$ animals that do not express any Tavi alleles (Figure 3.8.A,B). The Avi antibody detects several cross-reacting proteins, most notably a 50kDa protein that is highly expressed in the brain at both P7 and P42 and a weaker cross-reacting band at 37kDa at P7. Several endogenous biotinylated proteins are also detected by streptavidin in the molecular size around MBD2, particularly a 37kDa protein in the heart, liver, kidney and small intestine at P42 (Figure 3.8.A,B; denoted by *).

Western blot analysis of protein lysate from *Mbd2*$^{Tavi/Tavi}$*; R26*$^{BirA/+}$ animals showed that all three isoforms of MBD2 are partially obscured by the cross-reacting bands detected by the Avi antibody, particularly in the brain (Figure 3.8.C,D). However, MBD2a^{Tavi} and MBD2b^{Tavi} are clearly

detected by streptavidin in multiple tissues at both P7 and P42. By examining the merged images from the streptavidin and Avi antibody signals (yellow bands), we concluded that the three isoforms of MBD2^{Tavi} are expressed highly in multiple tissues including the heart, lung, liver, kidney and colon at P7 and P42. MBD2d^{Tavi} appears to be expressed at a lower level than the 2a and 2b isoforms in all tissues examined, particularly at P42. These isoforms are expressed in the brain, but at a lower level compared than other tissues. Interestingly, all MBD2^{Tavi} isoforms are not expressed in spleen or small intestine at P7, but become up-regulated in these tissues at P42 (Figure 3.8.C,D).

We next sought to place MBD2 spatiotemporal expression patterns into the context of the MBD family. Therefore, we surveyed MBD1, MeCP2 and MBD3 expression in the same set of tissues and time points included in our MBD2 study. We used the Tavi-tag system to analyze MBD1 expression. First, we identified cross-reacting proteins detected by the Avi antibody and endogenously biotinylated proteins by analyzing protein lysate from *R26*$^{BirA/+}$ animals (Figure 3.9.A,B). At the molecular size around MBD1, the Avi antibody detected only a minor cross-reacting band at 75kDa in the kidney at P42 (denoted by *). Several endogenous biotinylated proteins are detected by streptavidin, particularly a 75kDa protein with significant expression in all tissues examined at P7 and P42 (denoted by *) (Figure 3.9.A,B).

We then used *Mbd1*$^{Tavi/Tavi}$*; R26*$^{BirA/+}$ mice to perform western blots with streptavidin and the Avi antibody to detect biotinylated MBD1^{Tavi} expression (Figure 3.9.C,D). Streptavidin and the Avi antibody both detect biotinylated MBD1a^{Tavi} and MBD1b^{Tavi}. In order to examine the untagged MBD1d isoform, we also performed western blots with an antibody against MBD1 and included brain lysate from *Mbd1* null mice to specifically identify MBD1 isoforms (Figure 3.9.C,D). The MBD1 antibody detects the untagged MBD1d isoform in addition to the two biotinylated Tavi-tagged isoforms (MBD1 antibody and streptavidin merged images, note red unbiotinylated MBD1d band). We found that at P7, the three MBD1 isoforms are all highly expressed in the brain, consistent with a previously reported role for MBD1 in neural stem cells (Liu et al., 2010). Notably, MBD1 is barely detectable in non-neuronal tissues at P7. In addition, the expression of

all MBD1 isoforms is significantly reduced in P42 brains compared to P7 while remaining nearly undetectable in other tissues.

We then assessed MeCP2 and MBD3 expression in P7 and P42 wildtype animals using antibodies against each protein (Figure 3.10). The specificity and reliability of these antibodies allowed us to complete the expression survey. Consistent with previous findings (Shahbazian et al., 2002), we found that MeCP2 is highly expressed in the brain at P7 and P42, but is also expressed relatively highly in the lung and colon. Developmentally, MeCP2 expression is up-regulated in the heart and liver but down-regulated in the lung, kidney and colon in adult tissues, while remaining consistently high in the brain (Figure 3.10.A,B). Strikingly, we found that MBD3 is highly expressed in the brain with weakly detectable expression in the colon at P7 with undetectable expression in all other tissues examined (Figure 3.10.C). Similarly to MBD1 (Figure 3.9.D), MBD3 is significantly downregulated in the brain at P42 while remaining undetectable in all other tissues with the exception of the colon (Figure 3.10.D). These findings are in notable contrast to the expression patterns of MBD2, which is widely expressed in multiple tissue types. Our side-by-side comparison of MBD expression levels reveals that MBD2 is distinct from MBD1, MeCP2, and MBD3 in that it is highly expressed across multiple non-neuronal tissues. In contrast, MBD1, MeCP2, and MBD3 are highly enriched in the brain, consistent with their well-described neuronal functions (Allan et al., 2008; Guy et al., 2001). Our findings on the spatiotemporal expression patterns of the MBD proteins are summarized in Figure 3.11.

Our biotin-tagging approach also allows for direct quantitative comparison of $MBD2^{Tavi}$ and $MBD1^{Tavi}$ protein expression by measuring the streptavidin signal, an approach that is not possible with different antibodies. We quantified the relative expression of $MBD2a^{Tavi}$ and $MBD1a^{Tavi}$ by normalizing the streptavidin signal to the H3 antibody signal for the brain, lung, and colon at P7 and P42, three tissues where both MBD2 and MBD1 expression were detected (average of three representative western blots) (Figure 3.12). This analysis demonstrated that $MBD2a^{Tavi}$ is expressed significantly higher in the lung and colon compared to the brain at both developmental time points, P7 and P42 (Figure 3.12.A). In contrast, $MBD1a^{Tavi}$ is expressed

significantly higher in the brain compared to the lung and colon at P7 and P42 (Figure 3.12.B). We also assessed the temporal expression changes for MBD2a^{Tavi} and MBD1a^{Tavi} specifically in the brain (Figure 3.12.C). We found that MBD2a^{Tavi} expression levels in the brain do not significantly change from P7 to P42, but MBD1a^{Tavi} is significantly down-regulated at P42 compared to P7. In P42 brains, though the expression of MBD2a^{Tavi} is significantly higher than MBD1a^{Tavi}, it is relatively lower than MeCP2 (Figure 3.12.C and 3.10.B). Together, the distinct spatiotemporal expression patterns of MBD2 in comparison to MBD1 and MeCP2 appear to underlie the distinct behavioral phenotypes observed in each individual MBD gene null mouse model.

MBD2 is expressed widely throughout the brain and specifically in small intestine and colon epithelial crypt cells in adult mice

In order to examine MBD2 spatial expression in more detail, we took advantage of the *Mbd2* null allele, which contains a *LacZ* allele that replaces the *Mbd2* coding exon 2 (Hendrich et al., 2001). Therefore, we were able to use *Mbd2*$^{-/-}$ mice with β-gal staining to visualize where endogenous MBD2 is expressed. A similar approach has been used to determine MBD1 expression in the brain, as the *Mbd1* null allele also contains a *LacZ* allele (Zhao et al., 2003). We examined β-gal staining throughout the brain, including the olfactory bulb, prefrontal cortex, striatum, hippocampus, and cerebellum in P60 wildtype and *Mbd2*$^{-/-}$ mice. We also used Nissl staining of adjacent cryosections to visualize the anatomy of each region. In wildtype mice, no β-gal staining is visible, as expected (Figure 3.13.A). In *Mbd2*$^{-/-}$ mice, we observed β-gal staining throughout the brain, which implies that MBD2 is endogenously expressed throughout all brain regions examined here (Figure 3.13.B). Certain regions such as the hippocampus and the cerebellum show intense staining, but this is reflective of higher cell density rather than increased MBD2 expression as increased staining intensity is also observed with Nissl staining. These results corroborate our findings that MBD2 is expressed in the adult mouse brain using western blots to detect MBD2^{Tavi} expression (Figure 3.8).

We also extended our analysis of MBD2 spatial expression to the gastrointestinal tract, as there is evidence that the regulation of DNA methylation is essential in the maintenance of epithelial crypt cells (Sheaffer et al., 2014). Additionally, MBD2 has been proposed to affect tumorigenesis in colorectal cancer models (Sansom et al., 2003). We used the same β-gal staining strategy with *Mbd2*$^{-/-}$ mice as for the brain and examined MBD2 expression in the jejunum of the small intestine and the colon of P60 wildtype and *Mbd2*$^{-/-}$ mice. We found that MBD2 is expressed specifically in the crypt epithelial cells in the small intestine and colon, which house proliferating undifferentiated stem cells (Figure 3.14.A) (Humphries and Wright, 2008; Tan and Barker, 2014). We also verified the spatial expression of MBD2 by fractioning epithelial cells from the small intestine into villi and crypt populations and isolating colon crypt epithelial cells from *R26*$^{BirA/+}$ and *Mbd2*$^{Tavi/Tavi}$*; R26*$^{BirA/+}$ mice for western blot analysis. Using the anti-Avi antibody and streptavidin to detect MBD2^{Tavi} by western blotting, we determined that MBD2 is expressed specifically in the crypt cellular populations of the small intestine and colon with undetectable expression in small intestine villi (Figure 3.14.B). Together, this evidence suggests that in the gastrointestinal tract MBD2 may have a specific role in proliferating crypt epithelial stem cells.

DISCUSSION

In this study, we describe a novel biotin-tagging system for MBD2 and MBD1 and demonstrate the utility of this system for the study of MBD functions *in vivo*. We found that an affinity-tagged allele of MBD2 allows for the detection and immunoprecipitation of MBD2 in order to examine different protein isoforms, *in vivo* binding partners, chromatin localization, and spatiotemporal expression patterns. We found that MBD2 interacts with a distinct set of protein partners compared to MeCP2 *in vivo*, and is anti-correlated with the presence of activating histone marks at certain genomic loci. We also found that MBD2 is highly expressed in many tissues and that MBD2 expression increases significantly in spleen and small intestine in adult

mice. In contrast, MBD1, MeCP2, and MBD3 are primarily expressed in the brain. This study provides new genetic tools and identifies new areas for future studies of MBD function *in vivo*.

To investigate the *in vivo* function and expression of MBD2 in context of the MBD protein family, we used a biotin-tagging approach that we also applied to MBD1 (Figures 3.2 and 3.3). This approach advantageously allows for the precise detection of MBD2 from multiple tissues *in vivo*, while avoiding unreliable antibodies that are especially problematic for MBD2. We were also able to identify multiple isoforms of MBD2 that are not recognized by MBD2 antibodies alone (Figure 3.4). It is especially important to differentiate between the isoforms of MBD2 *in vivo*, as there is strong evidence that different isoforms of MBD2 have different interactions with the NuRD complex and different functions, particularly in ESCs (Lu et al., 2014; Tan and Nakielny, 2006). The MBD2d isoform has been observed in HeLa cells expressing endogenous MBD2 and is consistently identified in all tissues examined in this study (Figure 3.8). Therefore, it is unlikely to be a simple protein degradation product due to technical artifacts and may represent a cleavage event or post-translational modification of MBD2a. This isoform is also unlikely to arise from an alternatively transcribed or spliced transcript because previous examination of MBD2 in cDNA libraries identified only the transcripts corresponding to MBD2a/b and MBD2c (Figure 3.2.A) (Hendrich and Bird, 1998).

Previous studies have established that MBD2 is a key component of the NuRD complex, while MeCP2 is associated with the NCoR/SMRT and SIN3A co-repressor complexes, amongst other functions (Lyst et al., 2013; Nan et al., 1998; Ng et al., 1999; Zhang et al., 1999). However, in the case of MBD2, these results are exclusively from cultured cells and little is known about MBD2 *in vivo* functions. The Tavi-tag approach we developed allowed us to determine that MBD2 is associated with NuRD *in vivo*, and under these conditions has stronger interactions with HDAC1 than MeCP2 (Figure 3.6.A,B). We found essentially equivalent results in the brain, lung, and colon, which suggests that the interactions of MBD2 with NuRD are ubiquitous. There is evidence that post-translational modifications of MBD2a specifically affect NuRD interactions (Tan and Nakielny, 2006). However, our co-immunoprecipitation results do not support this as we

found that all isoforms of MBD2 are associated with the NuRD complex (Figure 3.6.D). It is possible that this specific post-translational modification does not occur in the brain *in vivo*, or that there are additional regulatory mechanisms determining MBD2 interactions with NuRD.

Previous work on the genome-wide binding patterns of MBD2 have been limited to cultured cells, often with over-expressed alleles of MBD2, similar to studies of MBD2 binding partners (Baubec et al., 2013; Günther et al., 2013; Menafra et al., 2014). We used the Tavi-tag approach to perform ChIP-qPCR for MBD2 to better understand where MBD2 is localized *in vivo.* Previous studies have found that MBD2 is localized at areas of high mCG density, but is also associated with active transcription. The localization of MBD2 to actively transcribed sites may depend on interactions with NuRD (Baubec et al., 2013). We found that $MBD2^{Tavi}$ shows reduced binding at the enhancers of constitutively active genes that have activating histone marks compared to gene-poor inactive regions (Figure 3.7). This result supports previously published findings. However, in order to have a complete understanding of MBD2 function additional loci must be examined. The NuRD complex and other co-repressors may function as modulators of transcriptional activity instead of just repressors, which is supported by ChIP-seq data (Baubec et al., 2013; Reynolds et al., 2013). Therefore, it would be informative to compare MBD2 binding at constitutively active genes to genes that have more active modulation of their expression, such as lowly expressed or cell-type specific genes. Additionally, MBD2 binding and mCG density *in vivo* could be examined to determine if MBD2 binds to DNA in a mCG-density dependent manner, as has been shown in ESCs (Baubec et al., 2013).

We also used the Tavi-tag approach to quantitatively analyze the different spatiotemporal expression patterns of MBD2 and MBD1 and compared these results to parallel analysis of MeCP2 and MBD3 using antibodies (Figures 3.8-12). This strategy allowed us to perform a side-by-side, quantitative comparison of MBD2 and MBD1 expression, while avoiding the use of unreliable antibodies for MBD2. Our spatiotemporal expression survey demonstrates that MBD2 is distinct from MBD1, MeCP2, and MBD3 as it is highly expressed in many tissues instead of being primarily expressed in the brain. We also observed that the three isoforms of MBD2 do not

show appreciable differences in expression levels between tissues or temporally, and instead are co-expressed consistently.

In order to gain a more precise spatial map of MBD2 expression in the brain, we performed β-gal staining in *Mbd2*$^{-/-}$ mice (Figure 3.13). Our results show that MBD2 is expressed constitutively throughout all regions of the brain examined. This result is congruent with our western blot data that MBD2 is expressed constitutively when examined at the resolution of western blots with whole tissue lysate (Figure 3.8). The finding that MBD3 is nearly exclusively expressed in the brain result is especially striking, as MBD3 and MBD2 form mutually exclusive complexes with the NuRD complex (Le Guezennec et al., 2006). A recent study found that MBD3, but not MBD2, interacts with a brain-specific NuRD component CHD5, as opposed to CHD4 (Potts et al., 2011). This finding further supports the hypothesis that NuRD-related functions in the brain may be primarily mediated by MBD3 and not MBD2. To extend this hypothesis, it is possible that in peripheral tissues MBD2 is the primary component of NuRD where MBD3 is not expressed. Our results show that MBD2 interacts with NuRD in a ubiquitous fashion across three tissues with variable MBD3 expression (Figure 3.6). Because MBD3 is not expressed or undetectable in these tissues, we hypothesize that NuRD primarily interacts with MBD2 in these cell types.

Our finding that MBD2 expression increases significantly in the spleen and small intestine from P7 to P42 is intriguing in the context of previous studies on the role of MBD2 in immunity and the small intestine (Figure 3.8.C,D) (Berger et al., 2007; Cook et al., 2015; Phesse et al., 2008; Sansom et al., 2003; Wang et al., 2013; Zhong et al., 2014). Precise temporal control of methylation and demethylation is essential for the development and differentiation of both T cells (Sellars et al., 2015) and intestinal epithelial crypt cells (Sheaffer et al., 2014), indicating that MBD2 may contribute to the interpretation of DNA methylation in these tissues. For example, MBD2 has a role in T cell development that is partially dependent on the methylation status of critical genes such as Foxp3 (Lal et al., 2009; Wang et al., 2013). MBD2 can also indirectly affect T cell activation and differentiation through its functions in dendritic cells (Cook et al., 2015).

Interestingly, both MeCP2 and MBD1 have also been implicated in innate and adaptive immunity (Cronk et al., 2015; Theoharides et al., 2015; Waterfield et al., 2014) indicating that MBD family proteins may have a wider role in these systems. However, although it is apparent that NuRD is essential for lymphocyte development, a precise role for MBD3 in these processes has not been identified (Dege and Hagman, 2014b).

In the intestine, loss of MBD2 is linked to altered gene expression (Berger et al., 2007). MBD2 has also been identified as a potential target for cancer therapeutic intervention. Loss of MBD2 is protective against tumorigenesis in a mouse model of colorectal cancer by downregulating Wnt signaling (Phesse et al., 2008; Sansom et al., 2003). In addition, MBD2 contributes to silencing of aberrantly hypermethylated tumor suppressor genes linked to colon cancer (Martin et al., 2008). Our results show that MBD2 is upregulated in the adult small intestine compared to expression at P7 (Figure 3.8.C,D). More specifically, we used parallel approaches to show that MBD2 is expressed in the proliferating, undifferentiated crypt stem cells of the small intestine and colon, and is not detectable in the differentiated epithelial villi cells of the small intestine (Figure 3.14). These results indicate that MBD2 may have a role specifically in undifferentiated, proliferating cells in this tissue. MBD3 has an essential role in maintaining gene expression programs and cell proliferation in the colon (Aguilera et al., 2011). MBD2 may have similar functions in the gastrointestinal tract. However, it is important to note that the histology of the small intestine and colon in *Mbd2*$^{-/-}$ mice appears equivalent to wildtype in our preliminary results and further work is required to characterize any MBD2-related phenotypes in this tissue.

The results of this work reveal many new directions for the study of MBD2 *in vivo* functions. First, further investigation is necessary to characterize the MBD2d isoform we observed in multiple tissues at young and adult time points and to determine if this isoform is biologically relevant (Figure 3.8). For example, certain treatments to remove chemical modifications may reveal if MBD2d is simply an unmodified form of MBD2a that consequentially has a lower molecular weight. Additional work to investigate the *in vivo* binding partners of MBD2 is also required to determine the dynamics of interactions between NuRD and MBD2 or MBD3. A

previous study suggested that most NuRD is in complex with MBD3 and not MBD2 in mammalian cells (Zhang et al., 1999). This may be the case *in vivo* in cell types where MBD2 and MBD3 are co-expressed including the brain and colon, but it is unclear how these interactions may differ in most peripheral tissues where MBD3 expression is very low.

The transgenic mice developed in this study could also be used to further examine MBD2 genome-wide localization patterns using streptavidin-mediated ChIP-seq. This approach would allow for a more thorough characterization of MBD2 localization, especially in conjunction with additional histone mark ChIP-seq analysis. These experiments may be combined with additional ChIP-seq or gene expression analysis in *Mbd2* null mice in order to examine how loss of MBD2 may affect the chromatin state and particularly histone acetylation. The Tavi-tag system can also be modified to allow for cell-type specific biotinylation of the tagged proteins. With conditional expression of BirA biotin ligase under control of a cell-type specific Cre recombinase, any of the experiments described here may be performed in a cell-type specific manner. This approach may be especially applicable to tissues such as the small intestine where MBD2 is expressed in a distinct sub-population of the tissue (Figure 3.14).

In summary, our study describes the *in vivo* binding partners and spatiotemporal expression patterns for MBD2 relative to the related proteins MBD1, MeCP2 and MBD3. We found that MBD2 is associated with a unique set of co-factors compared to MeCP2 *in vivo* and MBD2 localization to chromatin is anti-correlated with activating transcription marks. In contrast to MBD1, MeCP2, and MBD3, MBD2 is widely expressed in non-neuronal peripheral tissues. Our findings provide new insights into the functions of MBD2 and also provide genetic tools to investigate these functions *in vivo.*

CHAPTER 3 FIGURES

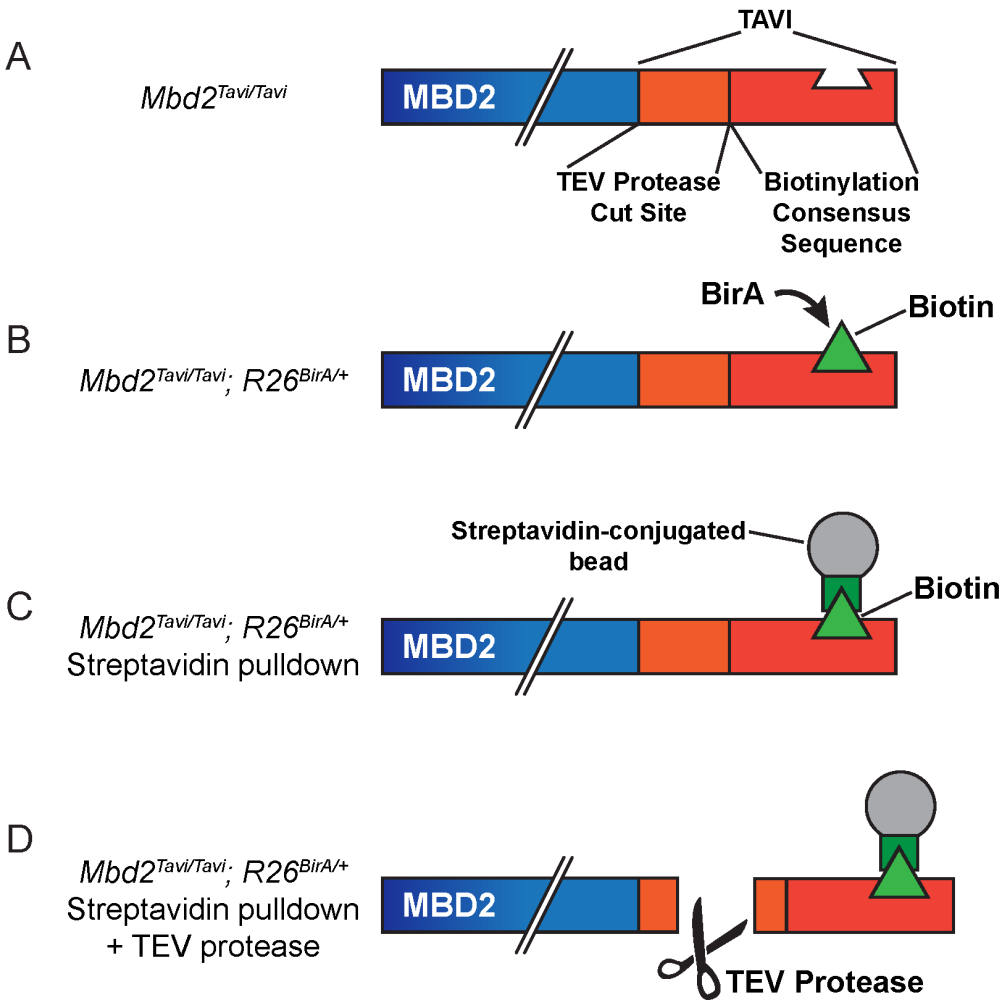

Figure 3.1. Schematic of biotin-affinity tagging approach.
(A) *Mbd2*$^{Tavi/Tavi}$ mice express an allele of MBD2 with a C-terminal biotinylation consensus sequence. **(B)** MBD2^{Tavi} is constitutively biotinylated in the presence of BirA biotin ligase in *Mbd2*$^{Tavi/Tavi}$*; R26*$^{BirA/+}$ mice. **(C)** Biotinylated MBD2^{Tavi} can be pulled down with streptavidin-conjugated beads for further downstream applications. **(D)** Treatment with TEV protease cleaves MBD2^{Tavi} between the endogenous protein coding sequence and C-terminal biotin consensus sequence. Schematic diagrams are not to scale.

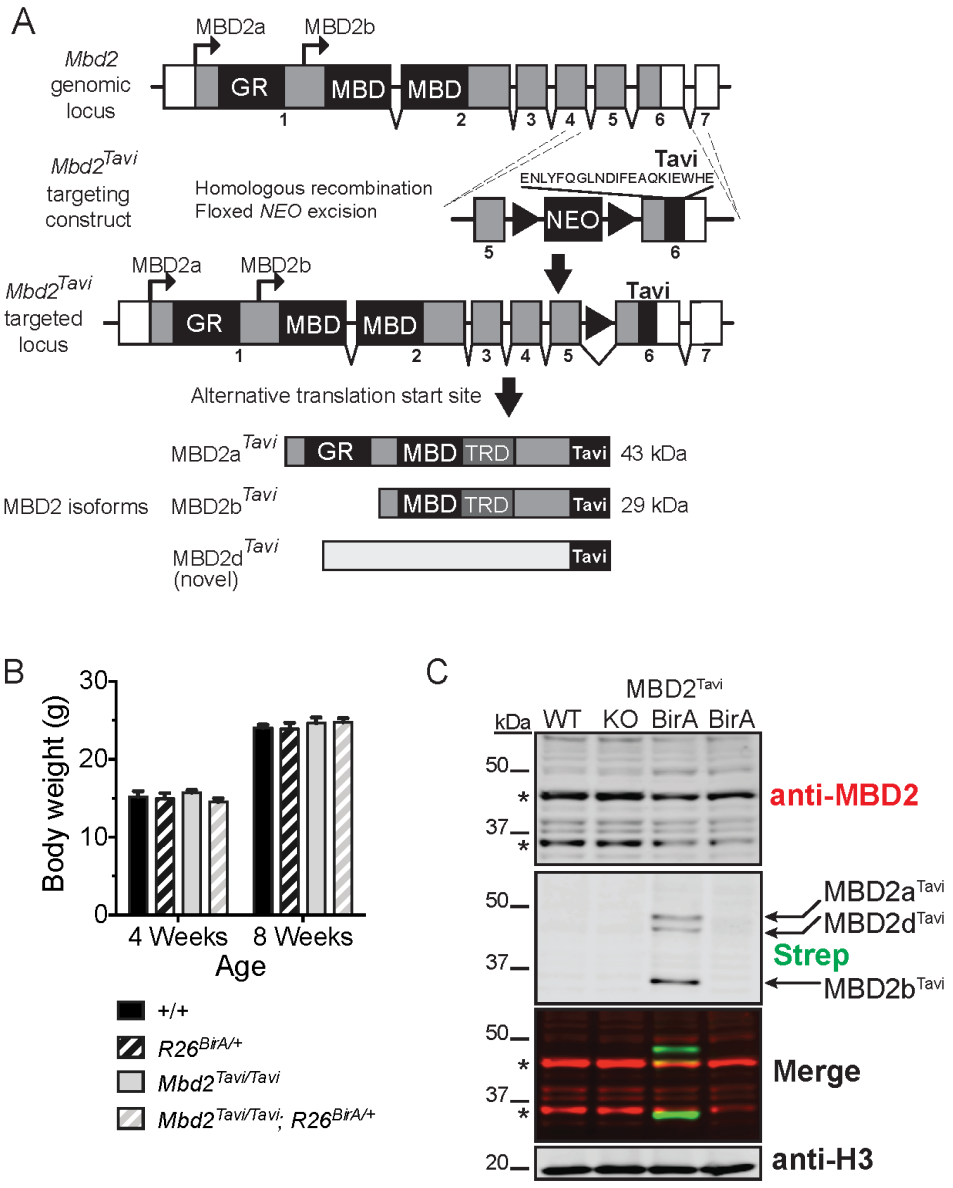

Figure 3.2. Development of *Mbd2*^{Tavi} knockin mice.
(A) Targeting strategy for generating *Mbd2*^{Tavi} knockin mice. The Tavi tag is inserted into exon 6. Two documented isoforms from alternative translation start sites, MBD2a^{Tavi} and MBD2b^{Tavi}, are expressed. A third newly found isoform, MBD2d, is also Tavi-tagged and expressed (GR, GR repeat region; TRD, transcriptional repression domain). **(B)**, *Mbd2*$^{Tavi/Tavi}$ (n = 8) and *Mbd2*$^{Tavi/Tavi}$; *R26*$^{BirA/+}$ (n = 7) mice have equivalent body weight to wildtype (+/+, n = 7) and *R26*$^{BirA/+}$ (n = 5) mice (two-way ANOVA). Data are presented as mean ±SEM. **(C)** Detection of MBD2 isoforms in the brain. An antibody against MBD2 detects cross-reacting bands in wildtype (WT) and *Mbd2*$^{-/-}$ (KO) brain lysate. Three isoforms of MBD2^{Tavi} are specifically biotinylated and detected by streptavidin in *Mbd2*$^{Tavi/Tavi}$; *R26*$^{BirA/+}$, but not *R26*$^{BirA/+}$, brain lysate. Cross-reacting and endogenously biotinylated proteins are denoted by *.

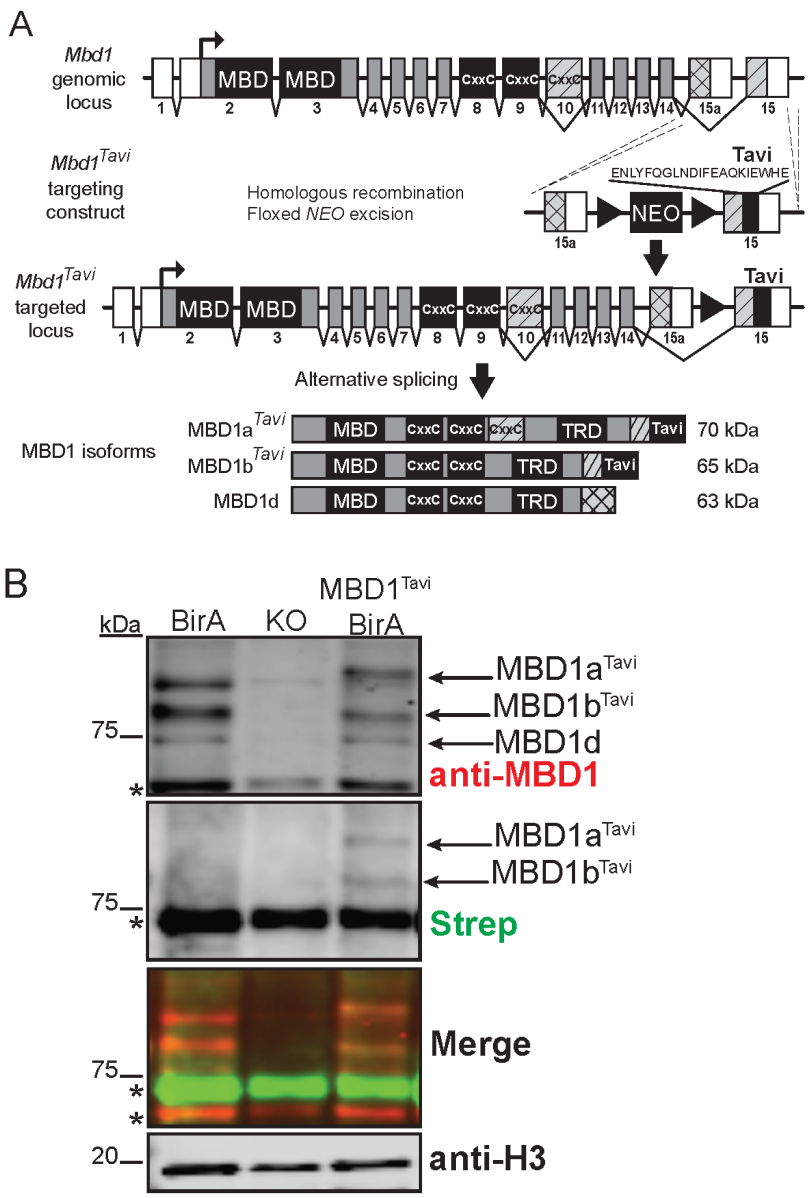

Figure 3.3. Development of *Mbd1^{Tavi}* knockin mice.
(A) Targeting strategy for generating *Mbd1^{Tavi}* knockin mice. The Tavi tag is inserted into exon 15, which is included in MBD1a^{Tavi} and MBD1b^{Tavi}, but not in the alternatively spliced isoform MBD1d (CxxC, CxxC zinc finger DNA-binding domain; TRD, transcriptional repression domain). **(B)** An antibody against MBD1 detects three MBD1 isoforms that are present in *R26$^{BirA/+}$* and *Mbd1$^{Tavi/Tavi}$; R26$^{BirA/+}$*, but not *Mbd1$^{-/-}$* (KO), P7 brain lysate. Two MBD1^{Tavi} isoforms are biotinylated and detected by streptavidin specifically in lysate from *Mbd1$^{Tavi/Tavi}$; R26$^{BirA/+}$* mice (merged image, yellow bands). Cross-reacting and endogenously biotinylated proteins are denoted by *.

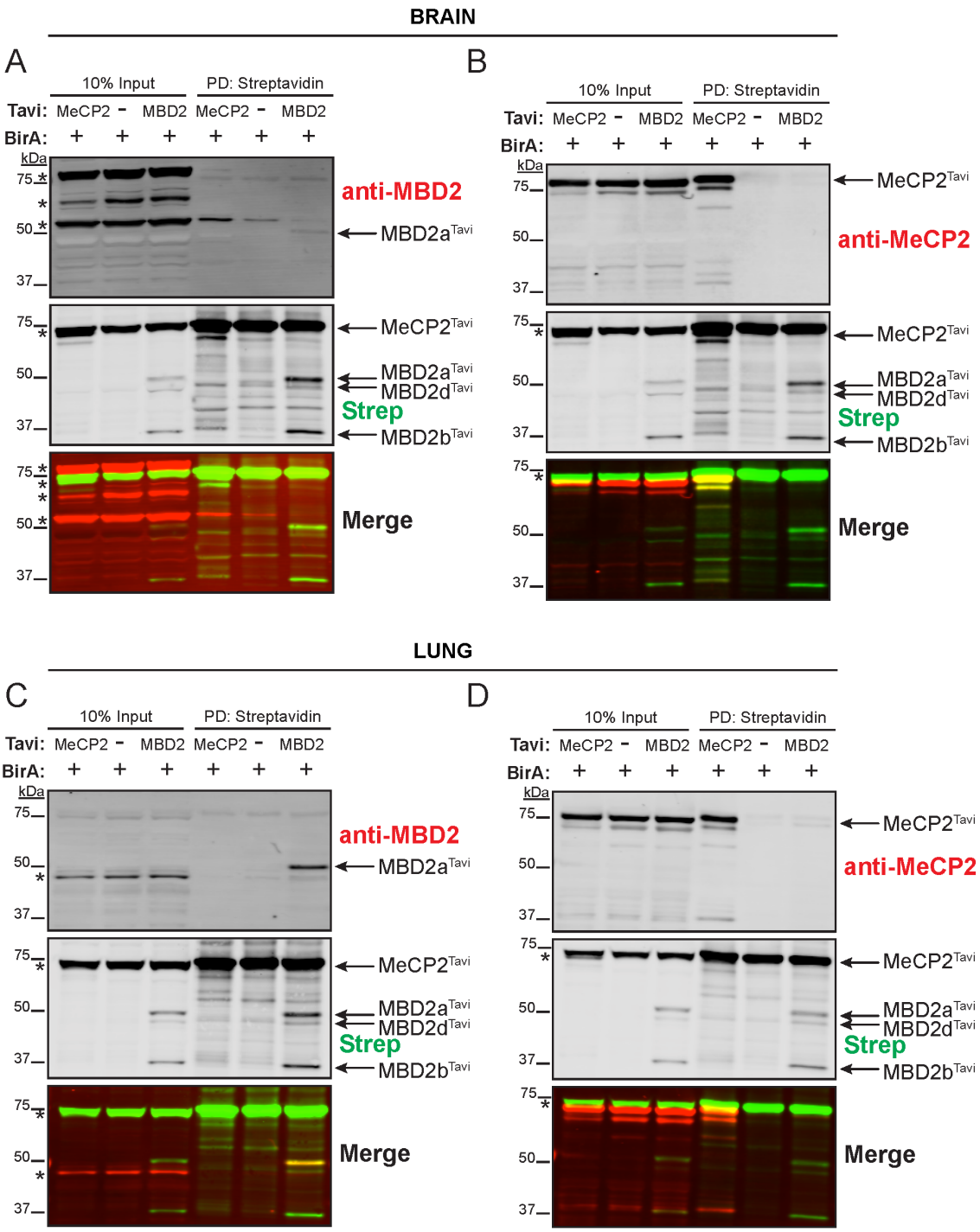

Figure 3.4. Streptavidin-mediated pulldown of biotinylated MBD2^{Tavi} compared to detection of MBD2 with an antibody.

Figure 3.4. Streptavidin-mediated pulldown of biotinylated MBD2^{Tavi} compared to detection of MBD2 with an antibody.
(A) Streptavidin pulldown of biotinylated MBD2^{Tavi} from brain lysate reveals three isoforms of MBD2^{Tavi}. Only MBD2a^{Tavi} is detected by an antibody against MBD2 after enrichment. **(B)** Streptavidin pulldown of MeCP2^{Tavi} from brain lysate shows specific detection of MeCP2^{Tavi} with an antibody against MeCP2. Streptavidin detects an endogenously biotinylated protein at 75kDa that partially obscures MeCP2. **(C)** Streptavidin pulldown of biotinylated MBD2^{Tavi} from lung lysate reveals three isoforms of MBD2^{Tavi}. Only MBD2a^{Tavi} is detected by an antibody against MBD2 after enrichment. **(D)** Streptavidin pulldown of MeCP2^{Tavi} from lung lysate shows specific detection of MeCP2^{Tavi} with an antibody against MeCP2. Cross-reacting and endogenously biotinylated proteins are denoted by *.

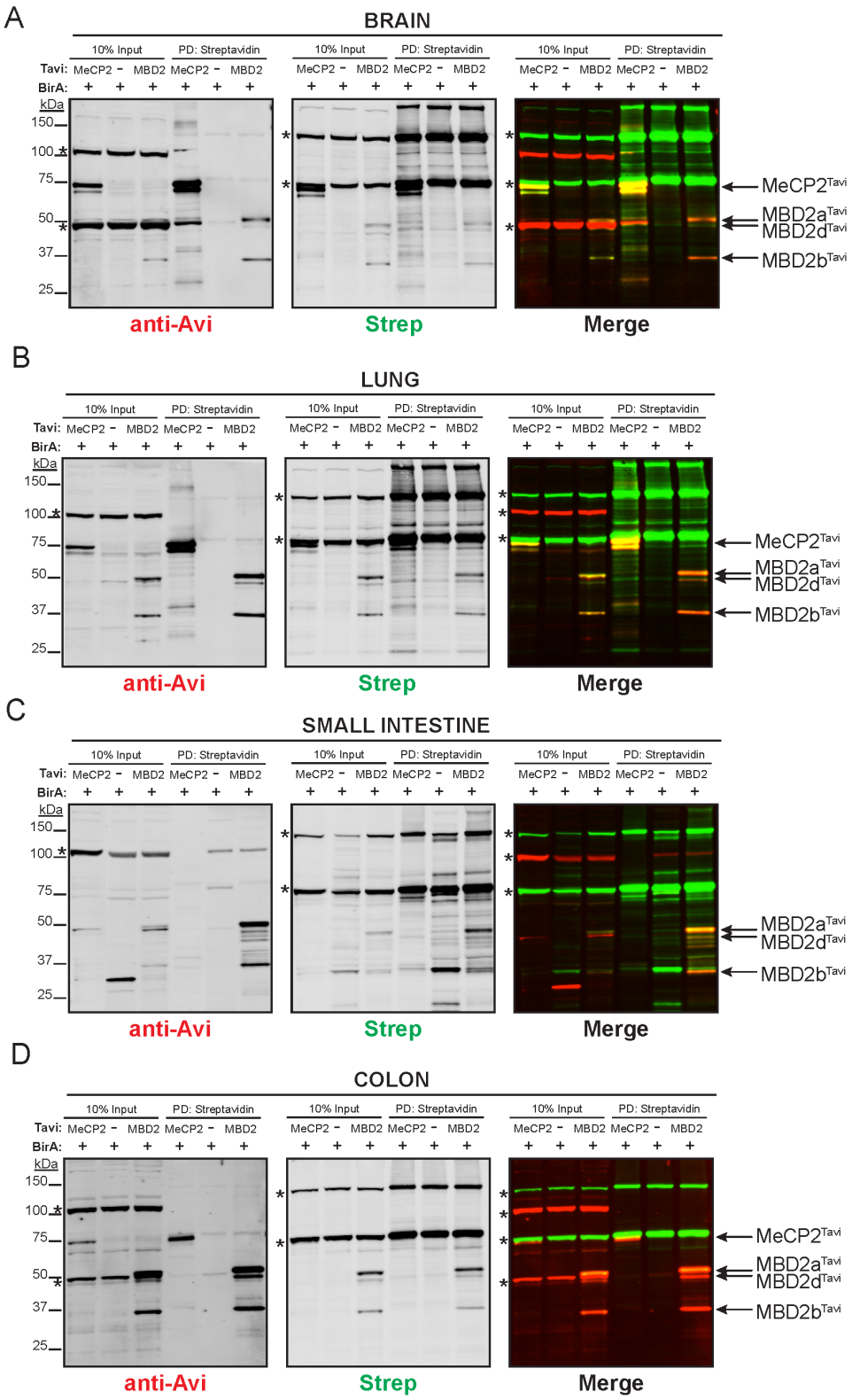

Figure 3.5. Different isoforms of biotinylated MBD2^{Tavi} can be detected with streptavidin in multiple tissues.

Figure 3.5. Different isoforms of biotinylated MBD2^{Tavi} can be detected with streptavidin in multiple tissues.
(A) Streptavidin pulldown and western blot with of biotinylated MBD2^{Tavi} from brain lysate reveals three isoforms of biotinylated MBD2^{Tavi} and biotinylated MeCP2^{Tavi}. In the brain, a non-specific cross-reacting band detected by the Avi antibody partially obscures MBD2a^{Tavi} and MBD2d^{Tavi}. MeCP2^{Tavi} is partially obscured by an endogenous biotinylated protein of 75kDa. **(B)** Biotinylated isoforms of MBD2^{Tavi} and MeCP2^{Tavi} are detected by streptavidin and Avi antibody and enriched with streptavidin pulldown in lung lysate. **(C)** Three isoforms of MBD2^{Tavi} are detected by streptavidin and Avi antibody and enriched with streptavidin pulldown in small intestine lysate. MeCP2 is not detectable in the small intestine. **(D)** Three isoforms of MBD2^{Tavi} and MeCP2^{Tavi} are detected by streptavidin and Avi antibody and enriched with streptavidin pulldown in colon lysate. Cross-reacting and endogenously biotinylated proteins are denoted by *.

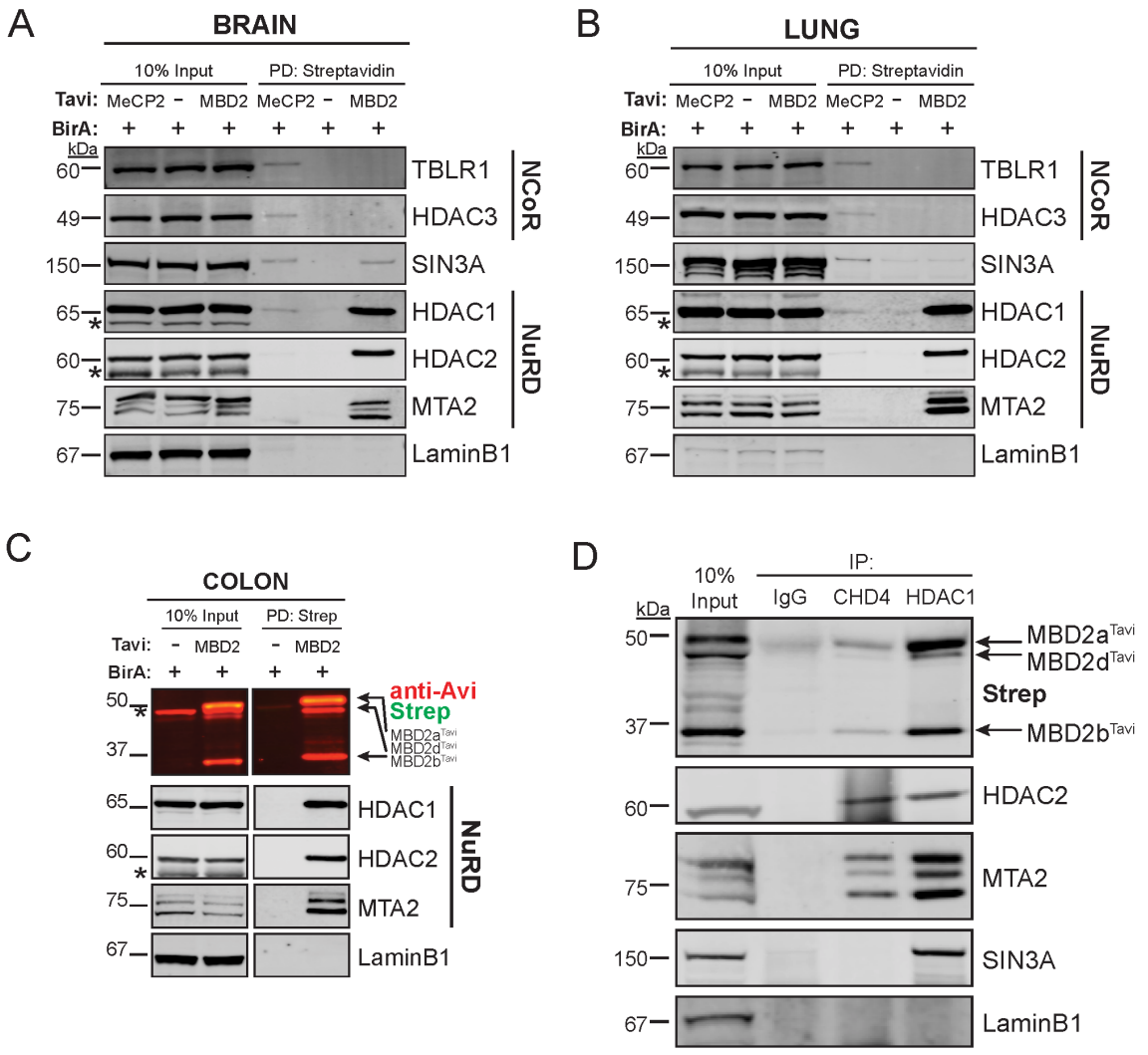

Figure 3.6. Distinct *in vivo* binding partners of MBD2 and MeCP2 in the brain and lung and ubiquitous MBD2-NuRD interactions across tissues.
Streptavidin pulldown and western blot from brain **(A)** and lung **(B)** lysate shows strong interactions between MBD2^{Tavi} and components of the NuRD complex, including HDAC1, HDAC2 and MTA2. MBD2^{Tavi} interacts weakly with SIN3A. MeCP2^{Tavi} interacts with the NCoR complex, including TBLR1 and HDAC3, and weak interaction with HDAC1 and SIN3A. Neither protein interacts with LaminB1 as expected. **(C)** MBD2 interacts with the NuRD complex in the colon similarly to the brain and lung. **(D)** Three isoforms of MBD2^{Tavi} are co-immunoprecipitated with components of the NuRD complex, including CHD4 and HDAC1. MBD2^{Tavi} shows weaker interaction with CHD4 compared to HDAC1. Interactions between other components of the NuRD complex, including HDAC2 and MTA2, and between HDAC1 and SIN3A were verified as controls. Cross-reacting and endogenously biotinylated proteins are denoted by *.

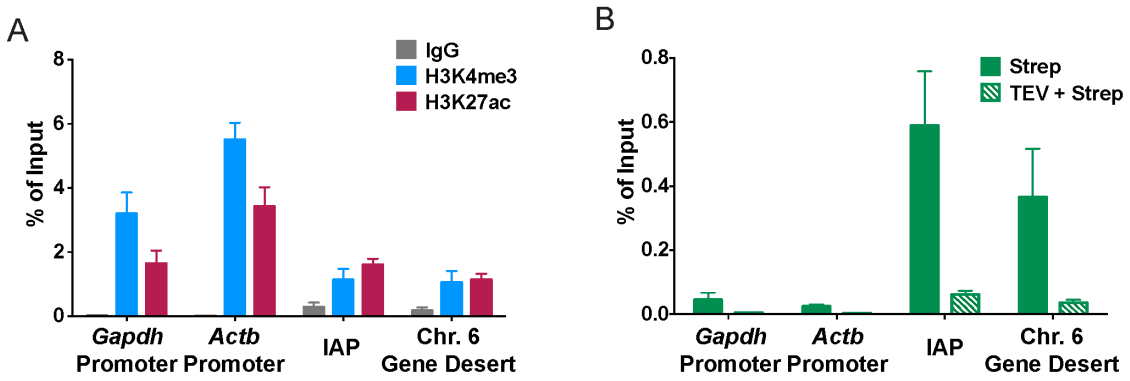

Figure 3.7. MBD2 is depleted at genomic loci with activating histone marks.
(A) ChIP-qPCR analysis in the cortex of adult *Mbd2*$^{Tavi/Tavi}$*; R26*$^{BirA/+}$ mice for activating histone marks H3K4me3 and H3K27ac shows enrichment at constitutively expressed loci, including the *Gapdh* and *Actb* promoters, and relatively lower enrichment at transcriptionally inactive regions, including IAP elements and a gene desert region of chromosome 6 (*n* = 3 biological replicates). **(B)** Streptavidin ChIP-qPCR in the cortex of adult *Mbd2*$^{Tavi/Tavi}$*; R26*$^{BirA/+}$ mice shows MBD2^{Tavi} is enriched at transcriptionally repressed repetitive and intergenic regions, and depleted at loci with enrichment of activating histone marks including *Gapdh* and *Actb* promoters. Pre-treatment with TEV protease cleaves the Tavi tag and returns the ChIP signal to background levels, demonstrating specificity of streptavidin ChIP with Tavi-tagged MBD2 (*n* = 3 biological replicates).

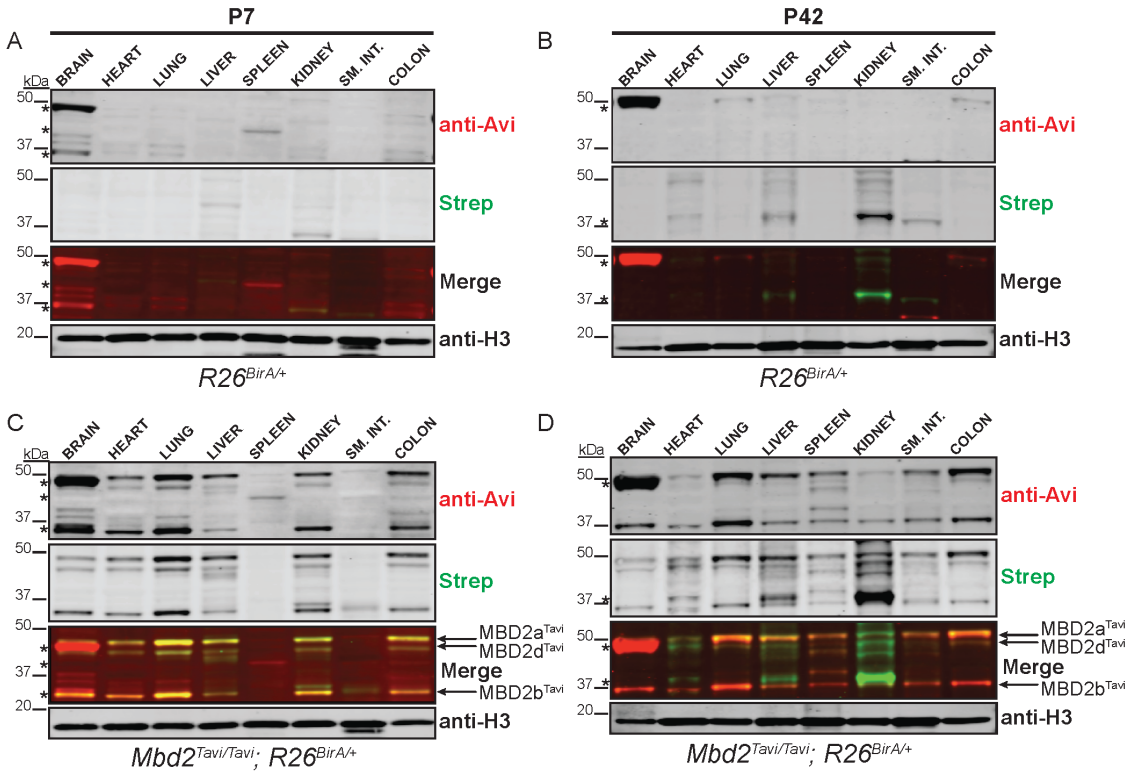

Figure 3.8. Spatiotemporal expression of MBD2 at P7 and P42.
(A) and **(B)** Western blot analysis with lysate from *R26*$^{BirA/+}$ mice reveals cross-reacting proteins detected by the Avi antibody and endogenously biotinylated proteins detected by streptavidin, denoted by *. **(C)** and **(D)** Three isoforms of MBD2^{Tavi} (MBD2a^{Tavi}, MBD2b^{Tavi} and MBD2d^{Tavi}) are biotinylated and detected by streptavidin and the Avi antibody. All isoforms of MBD2^{Tavi} are highly expressed throughout the body at P7, but are not expressed in spleen and small intestine. All isoforms of MBD2^{Tavi} are highly expressed throughout the body at P42, with up-regulation in spleen and small intestine compared to P7.

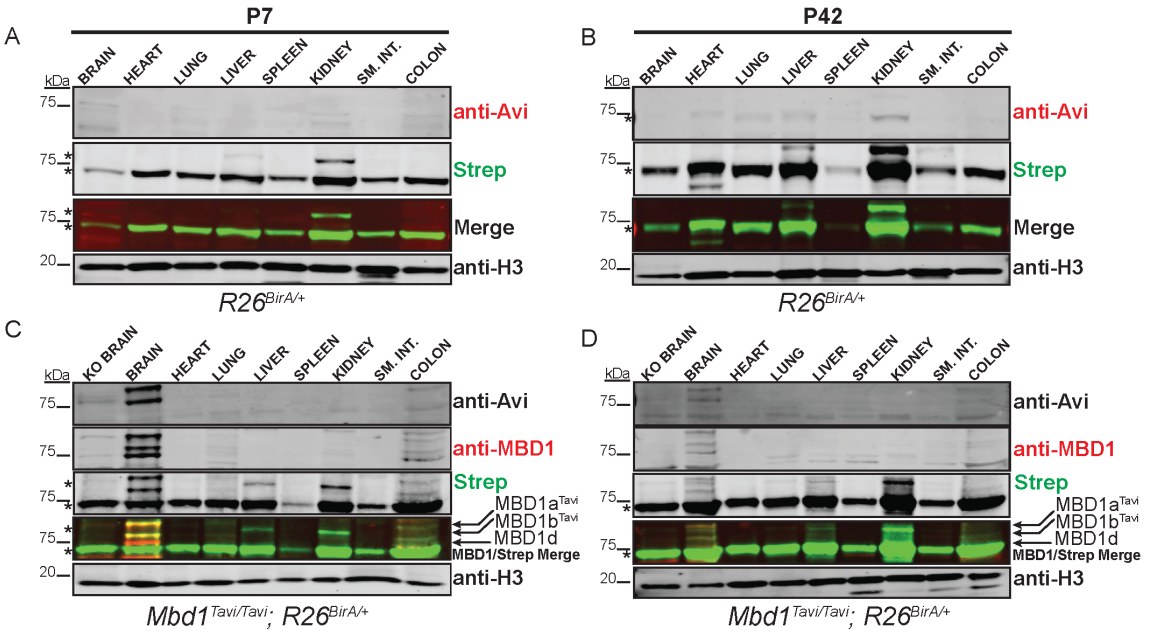

Figure 3.9. Spatiotemporal expression of MBD1 at P7 and P42.
(A) and **(B)** Western blot analysis with lysate from *R26*$^{BirA/+}$ mice reveals cross-reacting proteins detected by the Avi antibody and endogenously biotinylated proteins detected by streptavidin, denoted by *. **(C)** and **(D)** Two isoforms of MBD1^{Tavi} (MBD1a^{Tavi} and MBD1b^{Tavi}) are biotinylated and detected by the Avi antibody and streptavidin. An antibody against MBD1 also detects MBD1d, compared to *Mbd1* null brain lysate (KO brain). All three isoforms are highly expressed in the brain and show down-regulation at P42 compared to P7.

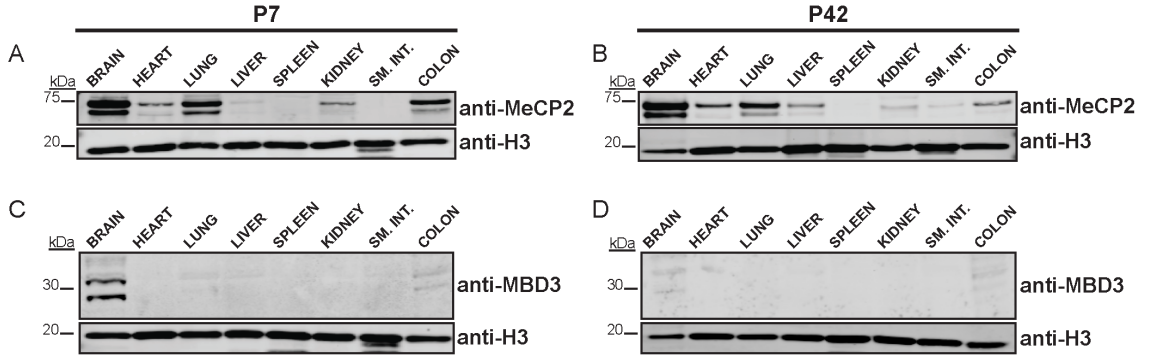

Figure 3.10. MeCP2 is consistently highly expressed in the brain while MBD3 is downregulated in the adult brain.
(A) and **(B)**, MeCP2 is highly expressed in the brain at P7 and P42 as detected by an antibody against MeCP2 using lysate from wildtype animals. MeCP2 is also expressed in other tissues including the lung and colon. **(C)** and **(D)**, MBD3 is highly expressed as a doublet band in the brain at P7 with lowly detectable expression at P42. MBD3 is also lowly detectable in the colon at P7 and P42.

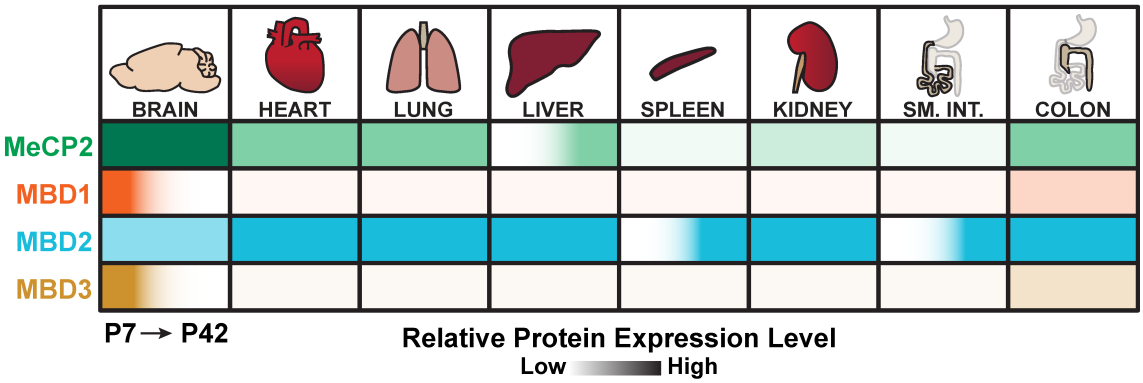

Figure 3.11. Summary of MBD protein spatiotemporal expression patterns.
In the brain, MeCP2, MBD1, MBD2 and MBD3 are highly expressed at P7, but only MeCP2 and MBD2 remain highly expressed at P42. In other tissues, MBD1 and MBD3 are undetectable with the exception of the colon. MBD2 is highly expressed across all tissues examined, and is upregulated in the spleen and small intestine at P42 compared to P7.

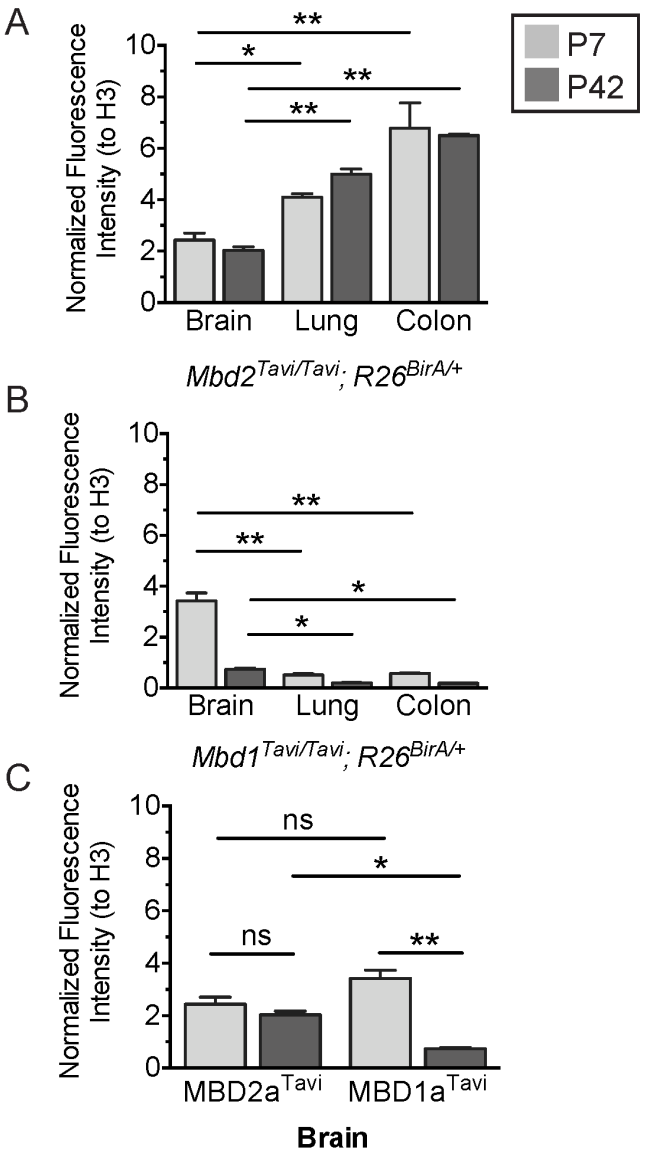

Figure 3.12. Quantification of MBD2a^{Tavi} and MBD1a^{Tavi} expression levels.
Expression levels of biotinylated MBD2a^{Tavi} and MBD1a^{Tavi} were determined by normalizing the fluorescence levels of streptavidin to H3 (average of three representative western blots). **(A)** MBD2a^{Tavi} is expressed significantly higher in the lung and colon compared to the brain at P7 and P42 (*P < 0.05, **P < 0.01, two-way ANOVA with Tukey's test). **(B)** MBD1a^{Tavi} is expressed significantly higher in the brain compared to the lung and colon at P7 and P42 (*P < 0.05, **P < 0.01, two-way ANOVA with Tukey's test). **(C)** MBD2a^{Tavi} expression in the brain does not significantly change from P7 to P42, but MBD1a^{Tavi} is significantly down-regulated in the brain at P42 compared to P7. At P42, MBD2a^{Tavi} is expressed significantly higher than MBD1a^{Tavi} in the brain (ns not significant, *P < 0.05, **P < 0.01, two-way ANOVA with Holm-Sidak multiple comparison test). All data are presented as mean ±SEM.

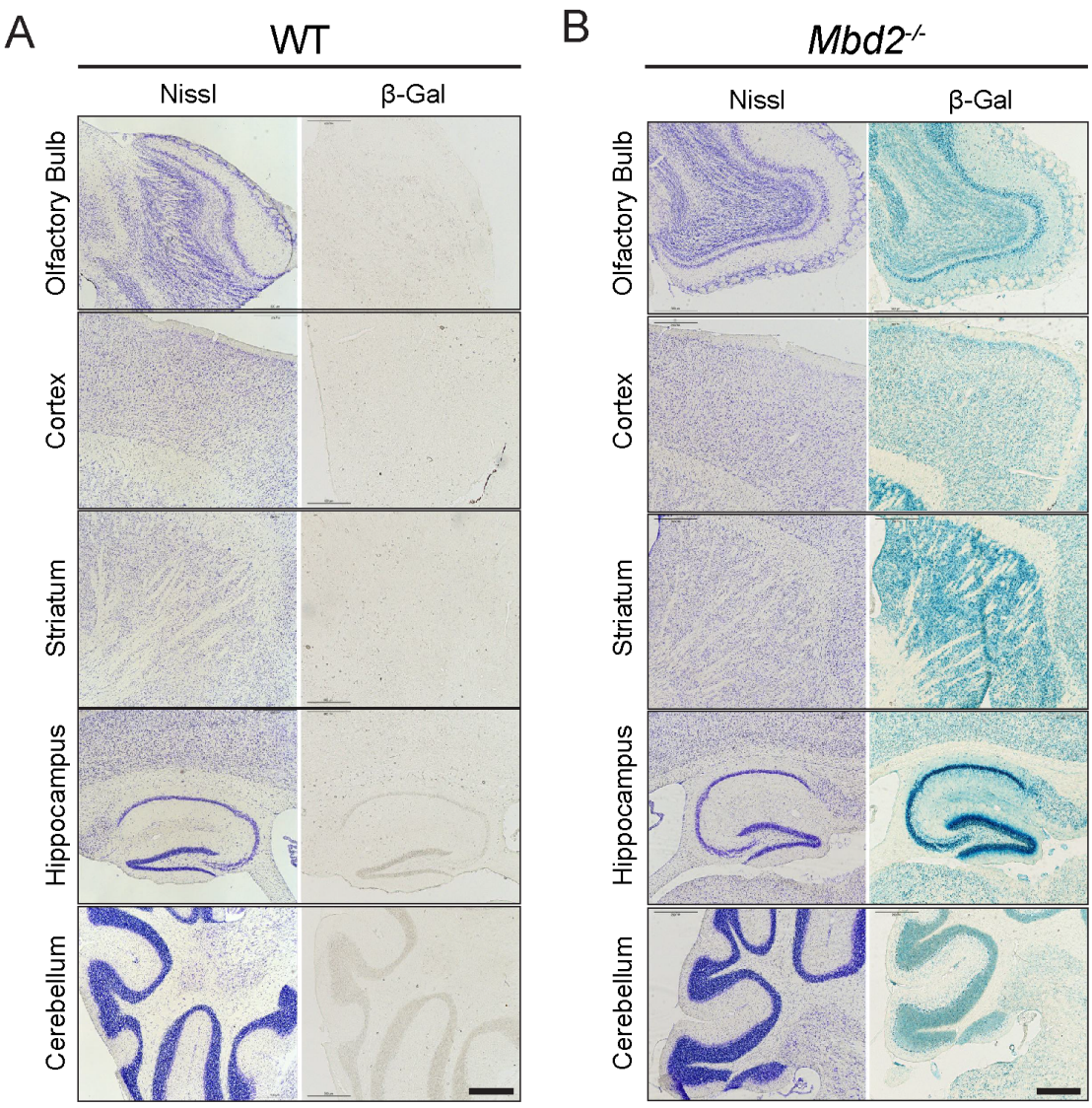

Figure 3.13. MBD2 expression throughout the adult brain is visualized with β-gal staining. **(A)** Representative β-gal staining of brain regions from P60 wildtype mice shows no staining (right). Nissl staining (left) allows for visualization of the tissue structure. **(B)** Representative β-gal staining of brain regions from P60 *Mbd2*$^{-/-}$ mice shows that MBD2 is expressed throughout all brain regions examined, including the olfactory bulb, cortex, striatum, hippocampus, and cerebellum (right). Nissl staining (left) allows for visualization of the tissue structure. Scale bars correspond to 500μm.

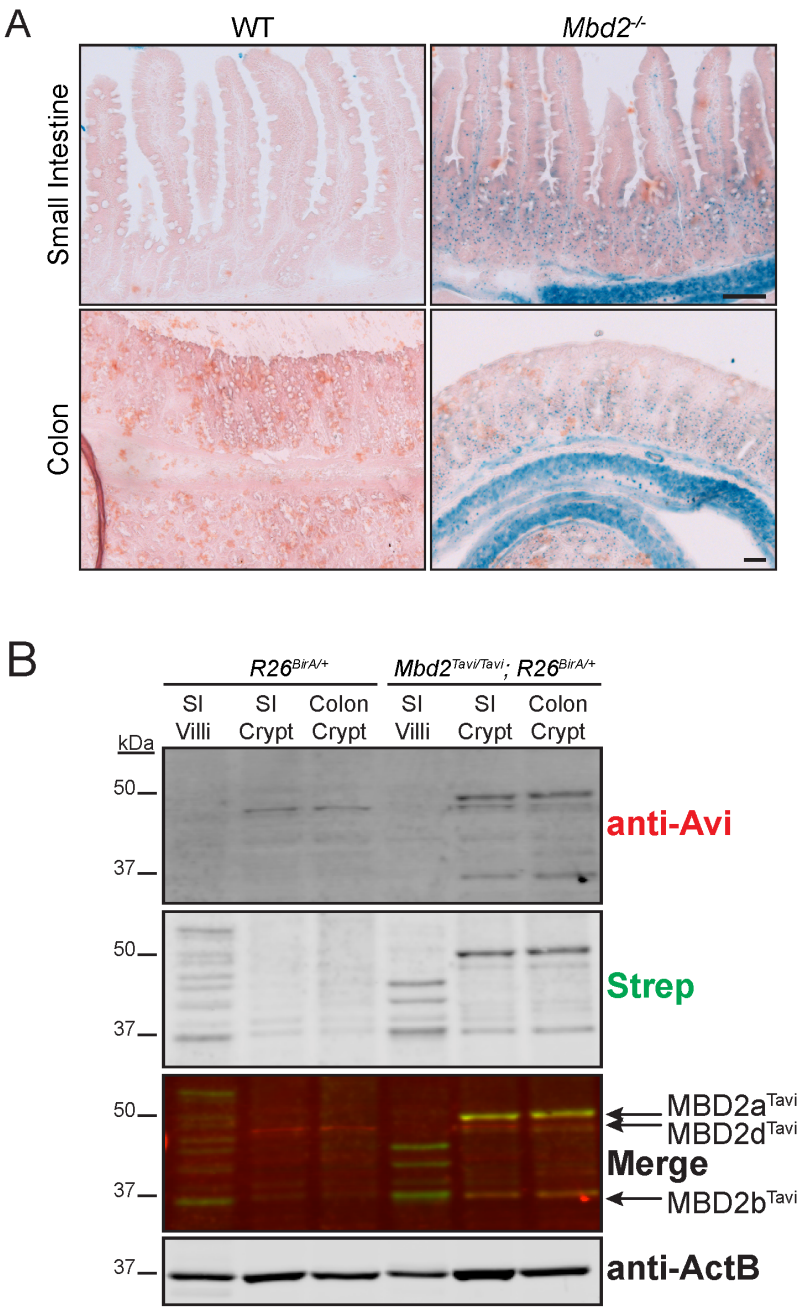

Figure 3.14. MBD2 is expressed specifically in epithelial crypt cells of the gastrointestinal tract.

(A) Representative β-gal staining of the small intestine (SI) and colon in P60 wildtype and *Mbd2*$^{-/-}$ mice. There is no staining in wildtype animals, and staining primarily in the epithelial crypt cells of both tissues in *Mbd2*$^{-/-}$ mice. **(B)** Western blot analysis of spatial expression of MBD2^{Tavi} in the small intestine and colon shows that MBD2 is primarily expressed in the epithelial crypt cells of both tissues with no detectable expression in villi epithelial cells. Scale bars correspond to 50μm.

CHAPTER 4: Discussion and Future Directions

In summary, I describe in Chapter 2 the results of the first thorough characterization of *Mbd2* null mice, with emphasis on behavioral phenotypes affected by related MBD proteins. In Chapter 3, I present my work on the generation of two novel transgenic mice with biotin-tagged endogenous MBD2 or MBD1. I also show the utilization of these mice to explore MBD2 functions and spatiotemporal expression in the context of the MBD protein family. Together, this study shows several unexpected findings and reveals new insights into MBD2 function *in vivo*. These results elucidate new directions and provide novel genetic tools for further study of MBD2 functions.

Interpretation of *Mbd2* null mice phenotypes

The majority of MBD proteins have been implicated in brain function in human disease and mouse models. Of the MBD proteins, MeCP2, MBD1 and MBD3 are arguably the most similar to MBD2 in terms of their DNA binding properties or co-repressor interactions (Baubec et al., 2013; Le Guezennec et al., 2006). All of these MBD proteins, and also MBD5, which does not bind to methylated DNA but is associated with heterochromatin, have been shown to directly affect neuronal functions. All of these MBD protein null mice, with the exception of brain-specific *Mbd3* null mice which are perinatal lethal, also have notable behavioral deficits in addition to underlying cellular phenotypes (Allan et al., 2008; Camarena et al., 2014; Guy et al., 2001; Knock et al., 2015; Zhao et al., 2003). It is also well established that DNA methylation and co-repressor protein activity, such as histone deacetylases associated with NuRD or the NCoR complexes, are essential for brain function (Guan et al., 2009; Guo et al., 2011; McQuown et al., 2011). Due to these findings, researchers in the MBD protein field have speculated that MBD2 may have similar brain-related functions (Baubec and Schübeler, 2014; Du et al., 2015). Prior to my thesis work, the only described behavioral or potentially brain-related phenotype of *Mbd2* null (*Mbd2*$^{-/-}$) mice was impaired pup nurturing and retrieval (Hendrich et al., 2001). This maternal behavior

phenotype has been referenced to support a role for MBD2 in brain function and behavior, although these phenotypes have complex etiologies (Du et al., 2015; Gammie, 2005).

With this evidence, it is surprising that we found *Mbd2*$^{-/-}$ mice are equivalent to wildtype and heterozygous littermates in most behavioral tests. *Mbd2*$^{-/-}$ mice show subtle changes on several behavioral tests and other measures, including home-cage hypoactivity, impaired nesting, low body weight associated with hypophagia, altered hypothalamic peptide expression, and few changes in striatal gene expression. These phenotypes are complex, multigenic, and interdependent, and therefore interpretation of their etiologies is challenging. Additionally, these phenotypes may be partially dependent on MBD2 functions in peripheral tissues. Specifically, MBD2 has been shown to affect gene expression in the gastrointestinal tract and in multiple immune cell types (Berger et al., 2007; Cook et al., 2015; Wang et al., 2013).

Assuming that loss of MBD2 does have effects in peripheral tissues, this further complicates the interpretation of these phenotypes because these systems are interrelated. First, the gastrointestinal system has an essential role in immune system homeostasis (Macdonald and Monteleone, 2005). In addition, body weight is inexorably linked to energy homeostasis (Tou and Wade, 2002), which could in turn affect activity levels to produce the hypoactivity and nesting deficits we observed in *Mbd2*$^{-/-}$ mice. The results of the RNA-seq study to identify differentially expressed genes (DEGs) in the striatum of *Mbd2*$^{-/-}$ mice support that immune and metabolic phenotypes may be co-occurring to indirectly affect neuronal or behavioral outcomes. Two DEGs with a greater than 2-fold change increase in expression are transthyretin (*Ttr*) and lipocalin2 (*Lcn2*), which are both linked to responses to inflammatory, nutritional, or neural injury stress (Buxbaum and Reixach, 2009; Lee et al., 2009). Therefore, dysfunction in several systems upon constitutive loss of MBD2 could have a synergistic effect on body weight, food intake, and activity phenotypes.

The complexities of these phenotypes could be resolved with additional research. Specifically, *Mbd2* conditional null mice could be used to isolate tissue- or cell-type specific MBD2 functions. For example, by crossing a floxed-*Mbd2* allele to a mouse expressing Villin-Cre

recombinase (Madison et al., 2002) it would be possible delete *Mbd2* exclusively from the entire intestinal epithelium. Further examination of body weight, food intake and metabolic phenotypes between this mouse and the constitutive *Mbd2*$^{-/-}$ mouse could reveal if low body weight is linked directly to intestinal phenotypes. A similar approach could be taken to examine MBD2-related phenotypes in lymphoid cell types. For instance, a mouse expressing Cre recombinase specifically in FoxP3+ cells (Zhou et al., 2008) could be used to ablate MBD2 expression in Treg cells. These cell-type specific approaches may be especially relevant to study MBD2 in immune cell types, as MBD2 acts in multiple cell types that influence each other's maturation and function, such as CD4+ T cells and dendritic cells (Aoki et al., 2009; Cook et al., 2015).

Precedents for altered leptin or glucocorticoid receptor signaling in *Mbd2* null mice

It is possible that the phenotypes observed in *Mbd2*$^{-/-}$ mice do have neuronal origins that were not fully elucidated by the experiments described here. First, MBD2 may be affecting the regulation of hypothalamic leptin signaling, which in turn could affect food intake, activity levels, and body weight. We found that hypothalamic orexigenic and anorexigenic peptides showed altered expression in *Mbd2* mice, although our findings are not representative of a typical pattern of misregulation associated with reduced body weight in other mouse models (Yang et al., 2014a). Hypothalamic regulation of energy expenditure is regulated primarily by leptin and other nutritional signaling (Myers et al., 2008). Transthyretin, which is significantly upregulated in the striatum of *Mbd2*$^{-/-}$ mice, is also affected by leptin levels which supports that these mice may have altered leptin signaling (Rendenbach et al., 2013). Previous studies have shown that MeCP2 affects hypothalamic gene expression and hypothalamic leptin signaling (Ben-Shachar et al., 2009; Torres-Andrade et al., 2014). Furthermore, there is evidence that hypothalamic leptin expression in response to diet-induced obesity is directly regulated through DNA methylation and MBD2-related mechanisms (Shen et al., 2014). Therefore, additional experiments are warranted to determine if leptin is misregulated in *Mbd2*$^{-/-}$ mice. It would also be critical to identify if any leptin-related phenotypes are hypothalamic, other neuronal, or peripheral in origin.

Another possible neuronal origin for *Mbd2*$^{-/-}$ phenotypes is the misregulation of glucocorticoid receptor (GR) signaling. In this study, we hypothesized that altered striatal dopamine signaling may underlie many of the phenotypes of *Mbd2*$^{-/-}$ mice, as highly similar phenotypic profiles have been observed in mice with genetic or pharmacological disruption to this system (Gammie et al., 2008; Henschen et al., 2013; Jager et al., 2014; Palmiter, 2008). However, analysis of biogenic amine levels in the cortex and striatum showed that dopamine and its metabolites are equivalent between wildtype and *Mbd2*$^{-/-}$ mice. An alternative, parallel hypothesis is that altered GR signaling in *Mbd2*$^{-/-}$ mice could contribute to the maternal nurturing deficits and possibly other observed phenotypes in *Mbd2*$^{-/-}$ mice (Hendrich et al., 2001).

Maternal licking and grooming behaviors drive increased expression of GR in the hippocampus, which in turn affects the regulation of stress responses through the hypothalamic–pituitary–adrenal (HPA) axis (Liu et al., 1997). Maternal behavior is strongly influenced by stress, adverse events or other environmental cues and these behaviors can trans-generationally influence maternal behavior of female offspring through epigenetic mechanisms (Francis et al., 1999). The expression of GR in the hippocampus is regulated through methylation of the exon 1_7 promoter and recruitment of activating transcription factors, including nerve growth factor-inducible protein A (NGFI-A). Epigenetic changes at the GR exon 1_7 promoter in response to early environmental cues can persist into adulthood to affect stress responses (Weaver et al., 2004).

A recent study showed that MBD2 expression is upregulated in the hippocampus in response to maternal licking and grooming, and MBD2 is required for NGFI-A-dependent activation of GR expression. Interestingly, the GR exon 1_7 promoter is generally silenced by DNA methylation, but MBD2 and NGFI-A binding activates GR expression. This regulation appears to be MBD2-specific, as MeCP2 was not found to interact with the GR exon 1_7 promoter (Weaver et al., 2014). These findings evoke the similar mechanism of FoxP3 regulation in Treg cells, which is generally silenced by DNA methylation but becomes demethylated and actively transcribed dependent on MBD2 and TET-2 activity (Wang et al., 2013). However, it is unknown if activation

of GR is concurrent with demethylation of the exon 1_7 promoter in a similar MBD2-dependent manner. According to this model, a female *Mbd2*$^{-/-}$ mouse born to a heterozygous mother would have an attenuated GR expression response to maternal behavior, leading to long-term epigenetic changes at the GR locus. These epigenetic changes could in turn affect this *Mbd2*$^{-/-}$ female mouse's own maternal nurturing behaviors, as has been observed in female rats whose dams were exposed to environmental stress (Francis et al., 1999; Liu et al., 1997; Weaver et al., 2004).

Furthermore, if GR signaling is altered in other cell types in *Mbd2*$^{-/-}$ mice, this misregulation could have widespread phenotypic effects. Glucocorticoid signaling is regulated by the HPA axis in response to stress and circadian signals through ubiquitously expressed GRs (Kadmiel and Cidlowski, 2013). The specificity of glucocorticoid signaling throughout the body is achieved by tightly regulated cell-type specific expression levels and post-translational modification of different GR isoforms. The GR locus has multiple alternative first exons corresponding to different cell-type specific isoforms, each with their own promoter that is regulated through DNA methylation and transcription factor binding (Turner et al., 2010).

It is possible that MBD2 regulates methylation-dependent GR expression in other cell types similarly to the hippocampus. GR signaling is systemic and has broad anti-inflammatory, anti-proliferative, pro-apoptotic, and anti-angiogenic effects on nearly every organ or system in the body. GR signaling has been shown to affect stress responses, inflammatory responses, glucose and lipid regulation, and general systemic homeostasis (Kadmiel and Cidlowski, 2013). Therefore, it is conceivable that reduced or altered GR signaling in *Mbd2*$^{-/-}$ mice could underlie many of this mouse model's subtle, non-specific phenotypes, including impaired nurturing, hypoactivity, gene expression changes corresponding to stress or inflammation, and low body weight.

Potential functional redundancy amongst MBD proteins

Our results showed that loss of MBD2 surprisingly has only subtle effects on behavior that may be related to non-neuronal, systemic phenotypes, which suggests that MBD2 may be dispensable for brain function. However, our biochemical and spatiotemporal data show that MBD2 is expressed at young and adult ages and interacts with the NuRD complex in the brain, suggesting an active role. There are several possible models to address this discrepancy. First, it is possible that MBD2 does impair neuronal functions, but these changes may be too subtle or in too small a population of cells to produce robust changes in behavior. For example, loss of MBD2 affects maturation and proliferation of olfactory receptor neurons, but *Mbd2*$^{-/-}$ mice appear to have unaffected olfactory ability (Macdonald et al., 2010). Another possibility is that MeCP2, which is very highly expressed in the brain throughout development, is able to compensate for loss of MBD2 in the brain. Alternatively, it has been proposed that the MBD family proteins may be functionally redundant because transcriptional repression is generally maintained in single MBD null models (Baubec and Schübeler, 2014).

Our findings, as they stand alone, support the model of compensation or functional redundancy in regard to the role of MBD2 and other MBD proteins specifically in the brain. Our data on the spatiotemporal expression of the MBD proteins shows that the brain is unique in having relatively high levels of MeCP2, MBD1, MBD2 and MBD3 expression compared to other tissues, particularly at younger ages. Therefore it is possible that loss of MBD2 alone in this tissue may not cause severe disruptions. MeCP2, which is expressed very highly in the brain and is essential for brain function (Guy et al., 2001; Skene et al., 2010), may be the predominant MBD protein in this tissue and therefore could be able to compensate for loss of MBD2. Our co-pulldown results and previous studies show that MBD2 and MeCP2 have certain overlaps in their co-repressor protein interactions. Specifically, MBD2 and MeCP2 both interact with HDAC1 and SIN3A (Boeke et al., 2000; Nan et al., 1998) in addition to binding to DNA in a mCG-density dependent manner (Baubec et al., 2013). However, MeCP2 would not necessarily be able to compensate for all MBD2-specific functions with NuRD, as MeCP2 does not interact with all members of this complex.

However, genetic evidence argues that the MBD proteins are not able to fully compensate for each other. Loss of each MBD protein produces distinct phenotypes in mice, emphasizing the unique role for each MBD protein (Allan et al., 2008; Guy et al., 2001; Hendrich et al., 2001). Loss of both MBD2 and MeCP2 decreases survivability compared to loss of MeCP2 alone (Martín Caballero et al., 2009). Similarly, loss of MBD2 in mice heterozygous for a *Mbd3* null allele resulted in decreased viability compared to *Mbd3* heterozygous mice with wildtype MBD2 expression (Hendrich et al., 2001), indicating that MBD2 has other functions for which MeCP2 and MBD3 are unable to compensate. There is currently no information on the phenotype of mice null for both MBD1 and MBD2, which would help clarify any potential interactions between these two MBD proteins. This has been difficult to achieve because the two genes are less than 4 Mb apart on the same chromosome. A double null mouse for *Mbd2* and *Mbd3* would also be informative, but may be impossible to achieve because constitutive loss of MBD3 is embryonic lethal, while brain-specific ablation of MBD3 is perinatal lethal (Hendrich et al., 2001; Knock et al., 2015).

The argument that the MBD proteins are functionally redundant at the molecular level is most applicable to MBD2 and MBD3, which are very closely related both in their protein structure and as components of the NuRD complex (Hendrich and Bird, 1998; Le Guezennec et al., 2006). However, genetic and biochemical evidence suggests that MBD2 and MBD3 have quite distinct properties, which argues against this model. Despite the high level of conservation between MBD2 and MBD3, these proteins have entirely different DNA-binding capabilities, which is reflected in their distinct genome-wide binding profiles in cell lines (Baubec et al., 2013; Günther et al., 2013; Hashimoto et al., 2012a). MBD2 binds specifically to mCG and MBD3 binds with low and equivalent affinity to unmodified or modified cytosines (Hashimoto et al., 2012a; Spruijt et al., 2013). In studies of genome-wide localization, MBD2 is found at methylated CGIs at transcription start sites, promoters, and exons, with low enrichment at low mCG-dense regions, such as repetitive regions and intergenic sites (Baubec et al., 2013; Günther et al., 2013; Menafra et al., 2014). MBD2 is also localized at unmethylated, active sites dependent on interactions with NuRD

(Baubec et al., 2013). In contrast, MBD3 is found at more unmethylated sites with active transcription compared to MBD2 (Günther et al., 2013). One example of MBD2-specific transcriptional regulation occurs at the BRCA1-NBR2 locus in HeLa cells where MBD2, but not MeCP2 or MBD1, is highly expressed and binds to a constitutively methylated regulatory region (Auriol et al., 2005).

MBD2 and MBD3 also differ in their interactions with the NuRD complex, which could result in different tissue-specific functions. MBD3/NuRD may be the primary form of NuRD in the brain, as it is abundant in the cerebellum where it affects synaptic connectivity in addition to regulating cortical neuronal differentiation (Knock et al., 2015; Yamada et al., 2014). MBD3 also interacts with a brain-specific, alternate form of NuRD that incorporates CHD4 in place of CHD5. This interaction is specific for MBD3, but it is not clear what the functional significance of the CHD4/NuRD complex versus the CHD5/NuRD complex in the brain may be (Potts et al., 2011). MBD2 has isoform-specific interactions with NuRD that could have important functional consequences, particularly in ESCs (Baubec et al., 2013; Lu et al., 2014). MBD2 also has isoform-specific interactions with different protein complexes that may affect NuRD interactions, and different genome-wide localization (Baubec et al., 2013; Tan and Nakielny, 2006). However, our results did not reveal a notable difference in binding to components of the NuRD complex between MBD2 isoforms. This may be due to experimental limitations, which did not permit the detection of subtle differences in NuRD interactions, or this mechanism may not occur in the brain *in vivo*. It is not clear if the other binding partners for MBD2 represent specific, NuRD-independent functions, or if they serve to mediate the interactions between MBD2 and NuRD. Either of these scenarios would necessarily indicate that any NuRD-independent MBD2 functions are also dispensable for brain function. If MBD2 does have distinct functions independent of NuRD, this again raises the question of why loss of MBD2 does not result in a more severe phenotype.

Although our results fit the MBD protein functional redundancy model in the brain, they do not support functional redundancy in peripheral tissues. We found that MBD2 is ubiquitously

expressed across all tissues examined at adult ages, and most tissues at postnatal day 7. MeCP2 is more widely expressed compared to MBD1 and MBD3, but is not co-expressed in all tissues with MBD2 expression. MBD3 and MBD1 expression is undetectable in the peripheral tissues examined, with the exception of the colon. Therefore, even if some level of functional redundancy exists among these proteins, this cannot be occurring in tissues such as the spleen or small intestine, where MBD2 is the only MBD protein expressed.

Our spatiotemporal expression profiling also raises important new questions about the *in vivo* dynamics of the NuRD complex and MBD2 or MBD3. Biochemical evidence has shown that MBD2 and MBD3 are mutually exclusive in the NuRD complex, and that the presence of the MBD protein is necessary for NuRD complex formation and function (Le Guezennec et al., 2006; Ramírez et al., 2012; Saito and Ishikawa, 2002). It is also apparent that the NuRD complex is essential in many tissues and biological processes, including development and tumorigenesis (Torchy et al., 2015). We found that MBD2 is associated with NuRD ubiquitously in three representative tissues. Our expression data on MBD2 and MBD3 suggest that in adult peripheral tissues, NuRD complex functions must depend primarily on MBD2, as MBD2 is highly expressed but MBD3 is not detectable. Our expression data for MBD3 indicate that MBD3 may be acting at early time points, particularly in the brain. This hypothesis is supported by mouse genetic studies that show that a constitutive loss of MBD3 is embryonic lethal, while a brain-specific conditional *Mbd3* null allele is perinatal lethal with neuronal deficits (Hendrich et al., 2001; Knock et al., 2015).

However, if MBD2 is indeed the primary acting MBD protein in adult peripheral tissues, this model again poses the question of why *Mbd2*$^{-/-}$ mice show relatively subtle phenotypes. This question can only be answered once the precise *in vivo* functions of MBD2 and the other MBD proteins have been defined. It is clear from genetic, biochemical and expression evidence that MBD2 has distinct properties from the other MBD proteins. Therefore, other explanations for the absence of a relatively robust *Mbd2*$^{-/-}$ phenotype besides functional redundancy must be considered.

Models of MBD2 function and outstanding questions

An essential goal of the MBD protein field that remains unresolved is defining the precise functions of these proteins. Surprisingly, attempts to identify specific methylated loci that show direct transcriptional regulation by the MBD proteins have been mostly unsuccessful. Ablation of the MBD encoding genes, including *Mecp2*, *Mbd2,* or *Mbd3*, produces many subtle transcriptional changes without a clear tendency for aberrant upregulation that would be expected according to models of MBD proteins being simple transcriptional repressors (Chahrour et al., 2008; Günther et al., 2013). This is especially surprising in the case of MeCP2, because loss or mutation of this gene has severe phenotypic consequences (Amir et al., 1999). For MeCP2, this inconsistency may be due to the fact that this protein has many other proposed functions, such as chromatin organization or stability, that may not necessarily correspond to large, consistent transcriptional changes upon loss of MeCP2 (Maunakea et al., 2013; Pohodich and Zoghbi, 2015; Skene et al., 2010). The picture is less clear for the other MBD proteins, including MBD2. The only described functions for MBD2 involve interactions with NuRD or other transcriptional activators and repressors, with no proposed major alternative functions (Angrisano et al., 2006; Ramírez et al., 2012). However, there is increasing evidence that the functions of MBD2 with NuRD are more dynamic and complex than originally realized when this protein complex was first identified (Baubec et al., 2013; Feng and Zhang, 2001).

These questions are challenging to resolve because it is experimentally difficult to distinguish between functions that are MBD2-specific rather than mediated by the NuRD complex as a whole, while the role of MBD3 must also be considered. We anticipate that our spatiotemporal expression results will aid in resolving this matter. Studying NuRD complex formation and function in a tissue where MBD2 is exclusively expressed may provide insights into MBD2-specific functions without the complication of MBD3/NuRD activity. Conversely, it would be valuable to compare MBD2/NuRD function to MBD3/NuRD function in the brain of young animals,

where these proteins are co-expressed, using conditional loss of MBD2 or MBD3 to examine questions of how the NuRD complex forms and functions with either protein.

One possible model for these interactions in tissues with MBD2 and MBD3 co-expression is that MBD3 is essential for NuRD formation and function, while MBD2 represents a more transient member of NuRD that is required to fine-tune NuRD function, and thus may be expendable. One study determined that most NuRD complexes contain MBD3 rather than MBD2 (Zhang et al., 1999), but this study was limited to cultured cells, and the dynamics of these interactions *in vivo* have not been fully determined. This scenario is supported by the distinct functions of MBD2 and MBD3 in ESCs. MBD3 is absolutely required for embryogenesis, while complete ablation of MBD2 does not compromise survivability or fertility (Hendrich et al., 2001). However, loss or overexpression of an individual isoform of MBD2 regulates the balance between differentiation and proliferation of pluripotent cells (Lu et al., 2014).

The different isoforms of MBD2 introduce further complications into models of MBD2/NuRD function. With a few important exceptions, most studies of MBD2 do not acknowledge or distinguish between the multiple alternatively spliced or translated isoforms. A recent study described opposing functions for MBD2a and MBD2c in the differentiation or proliferation of ESCs (Lu et al., 2014). Biochemical evidence shows that MBD2a, MBD2b, and MBD2c, which is only expressed in the testes and ESCs, have different interactions with NuRD and other protein complexes and are recruited to DNA differently (Baubec et al., 2013; Lu et al., 2014; Tan and Nakielny, 2006). These multiple forms of MBD2 may have distinct roles in other cell types that have yet to be fully explored. Similarly to the situation in ESCs, it is possible that complete deletion of MBD2 does not have large phenotypic effects, as we have observed. Disrupting the balance of MBD2 isoform expression could be more detrimental to NuRD function and therefore produce more robust phenotypes similarly to loss of MBD3.

Finally, another possible explanation for the absence of large transcriptional changes or overt phenotypes in *Mbd2*$^{-/-}$ mice is combinatorial action or redundancy among transcriptional and epigenetic regulatory mechanisms. There are multiple interdependent epigenetic mechanisms,

such as histone modifications and nucleosome spacing, to safeguard chromatin and transcriptional stability. This idea of epigenetic “resilience” means that multiple mechanisms of transcriptional regulation can co-exist at a single locus, so that upon loss of one component, the transcriptional program or epigenetic state is still maintained (Perissi et al., 2010). This concept is especially relevant to induced pluripotent stem cells, which tend to maintain certain epigenetic signatures even after reprogramming (Hochedlinger and Jaenisch, 2015). An example of MBD2 activity in this kind of regulation occurs at the *Xist* locus. Small amounts of aberrant *Xist* transcript are detectable in the absence of MBD2, but not other MBD proteins. However, other silencing mechanisms including HDAC activity were intact in *Mbd2* null cells to partially maintain *Xist* repression (Barr et al., 2007).

This model also allows for more dynamic responses at a single locus, which is supported by evidence that DNA methylation and co-repressors such as NuRD may in fact modulate both transcriptional activation and repression depending on the epigenomic context (Reynolds et al., 2013; Suzuki and Bird, 2008). DNA methylation can be associated with active transcription, possibly through the binding of activating transcription factors that bind specifically to methylated DNA sequences, many with developmental or cell-type specificity (Spruijt et al., 2013). Furthermore, the MBD proteins, including MBD2 and NuRD, are localized at many transcriptionally active sites (Baubec et al., 2013; Günther et al., 2013). These findings argue for a more dynamic picture of methylation-mediated transcriptional regulation than straightforward repression by the MBD proteins and their corresponding co-repressor proteins (Reynolds et al., 2013).

In conclusion, MBD2 is an integral part of the NuRD complex with many unanswered questions regarding its molecular and biological functions. We have shown for the first time that loss of MBD2 surprisingly produces few subtle phenotypes, in comparison to mice with loss of other MBD proteins (Guy et al., 2001; Hendrich et al., 2001; Zhao et al., 2003). We also introduced valuable genetic tools for the study of MBD2 *in vivo*. We generated two novel transgenic mouse lines with endogenous biotin-tagged MBD2 or MBD1, which can be used for

numerous experimental applications. We employed these mice to show that MBD2 is expressed and associates with the NuRD complex ubiquitously, while the expression of other MBD proteins is largely restricted to the brain. The spatiotemporal expression patterns of MBD2 support potential functions in several peripheral tissues. These findings also address important questions about functional redundancy amongst the MBD proteins as well as the dynamics of the NuRD complex with MBD2 and MBD3 *in vivo*. Future investigations into MBD2 functions may have important implications for the study of pluripotency, immunity and cancer.

BIBLIOGRAPHY

Agarwal, N., Hardt, T., Brero, A., Nowak, D., Rothbauer, U., Becker, A., et al. (2007). MeCP2 interacts with HP1 and modulates its heterochromatin association during myogenic differentiation. *Nucleic Acids Res.* 35, 5402–5408. doi:10.1093/nar/gkm599.

Aguilera, C., Nakagawa, K., Sancho, R., Chakraborty, A., Hendrich, B., and Behrens, A. (2011). c-Jun N-terminal phosphorylation antagonises recruitment of the Mbd3/NuRD repressor complex. *Nature* 469, 231–235. doi:10.1038/nature09607.

Alabert, C., Bukowski-Wills, J.-C., Lee, S.-B., Kustatscher, G., Nakamura, K., de Lima Alves, F., et al. (2014). Nascent chromatin capture proteomics determines chromatin dynamics during DNA replication and identifies unknown fork components. *Nat. Cell Biol.* 16, 281–293. doi:10.1038/ncb2918.

Allan, A. M., Liang, X., Luo, Y., Pak, C., Li, X., Szulwach, K. E., et al. (2008). The loss of methyl-CpG binding protein 1 leads to autism-like behavioral deficits. *Hum. Mol. Genet.* 17, 2047–2057. doi:10.1093/hmg/ddn102.

Álvarez-Errico, D., Vento-Tormo, R., Sieweke, M., and Ballestar, E. (2014). Epigenetic control of myeloid cell differentiation, identity and function. *Nat. Rev. Immunol.* 15, 7–17. doi:10.1038/nri3777.

Amir, R. E., Van den Veyver, I. B., Wan, M., Tran, C. Q., Francke, U., and Zoghbi, H. Y. (1999). Rett syndrome is caused by mutations in X-linked MECP2, encoding methyl-CpG-binding protein 2. *Nat. Genet.* 23, 185–188. doi:10.1038/13810.

Angrisano, T., Lembo, F., Pero, R., Natale, F., Fusco, A., Avvedimento, V. E., et al. (2006). TACC3 mediates the association of MBD2 with histone acetyltransferases and relieves transcriptional repression of methylated promoters. *Nucleic Acids Res.* 34, 364–372. doi:10.1093/nar/gkj400.

Aoki, K., Sato, N., Yamaguchi, A., Kaminuma, O., Hosozawa, T., and Miyatake, S. (2009). Regulation of DNA demethylation during maturation of CD4+ naive T cells by the conserved noncoding sequence 1. *J. Immunol. Baltim. Md 1950* 182, 7698–7707. doi:10.4049/jimmunol.0801643.

Auriol, E., Billard, L.-M., Magdinier, F., and Dante, R. (2005). Specific binding of the methyl binding domain protein 2 at the BRCA1-NBR2 locus. *Nucleic Acids Res.* 33, 4243–4254. doi:10.1093/nar/gki729.

Bader, S., Walker, M., McQueen, H. A., Sellar, R., Oei, E., Wopereis, S., et al. (2003). MBD1, MBD2 and CGBP genes at chromosome 18q21 are infrequently mutated in human colon and lung cancers. *Oncogene* 22, 3506–3510. doi:10.1038/sj.onc.1206574.

Balada, E., Ordi-Ros, J., Serrano-Acedo, S., Martinez-Lostao, L., and Vilardell-Tarrés, M. (2007). Transcript overexpression of the MBD2 and MBD4 genes in CD4+ T cells from systemic lupus erythematosus patients. *J. Leukoc. Biol.* 81, 1609–1616. doi:10.1189/jlb.0107064.

Ballas, N., Grunseich, C., Lu, D. D., Speh, J. C., and Mandel, G. (2005). REST and its corepressors mediate plasticity of neuronal gene chromatin throughout neurogenesis. *Cell* 121, 645–657. doi:10.1016/j.cell.2005.03.013.

Ballestar, E., Pile, L. A., Wassarman, D. A., Wolffe, A. P., and Wade, P. A. (2001). A Drosophila MBD family member is a transcriptional corepressor associated with specific genes. *Eur. J. Biochem. FEBS* 268, 5397–5406.

Barr, H., Hermann, A., Berger, J., Tsai, H.-H., Adie, K., Prokhortchouk, A., et al. (2007). Mbd2 contributes to DNA methylation-directed repression of the Xist gene. *Mol. Cell. Biol.* 27, 3750–3757. doi:10.1128/MCB.02204-06.

Basta, J., and Rauchman, M. (2015). The nucleosome remodeling and deacetylase complex in development and disease. *Transl. Res.* 165, 36–47. doi:10.1016/j.trsl.2014.05.003.

Baubec, T., Colombo, D. F., Wirbelauer, C., Schmidt, J., Burger, L., Krebs, A. R., et al. (2015). Genomic profiling of DNA methyltransferases reveals a role for DNMT3B in genic methylation. *Nature* 520, 243–247. doi:10.1038/nature14176.

Baubec, T., Ivánek, R., Lienert, F., and Schübeler, D. (2013). Methylation-dependent and -independent genomic targeting principles of the MBD protein family. *Cell* 153, 480–492. doi:10.1016/j.cell.2013.03.011.

Baubec, T., and Schübeler, D. (2014). Genomic patterns and context specific interpretation of DNA methylation. *Curr. Opin. Genet. Dev.* 25, 85–92. doi:10.1016/j.gde.2013.11.015.

Baylin, S. B., and Jones, P. A. (2011). A decade of exploring the cancer epigenome - biological and translational implications. *Nat. Rev. Cancer* 11, 726–734. doi:10.1038/nrc3130.

Baymaz, H. I., Fournier, A., Laget, S., Ji, Z., Jansen, P. W. T. C., Smits, A. H., et al. (2014). MBD5 and MBD6 interact with the human PR-DUB complex through their methyl-CpG-binding domain. *Proteomics*. doi:10.1002/pmic.201400013.

Benayed, R., Gharani, N., Rossman, I., Mancuso, V., Lazar, G., Kamdar, S., et al. (2005). Support for the Homeobox Transcription Factor Gene< i> ENGRAILED 2</i> as an Autism Spectrum Disorder Susceptibility Locus. *Am. J. Hum. Genet.* 77, 851–868.

Ben-Shachar, S., Chahrour, M., Thaller, C., Shaw, C. A., and Zoghbi, H. Y. (2009). Mouse models of MeCP2 disorders share gene expression changes in the cerebellum and hypothalamus. *Hum. Mol. Genet.* 18, 2431–2442. doi:10.1093/hmg/ddp181.

Berger, J., Sansom, O., Clarke, A., and Bird, A. (2007). MBD2 is required for correct spatial gene expression in the gut. *Mol. Cell. Biol.* 27, 4049–4057. doi:10.1128/MCB.02023-06.

Billard, L.-M., Magdinier, F., Lenoir, G. M., Frappart, L., and Dante, R. (2002). MeCP2 and MBD2 expression during normal and pathological growth of the human mammary gland. *Oncogene* 21, 2704–2712. doi:10.1038/sj.onc.1205357.

Bissonnette, J. M., Schaevitz, L. R., Knopp, S. J., and Zhou, Z. (2014). Respiratory phenotypes are distinctly affected in mice with common Rett syndrome mutations MeCP2 T158A and R168X. *Neuroscience* 267, 166–176. doi:10.1016/j.neuroscience.2014.02.043.

Blattler, A., and Farnham, P. J. (2013). Cross-talk between Site-specific Transcription Factors and DNA Methylation States. *J. Biol. Chem.* 288, 34287–34294. doi:10.1074/jbc.R113.512517.

Boeke, J., Ammerpohl, O., Kegel, S., Moehren, U., and Renkawitz, R. (2000). The minimal repression domain of MBD2b overlaps with the methyl-CpG-binding domain and binds directly to Sin3A. *J. Biol. Chem.* 275, 34963–34967. doi:10.1074/jbc.M005929200.

de Boer, E., Rodriguez, P., Bonte, E., Krijgsveld, J., Katsantoni, E., Heck, A., et al. (2003). Efficient biotinylation and single-step purification of tagged transcription factors in mammalian cells and transgenic mice. *Proc. Natl. Acad. Sci. U. S. A.* 100, 7480–7485. doi:10.1073/pnas.1332608100.

Bourc'his, D., Xu, G. L., Lin, C. S., Bollman, B., and Bestor, T. H. (2001). Dnmt3L and the establishment of maternal genomic imprints. *Science* 294, 2536–2539. doi:10.1126/science.1065848.

Bromberg-Martin, E. S., Matsumoto, M., and Hikosaka, O. (2010). Dopamine in motivational control: rewarding, aversive, and alerting. *Neuron* 68, 815–834. doi:10.1016/j.neuron.2010.11.022.

Buxbaum, J. N., and Reixach, N. (2009). Transthyretin: the servant of many masters. *Cell. Mol. Life Sci.* 66, 3095–3101. doi:10.1007/s00018-009-0109-0.

Cai, Y., Geutjes, E.-J., de Lint, K., Roepman, P., Bruurs, L., Yu, L.-R., et al. (2014). The NuRD complex cooperates with DNMTs to maintain silencing of key colorectal tumor suppressor genes. *Oncogene* 33, 2157–2168. doi:10.1038/onc.2013.178.

Camarena, V., Cao, L., Abad, C., Abrams, A., Toledo, Y., Araki, K., et al. (2014). Disruption of Mbd5 in mice causes neuronal functional deficits and neurobehavioral abnormalities consistent with 2q23.1 microdeletion syndrome. *EMBO Mol. Med.* 6, 1003–1015. doi:10.15252/emmm.201404044.

Campbell, P. M., Bovenzi, V., and Szyf, M. (2004). Methylated DNA-binding protein 2 antisense inhibitors suppress tumourigenesis of human cancer cell lines in vitro and in vivo. *Carcinogenesis* 25, 499–507. doi:10.1093/carcin/bgh045.

Cedar, H., and Bergman, Y. (2009). Linking DNA methylation and histone modification: patterns and paradigms. *Nat. Rev. Genet.* 10, 295–304. doi:10.1038/nrg2540.

Chahrour, M., Jung, S. Y., Shaw, C., Zhou, X., Wong, S. T. C., Qin, J., et al. (2008). MeCP2, a key contributor to neurological disease, activates and represses transcription. *Science* 320, 1224–1229. doi:10.1126/science.1153252.

Chatagnon, A., Bougel, S., Perriaud, L., Lachuer, J., Benhattar, J., and Dante, R. (2009). Specific association between the methyl-CpG-binding domain protein 2 and the hypermethylated region of the human telomerase reverse transcriptase promoter in cancer cells. *Carcinogenesis* 30, 28–34. doi:10.1093/carcin/bgn240.

Chatagnon, A., Perriaud, L., Nazaret, N., Croze, S., Benhattar, J., Lachuer, J., et al. (2011). Preferential binding of the methyl-CpG binding domain protein 2 at methylated transcriptional start site regions. *Epigenetics Off. J. DNA Methylation Soc.* 6, 1295–1307. doi:10.4161/epi.6.11.17875.

Cheh, M. A., Millonig, J. H., Roselli, L. M., Ming, X., Jacobsen, E., Kamdar, S., et al. (2006). En2 null mice display neurobehavioral and neurochemical alterations relevant to autism spectrum disorder. *Brain Res.* 1116, 166–176. doi:10.1016/j.brainres.2006.07.086.

Chen, T., and Dent, S. Y. R. (2014). Chromatin modifiers and remodellers: regulators of cellular differentiation. *Nat. Rev. Genet.* 15, 93–106. doi:10.1038/nrg3607.

Chen, T., Ueda, Y., Dodge, J. E., Wang, Z., and Li, E. (2003). Establishment and maintenance of genomic methylation patterns in mouse embryonic stem cells by Dnmt3a and Dnmt3b. *Mol. Cell. Biol.* 23, 5594–5605.

Conti, V., Gandaglia, A., Galli, F., Tirone, M., Bellini, E., Campana, L., et al. (2015). MeCP2 Affects Skeletal Muscle Growth and Morphology through Non Cell-Autonomous Mechanisms. *PLOS ONE* 10, e0130183. doi:10.1371/journal.pone.0130183.

Cook, P. C., Owen, H., Deaton, A. M., Borger, J. G., Brown, S. L., Clouaire, T., et al. (2015). A dominant role for the methyl-CpG-binding protein Mbd2 in controlling Th2 induction by dendritic cells. *Nat. Commun.* 6, 6920. doi:10.1038/ncomms7920.

Crawley, J. N. (2007). *What's wrong with my mouse?: behavioral phenotyping of transgenic and null mice*. 2nd ed. Hoboken, N.J: Wiley-Interscience.

Cronk, J. C., Derecki, N. C., Ji, E., Xu, Y., Lampano, A. E., Smirnov, I., et al. (2015). Methyl-CpG Binding Protein 2 Regulates Microglia and Macrophage Gene Expression in Response to Inflammatory Stimuli. *Immunity* 42, 679–691. doi:10.1016/j.immuni.2015.03.013.

Csankovszki, G., Nagy, A., and Jaenisch, R. (2001). Synergism of Xist Rna, DNA Methylation, and Histone Hypoacetylation in Maintaining X Chromosome Inactivation. *J. Cell Biol.* 153, 773–784. doi:10.1083/jcb.153.4.773.

Cukier, H. N., Lee, J. M., Ma, D., Young, J. I., Mayo, V., Butler, B. L., et al. (2012). The expanding role of MBD genes in autism: identification of a MECP2 duplication and novel alterations in MBD5, MBD6, and SETDB1. *Autism Res. Off. J. Int. Soc. Autism Res.* 5, 385–397. doi:10.1002/aur.1251.

Cukier, H. N., Rabionet, R., Konidari, I., Rayner-Evans, M. Y., Baltos, M. L., Wright, H. H., et al. (2010). Novel variants identified in methyl-CpG-binding domain genes in autistic individuals. *Neurogenetics* 11, 291–303. doi:10.1007/s10048-009-0228-7.

Deacon, R. M. (2006). Assessing nest building in mice. *Nat. Protoc.* 1, 1117–1119. doi:10.1038/nprot.2006.170.

Deaton, A. M., and Bird, A. (2011). CpG islands and the regulation of transcription. *Genes Dev.* 25, 1010–1022. doi:10.1101/gad.2037511.

Dege, C., and Hagman, J. (2014a). Mi-2/NuRD chromatin remodeling complexes regulate B and T-lymphocyte development and function. *Immunol. Rev.* 261, 126–140. doi:10.1111/imr.12209.

Dege, C., and Hagman, J. (2014b). Mi-2/NuRD chromatin remodeling complexes regulate B and T-lymphocyte development and function. *Immunol. Rev.* 261, 126–140. doi:10.1111/imr.12209.

Derks, S., Bosch, L. J. W., Niessen, H. E. C., Moerkerk, P. T. M., van den Bosch, S. M., Carvalho, B., et al. (2009). Promoter CpG island hypermethylation- and H3K9me3 and H3K27me3-mediated epigenetic silencing targets the deleted in colon cancer (DCC)

gene in colorectal carcinogenesis without affecting neighboring genes on chromosomal region 18q21. *Carcinogenesis* 30, 1041–1048. doi:10.1093/carcin/bgp073.

Desai, M. A., Webb, H. D., Sinanan, L. M., Scarsdale, J. N., Walavalkar, N. M., Ginder, G. D., et al. (2015). An intrinsically disordered region of methyl-CpG binding domain protein 2 (MBD2) recruits the histone deacetylase core of the NuRD complex. *Nucleic Acids Res.* 43, 3100–3113. doi:10.1093/nar/gkv168.

Devailly, G., Grandin, M., Perriaud, L., Mathot, P., Delcros, J.-G., Bidet, Y., et al. (2015). Dynamics of MBD2 deposition across methylated DNA regions during malignant transformation of human mammary epithelial cells. *Nucleic Acids Res.* doi:10.1093/nar/gkv508.

Dobin, A., Davis, C. A., Schlesinger, F., Drenkow, J., Zaleski, C., Jha, S., et al. (2013). STAR: ultrafast universal RNA-seq aligner. *Bioinformatics* 29, 15–21. doi:10.1093/bioinformatics/bts635.

Domcke, S., Bardet, A. F., Adrian Ginno, P., Hartl, D., Burger, L., and Schübeler, D. (2015). Competition between DNA methylation and transcription factors determines binding of NRF1. *Nature* 528, 575–579. doi:10.1038/nature16462.

Dos Santos, R. L., Tosti, L., Radzisheuskaya, A., Caballero, I. M., Kaji, K., Hendrich, B., et al. (2014). MBD3/NuRD Facilitates Induction of Pluripotency in a Context-Dependent Manner. *Cell Stem Cell*. doi:10.1016/j.stem.2014.04.019.

Du, Q., Luu, P.-L., Stirzaker, C., and Clark, S. J. (2015). Methyl-CpG-binding domain proteins: readers of the epigenome. *Epigenomics*, 1–23. doi:10.2217/epi.15.39.

Eberl, H. C., Spruijt, C. G., Kelstrup, C. D., Vermeulen, M., and Mann, M. (2013). A Map of General and Specialized Chromatin Readers in Mouse Tissues Generated by Label-free Interaction Proteomics. *Mol. Cell* 49, 368–378. doi:10.1016/j.molcel.2012.10.026.

Ebert, D. H., Gabel, H. W., Robinson, N. D., Kastan, N. R., Hu, L. S., Cohen, S., et al. (2013). Activity-dependent phosphorylation of MeCP2 threonine 308 regulates interaction with NCoR. *Nature* 499, 341–345. doi:10.1038/nature12348.

Endele, S., Rosenberger, G., Geider, K., Popp, B., Tamer, C., Stefanova, I., et al. (2010). Mutations in GRIN2A and GRIN2B encoding regulatory subunits of NMDA receptors cause variable neurodevelopmental phenotypes. *Nat. Genet.* 42, 1021–1026. doi:10.1038/ng.677.

Fairless, A. H., Shah, R. Y., Guthrie, A. J., Li, H., and Brodkin, E. S. (2011). Deconstructing Sociability, An Autism-Relevant Phenotype, in Mouse Models. *Anat. Rec. Adv. Integr. Anat. Evol. Biol.* 294, 1713–1725. doi:10.1002/ar.21318.

Fearon, E., Cho, K., Nigro, J., Kern, S., Simons, J., Ruppert, J., et al. (1990). Identification of a chromosome 18q gene that is altered in colorectal cancers. *Science* 247, 49–56. doi:10.1126/science.2294591.

Feng, J., Zhou, Y., Campbell, S. L., Le, T., Li, E., Sweatt, J. D., et al. (2010). Dnmt1 and Dnmt3a maintain DNA methylation and regulate synaptic function in adult forebrain neurons. *Nat. Neurosci.* 13, 423–430. doi:10.1038/nn.2514.

Feng, Q., and Zhang, Y. (2001). The MeCP1 complex represses transcription through preferential binding, remodeling, and deacetylating methylated nucleosomes. *Genes Dev.* 15, 827–832. doi:10.1101/gad.876201.

Filion, G. J. P., Zhenilo, S., Salozhin, S., Yamada, D., Prokhortchouk, E., and Defossez, P.-A. (2006). A family of human zinc finger proteins that bind methylated DNA and repress transcription. *Mol. Cell. Biol.* 26, 169–181. doi:10.1128/MCB.26.1.169-181.2006.

Francis, D., Diorio, J., Liu, D., and Meaney, M. J. (1999). Nongenomic transmission across generations of maternal behavior and stress responses in the rat. *Science* 286, 1155–1158.

Fujita, H., Fujii, R., Aratani, S., Amano, T., Fukamizu, A., and Nakajima, T. (2003a). Antithetic Effects of MBD2a on Gene Regulation. *Mol. Cell. Biol.* 23, 2645–2657. doi:10.1128/MCB.23.8.2645-2657.2003.

Fujita, N., Watanabe, S., Ichimura, T., Ohkuma, Y., Chiba, T., Saya, H., et al. (2003b). MCAF mediates MBD1-dependent transcriptional repression. *Mol. Cell. Biol.* 23, 2834–2843.

Fujita, N., Watanabe, S., Ichimura, T., Tsuruzoe, S., Shinkai, Y., Tachibana, M., et al. (2003c). Methyl-CpG binding domain 1 (MBD1) interacts with the Suv39h1-HP1 heterochromatic complex for DNA methylation-based transcriptional repression. *J. Biol. Chem.* 278, 24132–24138. doi:10.1074/jbc.M302283200.

Gabel, H. W., Kinde, B., Stroud, H., Gilbert, C. S., Harmin, D. A., Kastan, N. R., et al. (2015). Disruption of DNA-methylation-dependent long gene repression in Rett syndrome. *Nature* 522, 89–93. doi:10.1038/nature14319.

Gammie, S. C. (2005). Current models and future directions for understanding the neural circuitries of maternal behaviors in rodents. *Behav. Cogn. Neurosci. Rev.* 4, 119–135. doi:10.1177/1534582305281086.

Gammie, S. C., Edelmann, M. N., Mandel-Brehm, C., D'Anna, K. L., Auger, A. P., and Stevenson, S. A. (2008). Altered dopamine signaling in naturally occurring maternal neglect. *PloS One* 3, e1974. doi:10.1371/journal.pone.0001974.

Gao, H., Lukin, K., Ramírez, J., Fields, S., Lopez, D., and Hagman, J. (2009). Opposing effects of SWI/SNF and Mi-2/NuRD chromatin remodeling complexes on epigenetic reprogramming by EBF and Pax5. *Proc. Natl. Acad. Sci. U. S. A.* 106, 11258–11263. doi:10.1073/pnas.0809485106.

Gaskill, B. N., Karas, A. Z., Garner, J. P., and Pritchett-Corning, K. R. (2013). Nest Building as an Indicator of Health and Welfare in Laboratory Mice. *J. Vis. Exp.* doi:10.3791/51012.

Gnanapragasam, M. N., Scarsdale, J. N., Amaya, M. L., Webb, H. D., Desai, M. A., Walavalkar, N. M., et al. (2011). p66Alpha-MBD2 coiled-coil interaction and recruitment of Mi-2 are critical for globin gene silencing by the MBD2-NuRD complex. *Proc. Natl. Acad. Sci. U. S. A.* 108, 7487–7492. doi:10.1073/pnas.1015341108.

Goffin, D., Allen, M., Zhang, L., Amorim, M., Wang, I.-T. J., Reyes, A.-R. S., et al. (2012). Rett syndrome mutation MeCP2 T158A disrupts DNA binding, protein stability and ERP responses. *Nat. Neurosci.* 15, 274–283. doi:10.1038/nn.2997.

Guan, J.-S., Haggarty, S. J., Giacometti, E., Dannenberg, J.-H., Joseph, N., Gao, J., et al. (2009). HDAC2 negatively regulates memory formation and synaptic plasticity. *Nature* 459, 55–60. doi:10.1038/nature07925.

Günther, K., Rust, M., Leers, J., Boettger, T., Scharfe, M., Jarek, M., et al. (2013). Differential roles for MBD2 and MBD3 at methylated CpG islands, active promoters and binding to exon sequences. *Nucleic Acids Res.* 41, 3010–3021. doi:10.1093/nar/gkt035.

Guo, J. U., Ma, D. K., Mo, H., Ball, M. P., Jang, M.-H., Bonaguidi, M. A., et al. (2011). Neuronal activity modifies the DNA methylation landscape in the adult brain. *Nat. Neurosci.* 14, 1345–1351. doi:10.1038/nn.2900.

Guo, J. U., Su, Y., Shin, J. H., Shin, J., Li, H., Xie, B., et al. (2014). Distribution, recognition and regulation of non-CpG methylation in the adult mammalian brain. *Nat. Neurosci.* 17, 215–222. doi:10.1038/nn.3607.

Gu, P., Xu, X., Le Menuet, D., Chung, A. C.-K., and Cooney, A. J. (2011). Differential recruitment of methyl CpG-binding domain factors and DNA methyltransferases by the orphan receptor germ cell nuclear factor initiates the repression and silencing of Oct4. *Stem Cells Dayt. Ohio* 29, 1041–1051. doi:10.1002/stem.652.

Guy, J., Hendrich, B., Holmes, M., Martin, J. E., and Bird, A. (2001). A mouse Mecp2-null mutation causes neurological symptoms that mimic Rett syndrome. *Nat. Genet.* 27, 322–326. doi:10.1038/85899.

Hashimoto, H., Liu, Y., Upadhyay, A. K., Chang, Y., Howerton, S. B., Vertino, P. M., et al. (2012a). Recognition and potential mechanisms for replication and erasure of cytosine hydroxymethylation. *Nucleic Acids Res.* 40, 4841–4849. doi:10.1093/nar/gks155.

Hashimoto, H., Zhang, X., and Cheng, X. (2012b). Excision of thymine and 5-hydroxymethyluracil by the MBD4 DNA glycosylase domain: structural basis and implications for active DNA demethylation. *Nucleic Acids Res.* 40, 8276–8284. doi:10.1093/nar/gks628.

Hendrich, B., Abbott, C., McQueen, H., Chambers, D., Cross, S., and Bird, A. (1999). Genomic structure and chromosomal mapping of the murine and human Mbd1, Mbd2, Mbd3, and Mbd4 genes. *Mamm. Genome Off. J. Int. Mamm. Genome Soc.* 10, 906–912.

Hendrich, B., and Bird, A. (1998). Identification and characterization of a family of mammalian methyl-CpG binding proteins. *Mol. Cell. Biol.* 18, 6538–6547.

Hendrich, B., Guy, J., Ramsahoye, B., Wilson, V. A., and Bird, A. (2001). Closely related proteins MBD2 and MBD3 play distinctive but interacting roles in mouse development. *Genes Dev.* 15, 710–723. doi:10.1101/gad.194101.

Hendrich, B., and Tweedie, S. (2003). The methyl-CpG binding domain and the evolving role of DNA methylation in animals. *Trends Genet.* 19, 269–277. doi:10.1016/S0168-9525(03)00080-5.

Henschen, C. W., Palmiter, R. D., and Darvas, M. (2013). Restoration of dopamine signaling to the dorsal striatum is sufficient for aspects of active maternal behavior in female mice. *Endocrinology* 154, 4316–4327. doi:10.1210/en.2013-1257.

He, Y.-F., Li, B.-Z., Li, Z., Liu, P., Wang, Y., Tang, Q., et al. (2011). Tet-mediated formation of 5-carboxylcytosine and its excision by TDG in mammalian DNA. *Science* 333, 1303–1307. doi:10.1126/science.1210944.

Heyward, F. D., and Sweatt, J. D. (2015). DNA Methylation in Memory Formation: Emerging Insights. *The Neuroscientist* 21, 475–489. doi:10.1177/1073858415579635.

Hochedlinger, K., and Jaenisch, R. (2015). Induced Pluripotency and Epigenetic Reprogramming. *Cold Spring Harb. Perspect. Biol.* 7, a019448. doi:10.1101/cshperspect.a019448.

Holik, A. Z., Young, M., Krzystyniak, J., Williams, G. T., Metzger, D., Shorning, B. Y., et al. (2014). Brg1 Loss Attenuates Aberrant Wnt-Signalling and Prevents Wnt-Dependent Tumourigenesis in the Murine Small Intestine. *PLoS Genet.* 10, e1004453. doi:10.1371/journal.pgen.1004453.

Hosokawa, H., Tanaka, T., Suzuki, Y., Iwamura, C., Ohkubo, S., Endoh, K., et al. (2013). Functionally distinct Gata3/Chd4 complexes coordinately establish T helper 2 (Th2) cell identity. *Proc. Natl. Acad. Sci. U. S. A.* 110, 4691–4696. doi:10.1073/pnas.1220865110.

Howerton, A. R., Roland, A. V., and Bale, T. L. (2014). Dorsal raphe neuroinflammation promotes dramatic behavioral stress dysregulation. *J. Neurosci. Off. J. Soc. Neurosci.* 34, 7113–7123. doi:10.1523/JNEUROSCI.0118-14.2014.

Humphries, A., and Wright, N. A. (2008). Colonic crypt organization and tumorigenesis. *Nat. Rev. Cancer* 8, 415–424. doi:10.1038/nrc2392.

Hutchins, A. S., Artis, D., Hendrich, B. D., Bird, A. P., Scott, P., and Reiner, S. L. (2005). Cutting edge: a critical role for gene silencing in preventing excessive type 1 immunity. *J. Immunol. Baltim. Md 1950* 175, 5606–5610.

Hutchins, A. S., Mullen, A. C., Lee, H. W., Sykes, K. J., High, F. A., Hendrich, B. D., et al. (2002). Gene silencing quantitatively controls the function of a developmental trans-activator. *Mol. Cell* 10, 81–91.

Ichimura, T., Watanabe, S., Sakamoto, Y., Aoto, T., Fujita, N., and Nakao, M. (2005). Transcriptional repression and heterochromatin formation by MBD1 and MCAF/AM family proteins. *J. Biol. Chem.* 280, 13928–13935. doi:10.1074/jbc.M413654200.

Illingworth, R., Kerr, A., Desousa, D., Jørgensen, H., Ellis, P., Stalker, J., et al. (2008). A novel CpG island set identifies tissue-specific methylation at developmental gene loci. *PLoS Biol.* 6, e22. doi:10.1371/journal.pbio.0060022.

Ito, S., Shen, L., Dai, Q., Wu, S. C., Collins, L. B., Swenberg, J. A., et al. (2011). Tet proteins can convert 5-methylcytosine to 5-formylcytosine and 5-carboxylcytosine. *Science* 333, 1300–1303. doi:10.1126/science.1210597.

Jager, J., O'Brien, W. T., Manlove, J., Krizman, E. N., Fang, B., Gerhart-Hines, Z., et al. (2014). Behavioral Changes and Dopaminergic Dysregulation in Mice Lacking the Nuclear Receptor Rev-erbα. *Mol. Endocrinol.* 28, 490–498. doi:10.1210/me.2013-1351.

Jeffery, L., and Nakielny, S. (2004). Components of the DNA methylation system of chromatin control are RNA-binding proteins. *J. Biol. Chem.* 279, 49479–49487. doi:10.1074/jbc.M409070200.

Jirkof, P. (2014). Burrowing and nest building behavior as indicators of well-being in mice. *J. Neurosci. Methods* 234, 139–146. doi:10.1016/j.jneumeth.2014.02.001.

Jørgensen, H. F., Ben-Porath, I., and Bird, A. P. (2004). Mbd1 is recruited to both methylated and nonmethylated CpGs via distinct DNA binding domains. *Mol. Cell. Biol.* 24, 3387–3395.

Kadmiel, M., and Cidlowski, J. A. (2013). Glucocorticoid receptor signaling in health and disease. *Trends Pharmacol. Sci.* 34, 518–530. doi:10.1016/j.tips.2013.07.003.

Kaji, K., Caballero, I. M., MacLeod, R., Nichols, J., Wilson, V. A., and Hendrich, B. (2006). The NuRD component Mbd3 is required for pluripotency of embryonic stem cells. *Nat. Cell Biol.* 8, 285–292. doi:10.1038/ncb1372.

Kaji, K., Nichols, J., and Hendrich, B. (2007). Mbd3, a component of the NuRD co-repressor complex, is required for development of pluripotent cells. *Dev. Camb. Engl.* 134, 1123–1132. doi:10.1242/dev.02802.

Kanai, Y., Ushijima, S., Nakanishi, Y., and Hirohashi, S. (1999). Reduced mRNA expression of the DNA demethylase, MBD2, in human colorectal and stomach cancers. *Biochem. Biophys. Res. Commun.* 264, 962–966. doi:10.1006/bbrc.1999.1613.

Kernohan, K. D., Vernimmen, D., Gloor, G. B., and Bérubé, N. G. (2014). Analysis of neonatal brain lacking ATRX or MeCP2 reveals changes in nucleosome density, CTCF binding and chromatin looping. *Nucleic Acids Res.* 42, 8356–8368. doi:10.1093/nar/gku564.

Kersh, E. N. (2006). Impaired Memory CD8 T Cell Development in the Absence of Methyl-CpG-Binding Domain Protein 2. *J. Immunol.* 177, 3821–3826. doi:10.4049/jimmunol.177.6.3821.

Kim, T.-K., and Shiekhattar, R. (2015). Architectural and Functional Commonalities between Enhancers and Promoters. *Cell* 162, 948–959. doi:10.1016/j.cell.2015.08.008.

Knock, E., Pereira, J., Lombard, P. D., Dimond, A., Leaford, D., Livesey, F. J., et al. (2015). The methyl binding domain 3/nucleosome remodelling and deacetylase complex regulates neural cell fate determination and terminal differentiation in the cerebral cortex. *Neural Develop.* 10, 13. doi:10.1186/s13064-015-0040-z.

Komori, H. K., Hart, T., LaMere, S. A., Chew, P. V., and Salomon, D. R. (2015). Defining CD4 T cell memory by the epigenetic landscape of CpG DNA methylation. *J. Immunol. Baltim. Md 1950* 194, 1565–1579. doi:10.4049/jimmunol.1401162.

Laget, S., Joulie, M., Le Masson, F., Sasai, N., Christians, E., Pradhan, S., et al. (2010). The human proteins MBD5 and MBD6 associate with heterochromatin but they do not bind methylated DNA. *PloS One* 5, e11982. doi:10.1371/journal.pone.0011982.

Lai, A. Y., and Wade, P. A. (2011). Cancer biology and NuRD: a multifaceted chromatin remodelling complex. *Nat. Rev. Cancer* 11, 588–596. doi:10.1038/nrc3091.

Lal, G., Zhang, N., van der Touw, W., Ding, Y., Ju, W., Bottinger, E. P., et al. (2009). Epigenetic regulation of Foxp3 expression in regulatory T cells by DNA methylation. *J. Immunol. Baltim. Md 1950* 182, 259–273.

Lee, M. R., Prasain, N., Chae, H.-D., Kim, Y.-J., Mantel, C., Yoder, M. C., et al. (2013). Epigenetic regulation of NANOG by miR-302 cluster-MBD2 completes induced pluripotent stem cell reprogramming. *Stem Cells Dayt. Ohio* 31, 666–681. doi:10.1002/stem.1302.

Lee, S., Park, J.-Y., Lee, W.-H., Kim, H., Park, H.-C., Mori, K., et al. (2009). Lipocalin-2 Is an Autocrine Mediator of Reactive Astrocytosis. *J. Neurosci.* 29, 234–249. doi:10.1523/JNEUROSCI.5273-08.2009.

Le Guezennec, X., Vermeulen, M., Brinkman, A. B., Hoeijmakers, W. A. M., Cohen, A., Lasonder, E., et al. (2006). MBD2/NuRD and MBD3/NuRD, two distinct complexes with different biochemical and functional properties. *Mol. Cell. Biol.* 26, 843–851. doi:10.1128/MCB.26.3.843-851.2006.

Lei, W., Luo, Y., Lei, W., Luo, Y., Yan, K., Zhao, S., et al. (2009). Abnormal DNA methylation in CD4+ T cells from patients with systemic lupus erythematosus, systemic sclerosis, and dermatomyositis. *Scand. J. Rheumatol.* 38, 369–374. doi:10.1080/03009740902758875.

Lewis, J. D., Meehan, R. R., Henzel, W. J., Maurer-Fogy, I., Jeppesen, P., Klein, F., et al. (1992). Purification, sequence, and cellular localization of a novel chromosomal protein that binds to Methylated DNA. *Cell* 69, 905–914. doi:10.1016/0092-8674(92)90610-O.

Li, E., Beard, C., and Jaenisch, R. (1993). Role for DNA methylation in genomic imprinting. *Nature* 366, 362–365. doi:10.1038/366362a0.

Li, H., Yamagata, T., Mori, M., Yasuhara, A., and Momoi, M. Y. (2005). Mutation analysis of methyl-CpG binding protein family genes in autistic patients. *Brain Dev.* 27, 321–325. doi:10.1016/j.braindev.2004.08.003.

Lister, R., Mukamel, E. A., Nery, J. R., Urich, M., Puddifoot, C. A., Johnson, N. D., et al. (2013). Global epigenomic reconfiguration during mammalian brain development. *Science* 341, 1237905. doi:10.1126/science.1237905.

Lister, R., Pelizzola, M., Dowen, R. H., Hawkins, R. D., Hon, G., Tonti-Filippini, J., et al. (2009). Human DNA methylomes at base resolution show widespread epigenomic differences. *Nature* 462, 315–322. doi:10.1038/nature08514.

Liu, C. C., Ou, T. T., Wu, C. C., Li, R. N., Lin, Y. C., Lin, C. H., et al. (2011). Global DNA methylation, DNMT1, and MBD2 in patients with systemic lupus erythematosus. *Lupus* 20, 131–136. doi:10.1177/0961203310381517.

Liu, C., Teng, Z.-Q., Santistevan, N. J., Szulwach, K. E., Guo, W., Jin, P., et al. (2010). Epigenetic regulation of miR-184 by MBD1 governs neural stem cell proliferation and differentiation. *Cell Stem Cell* 6, 433–444. doi:10.1016/j.stem.2010.02.017.

Liu, D., Diorio, J., Tannenbaum, B., Caldji, C., Francis, D., Freedman, A., et al. (1997). Maternal care, hippocampal glucocorticoid receptors, and hypothalamic-pituitary-adrenal responses to stress. *Science* 277, 1659–1662.

Lopez-Serra, L., Ballestar, E., Ropero, S., Setien, F., Billard, L.-M., Fraga, M. F., et al. (2008). Unmasking of epigenetically silenced candidate tumor suppressor genes by removal of methyl-CpG-binding domain proteins. *Oncogene* 27, 3556–3566. doi:10.1038/sj.onc.1211022.

Luo, M., Ling, T., Xie, W., Sun, H., Zhou, Y., Zhu, Q., et al. (2013). NuRD blocks reprogramming of mouse somatic cells into pluripotent stem cells. *Stem Cells Dayt. Ohio* 31, 1278–1286. doi:10.1002/stem.1374.

Lu, X., Kovalev, G. I., Chang, H., Kallin, E., Knudsen, G., Xia, L., et al. (2008). Inactivation of NuRD component Mta2 causes abnormal T cell activation and lupus-like autoimmune disease in mice. *J. Biol. Chem.* 283, 13825–13833. doi:10.1074/jbc.M801275200.

Lu, Y., Loh, Y.-H., Li, H., Cesana, M., Ficarro, S. B., Parikh, J. R., et al. (2014). Alternative Splicing of MBD2 Supports Self-Renewal in Human Pluripotent Stem Cells. *Cell Stem Cell.* doi:10.1016/j.stem.2014.04.002.

Lyst, M. J., Ekiert, R., Ebert, D. H., Merusi, C., Nowak, J., Selfridge, J., et al. (2013). Rett syndrome mutations abolish the interaction of MeCP2 with the NCoR/SMRT co-repressor. *Nat. Neurosci.* 16, 898–902. doi:10.1038/nn.3434.

Macdonald, J. L., Verster, A., Berndt, A., and Roskams, A. J. (2010). MBD2 and MeCP2 regulate distinct transitions in the stage-specific differentiation of olfactory receptor neurons. *Mol. Cell. Neurosci.* 44, 55–67. doi:10.1016/j.mcn.2010.02.003.

Macdonald, T. T., and Monteleone, G. (2005). Immunity, inflammation, and allergy in the gut. *Science* 307, 1920–1925. doi:10.1126/science.1106442.

Madison, B. B., Dunbar, L., Qiao, X. T., Braunstein, K., Braunstein, E., and Gumucio, D. L. (2002). Cis elements of the villin gene control expression in restricted domains of the vertical (crypt) and horizontal (duodenum, cecum) axes of the intestine. *J. Biol. Chem.* 277, 33275–33283. doi:10.1074/jbc.M204935200.

Magdinier, F., and Wolffe, A. P. (2001). Selective association of the methyl-CpG binding protein MBD2 with the silent p14/p16 locus in human neoplasia. *Proc. Natl. Acad. Sci. U. S. A.* 98, 4990–4995. doi:10.1073/pnas.101617298.

Marhold, J., Kramer, K., Kremmer, E., and Lyko, F. (2004). The Drosophila MBD2/3 protein mediates interactions between the MI-2 chromatin complex and CpT/A-methylated DNA. *Dev. Camb. Engl.* 131, 6033–6039. doi:10.1242/dev.01531.

Martín Caballero, I., Hansen, J., Leaford, D., Pollard, S., and Hendrich, B. D. (2009). The methyl-CpG binding proteins Mecp2, Mbd2 and Kaiso are dispensable for mouse embryogenesis, but play a redundant function in neural differentiation. *PloS One* 4, e4315. doi:10.1371/journal.pone.0004315.

Martin, V., Jørgensen, H. F., Chaubert, A. S. B., Berger, J., Barr, H., Shaw, P., et al. (2008). MBD2-mediated transcriptional repression of the p14ARF tumor suppressor gene in human colon cancer cells. *Pathobiol. J. Immunopathol. Mol. Cell. Biol.* 75, 281–287. doi:10.1159/000151708.

Maunakea, A. K., Chepelev, I., Cui, K., and Zhao, K. (2013). Intragenic DNA methylation modulates alternative splicing by recruiting MeCP2 to promote exon recognition. *Cell Res.* 23, 1256–1269. doi:10.1038/cr.2013.110.

Maunakea, A. K., Nagarajan, R. P., Bilenky, M., Ballinger, T. J., D'Souza, C., Fouse, S. D., et al. (2010). Conserved role of intragenic DNA methylation in regulating alternative promoters. *Nature* 466, 253–257. doi:10.1038/nature09165.

McQuown, S. C., Barrett, R. M., Matheos, D. P., Post, R. J., Rogge, G. A., Alenghat, T., et al. (2011). HDAC3 is a critical negative regulator of long-term memory formation. *J. Neurosci. Off. J. Soc. Neurosci.* 31, 764–774. doi:10.1523/JNEUROSCI.5052-10.2011.

Meehan, R. R., Lewis, J. D., McKay, S., Kleiner, E. L., and Bird, A. P. (1989). Identification of a mammalian protein that binds specifically to DNA containing methylated CpGs. *Cell* 58, 499–507. doi:10.1016/0092-8674(89)90430-3.

Meissner, A. (2010). Epigenetic modifications in pluripotent and differentiated cells. *Nat. Biotechnol.* 28, 1079–1088. doi:10.1038/nbt.1684.

Mellén, M., Ayata, P., Dewell, S., Kriaucionis, S., and Heintz, N. (2012). MeCP2 binds to 5hmC enriched within active genes and accessible chromatin in the nervous system. *Cell* 151, 1417–1430. doi:10.1016/j.cell.2012.11.022.

Menafra, R., Brinkman, A. B., Matarese, F., Franci, G., Bartels, S. J. J., Nguyen, L., et al. (2014). Genome-Wide Binding of MBD2 Reveals Strong Preference for Highly Methylated Loci. *PLoS ONE* 9, e99603. doi:10.1371/journal.pone.0099603.

Mian, O. Y., Wang, S. Z., Zhu, S. Z., Gnanapragasam, M. N., Graham, L., Bear, H. D., et al. (2011). Methyl-binding domain protein 2-dependent proliferation and survival of breast cancer cells. *Mol. Cancer Res. MCR* 9, 1152–1162. doi:10.1158/1541-7786.MCR-11-0252.

Mitra, P., Xie, R.-L., Medina, R., Hovhannisyan, H., Zaidi, S. K., Wei, Y., et al. (2003). Identification of HiNF-P, a Key Activator of Cell Cycle-Controlled Histone H4 Genes at the Onset of S Phase. *Mol. Cell. Biol.* 23, 8110–8123. doi:10.1128/MCB.23.22.8110-8123.2003.

Mo, A., Mukamel, E. A., Davis, F. P., Luo, C., Henry, G. L., Picard, S., et al. (2015). Epigenomic Signatures of Neuronal Diversity in the Mammalian Brain. *Neuron* 86, 1369–1384. doi:10.1016/j.neuron.2015.05.018.

Morey, L., Brenner, C., Fazi, F., Villa, R., Gutierrez, A., Buschbeck, M., et al. (2008). MBD3, a component of the NuRD complex, facilitates chromatin alteration and deposition of epigenetic marks. *Mol. Cell. Biol.* 28, 5912–5923. doi:10.1128/MCB.00467-08.

Müller, H. M., Fiegl, H., Goebel, G., Hubalek, M. M., Widschwendter, A., Müller-Holzner, E., et al. (2003). MeCP2 and MBD2 expression in human neoplastic and non-neoplastic breast tissue and its association with oestrogen receptor status. *Br. J. Cancer* 89, 1934–1939. doi:10.1038/sj.bjc.6601392.

Müller-Tidow, C., Kügler, K., Diederichs, S., Klümpen, S., Möller, M., Vogt, U., et al. (2001). Loss of expression of HDAC-recruiting methyl-CpG-binding domain proteins in human cancer. *Br. J. Cancer* 85, 1168–1174. doi:10.1054/bjoc.2001.2041.

Musselman, C. A., Ramirez, J., Sims, J. K., Mansfield, R. E., Oliver, S. S., Denu, J. M., et al. (2012). Bivalent recognition of nucleosomes by the tandem PHD fingers of the CHD4 ATPase is required for CHD4-mediated repression. *Proc. Natl. Acad. Sci.* 109, 787–792. doi:10.1073/pnas.1113655109.

Myers, M. G., Cowley, M. A., and Münzberg, H. (2008). Mechanisms of leptin action and leptin resistance. *Annu. Rev. Physiol.* 70, 537–556. doi:10.1146/annurev.physiol.70.113006.100707.

Nan, X., Campoy, F. J., and Bird, A. (1997). MeCP2 is a transcriptional repressor with abundant binding sites in genomic chromatin. *Cell* 88, 471–481.

Nan, X., Ng, H. H., Johnson, C. A., Laherty, C. D., Turner, B. M., Eisenman, R. N., et al. (1998). Transcriptional repression by the methyl-CpG-binding protein MeCP2 involves a histone deacetylase complex. *Nature* 393, 386–389. doi:10.1038/30764.

Ng, H. H., Jeppesen, P., and Bird, A. (2000). Active repression of methylated genes by the chromosomal protein MBD1. *Mol. Cell. Biol.* 20, 1394–1406.

Ng, H. H., Zhang, Y., Hendrich, B., Johnson, C. A., Turner, B. M., Erdjument-Bromage, H., et al. (1999). MBD2 is a transcriptional repressor belonging to the MeCP1 histone deacetylase complex. *Nat. Genet.* 23, 58–61. doi:10.1038/12659.

Nicholson, T. B., Chen, T., and Richard, S. (2009). The physiological and pathophysiological role of PRMT1-mediated protein arginine methylation. *Pharmacol. Res.* 60, 466–474. doi:10.1016/j.phrs.2009.07.006.

Noh, K.-M., Wang, H., Kim, H. R., Wenderski, W., Fang, F., Li, C. H., et al. (2015). Engineering of a Histone-Recognition Domain in Dnmt3a Alters the Epigenetic Landscape and Phenotypic Features of Mouse ESCs. *Mol. Cell* 59, 89–103. doi:10.1016/j.molcel.2015.05.017.

Okano, M., Bell, D. W., Haber, D. A., and Li, E. (1999). DNA methyltransferases Dnmt3a and Dnmt3b are essential for de novo methylation and mammalian development. *Cell* 99, 247–257.

Otabi, H., Goto, T., Okayama, T., Kohari, D., and Toyoda, A. (2015). Subchronic and mild social defeat stress alter mouse nest building behavior. *Behav. Processes*. doi:10.1016/j.beproc.2015.10.018.

Palmiter, R. D. (2008). *Dopamine Signaling in the Dorsal Striatum Is Essential for Motivated Behaviors*. *Ann. N. Y. Acad. Sci.* 1129, 35–46. doi:10.1196/annals.1417.003.

Panayotis, N., Ghata, A., Villard, L., and Roux, J.-C. (2011). Biogenic amines and their metabolites are differentially affected in the Mecp2-deficient mouse brain. *BMC Neurosci.* 12, 47. doi:10.1186/1471-2202-12-47.

Parry, L., and Clarke, A. R. (2011). The Roles of the Methyl-CpG Binding Proteins in Cancer. *Genes Cancer* 2, 618–630. doi:10.1177/1947601911418499.

Pasciuto, E., Borrie, S. C., Kanellopoulos, A. K., Santos, A. R., Cappuyns, E., D'Andrea, L., et al. (2015). Autism Spectrum Disorders: Translating human deficits into mouse behavior. *Neurobiol. Learn. Mem.* doi:10.1016/j.nlm.2015.07.013.

Pastor, W. A., Aravind, L., and Rao, A. (2013). TETonic shift: biological roles of TET proteins in DNA demethylation and transcription. *Nat. Rev. Mol. Cell Biol.* 14, 341–356. doi:10.1038/nrm3589.

Pastor, W. A., Pape, U. J., Huang, Y., Henderson, H. R., Lister, R., Ko, M., et al. (2011). Genome-wide mapping of 5-hydroxymethylcytosine in embryonic stem cells. *Nature* 473, 394–397. doi:10.1038/nature10102.

Perissi, V., Jepsen, K., Glass, C. K., and Rosenfeld, M. G. (2010). Deconstructing repression: evolving models of co-repressor action. *Nat. Rev. Genet.* 11, 109–123. doi:10.1038/nrg2736.

Phesse, T. J., Parry, L., Reed, K. R., Ewan, K. B., Dale, T. C., Sansom, O. J., et al. (2008). Deficiency of Mbd2 attenuates Wnt signaling. *Mol. Cell. Biol.* 28, 6094–6103. doi:10.1128/MCB.00539-08.

Pohodich, A. E., and Zoghbi, H. Y. (2015). Rett syndrome: disruption of epigenetic control of postnatal neurological functions. *Hum. Mol. Genet.* doi:10.1093/hmg/ddv217.

Pontes, T. B., Chen, E. S., Gigek, C. O., Calcagno, D. Q., Wisnieski, F., Leal, M. F., et al. (2014). Reduced mRNA expression levels of MBD2 and MBD3 in gastric carcinogenesis. *Tumour Biol. J. Int. Soc. Oncodevelopmental Biol. Med.* 35, 3447–3453. doi:10.1007/s13277-013-1455-y.

Potts, R. C., Zhang, P., Wurster, A. L., Precht, P., Mughal, M. R., Wood, W. H., et al. (2011). CHD5, a brain-specific paralog of Mi2 chromatin remodeling enzymes, regulates expression of neuronal genes. *PloS One* 6, e24515. doi:10.1371/journal.pone.0024515.

Prokhortchouk, A., Hendrich, B., Jørgensen, H., Ruzov, A., Wilm, M., Georgiev, G., et al. (2001). The p120 catenin partner Kaiso is a DNA methylation-dependent transcriptional repressor. *Genes Dev.* 15, 1613–1618. doi:10.1101/gad.198501.

Prokhortchouk, A., Sansom, O., Selfridge, J., Caballero, I. M., Salozhin, S., Aithozhina, D., et al. (2006). Kaiso-deficient mice show resistance to intestinal cancer. *Mol. Cell. Biol.* 26, 199–208. doi:10.1128/MCB.26.1.199-208.2006.

Rais, Y., Zviran, A., Geula, S., Gafni, O., Chomsky, E., Viukov, S., et al. (2013). Deterministic direct reprogramming of somatic cells to pluripotency. *Nature* 502, 65–70. doi:10.1038/nature12587.

Ramírez, J., Dege, C., Kutateladze, T. G., and Hagman, J. (2012). MBD2 and multiple domains of CHD4 are required for transcriptional repression by Mi-2/NuRD complexes. *Mol. Cell. Biol.* 32, 5078–5088. doi:10.1128/MCB.00819-12.

Reed, D. R., Lawler, M. P., and Tordoff, M. G. (2008). Reduced body weight is a common effect of gene null in mice. *BMC Genet.* 9, 4. doi:10.1186/1471-2156-9-4.

Reese, B. E., Bachman, K. E., Baylin, S. B., and Rountree, M. R. (2003). The methyl-CpG binding protein MBD1 interacts with the p150 subunit of chromatin assembly factor 1. *Mol. Cell. Biol.* 23, 3226–3236.

Rendenbach, C., Ganswindt, S., Seitz, S., Barvencik, F., Huebner, A. K., Baranowsky, A., et al. (2013). Increased Expression of Transthyretin in Leptin-Deficient *ob/ob* Mice is not Causative for Their Major Phenotypic Abnormalities. *J. Neuroendocrinol.* 25, 14–22. doi:10.1111/j.1365-2826.2012.02366.x.

Reynolds, N., Latos, P., Hynes-Allen, A., Loos, R., Leaford, D., O'Shaughnessy, A., et al. (2012). NuRD suppresses pluripotency gene expression to promote transcriptional heterogeneity and lineage commitment. *Cell Stem Cell* 10, 583–594. doi:10.1016/j.stem.2012.02.020.

Reynolds, N., O'Shaughnessy, A., and Hendrich, B. (2013). Transcriptional repressors: multifaceted regulators of gene expression. *Dev. Camb. Engl.* 140, 505–512. doi:10.1242/dev.083105.

Robinson, M. D., McCarthy, D. J., and Smyth, G. K. (2010). edgeR: a Bioconductor package for differential expression analysis of digital gene expression data. *Bioinforma. Oxf. Engl.* 26, 139–140. doi:10.1093/bioinformatics/btp616.

Roloff, T. C., Ropers, H. H., and Nuber, U. A. (2003). Comparative study of methyl-CpG-binding domain proteins. *BMC Genomics* 4, 1.

Saito, M., and Ishikawa, F. (2002). The mCpG-binding domain of human MBD3 does not bind to mCpG but interacts with NuRD/Mi2 components HDAC1 and MTA2. *J. Biol. Chem.* 277, 35434–35439. doi:10.1074/jbc.M203455200.

Sansom, O. J. (2004). Loss of Apc in vivo immediately perturbs Wnt signaling, differentiation, and migration. *Genes Dev.* 18, 1385–1390. doi:10.1101/gad.287404.

Sansom, O. J., Berger, J., Bishop, S. M., Hendrich, B., Bird, A., and Clarke, A. R. (2003). Deficiency of Mbd2 suppresses intestinal tumorigenesis. *Nat. Genet.* 34, 145–147. doi:10.1038/ng1155.

Sapkota, Y., Mackey, J. R., Lai, R., Franco-Villalobos, C., Lupichuk, S., Robson, P. J., et al. (2014). Assessing SNP-SNP interactions among DNA repair, modification and metabolism related pathway genes in breast cancer susceptibility. *PloS One* 8, e64896. doi:10.1371/journal.pone.0064896.

Sarraf, S. A., and Stancheva, I. (2004). Methyl-CpG binding protein MBD1 couples histone H3 methylation at lysine 9 by SETDB1 to DNA replication and chromatin assembly. *Mol. Cell* 15, 595–605. doi:10.1016/j.molcel.2004.06.043.

Schoch, H., and Abel, T. (2014). Transcriptional co-repressors and memory storage. *Neuropharmacology* 80, 53–60. doi:10.1016/j.neuropharm.2014.01.003.

Schübeler, D. (2015). Function and information content of DNA methylation. *Nature* 517, 321–326. doi:10.1038/nature14192.

Schultz, M. D., He, Y., Whitaker, J. W., Hariharan, M., Mukamel, E. A., Leung, D., et al. (2015). Human body epigenome maps reveal noncanonical DNA methylation variation. *Nature*. doi:10.1038/nature14465.

Schwartz, M. W. (2005). Diabetes, Obesity, and the Brain. *Science* 307, 375–379. doi:10.1126/science.1104344.

Sekimata, M., Takahashi, A., Murakami-Sekimata, A., and Homma, Y. (2001). Involvement of a novel zinc finger protein, MIZF, in transcriptional repression by interacting with a methyl-CpG-binding protein, MBD2. *J. Biol. Chem.* 276, 42632–42638. doi:10.1074/jbc.M107048200.

Sellars, M., Huh, J. R., Day, K., Issuree, P. D., Galan, C., Gobeil, S., et al. (2015). Regulation of DNA methylation dictates Cd4 expression during the development of helper and cytotoxic T cell lineages. *Nat. Immunol.* 16, 746–754. doi:10.1038/ni.3198.

Shahbazian, M. D., Antalffy, B., Armstrong, D. L., and Zoghbi, H. Y. (2002). Insight into Rett syndrome: MeCP2 levels display tissue- and cell-specific differences and correlate with neuronal maturation. *Hum. Mol. Genet.* 11, 115–124.

Sheaffer, K. L., Kim, R., Aoki, R., Elliott, E. N., Schug, J., Burger, L., et al. (2014). DNA methylation is required for the control of stem cell differentiation in the small intestine. *Genes Dev.* 28, 652–664. doi:10.1101/gad.230318.113.

Shen, W., Wang, C., Xia, L., Fan, C., Dong, H., Deckelbaum, R. J., et al. (2014). Epigenetic modification of the leptin promoter in diet-induced obese mice and the effects of N-3 polyunsaturated fatty acids. *Sci. Rep.* 4, 5282. doi:10.1038/srep05282.

Shih, H.-Y., Sciumè, G., Poholek, A. C., Vahedi, G., Hirahara, K., Villarino, A. V., et al. (2014). Transcriptional and epigenetic networks of helper T and innate lymphoid cells. *Immunol. Rev.* 261, 23–49. doi:10.1111/imr.12208.

Shlyueva, D., Stampfel, G., and Stark, A. (2014). Transcriptional enhancers: from properties to genome-wide predictions. *Nat. Rev. Genet.* 15, 272–286. doi:10.1038/nrg3682.

Shukeir, N., Pakneshan, P., Chen, G., Szyf, M., and Rabbani, S. A. (2006). Alteration of the methylation status of tumor-promoting genes decreases prostate cancer cell invasiveness and tumorigenesis in vitro and in vivo. *Cancer Res.* 66, 9202–9210. doi:10.1158/0008-5472.CAN-06-1954.

Skene, P. J., Illingworth, R. S., Webb, S., Kerr, A. R. W., James, K. D., Turner, D. J., et al. (2010). Neuronal MeCP2 is expressed at near histone-octamer levels and globally alters the chromatin state. *Mol. Cell* 37, 457–468. doi:10.1016/j.molcel.2010.01.030.

Smith, Z. D., and Meissner, A. (2013). DNA methylation: roles in mammalian development. *Nat. Rev. Genet.* 14, 204–220. doi:10.1038/nrg3354.

Spruijt, C. G., Gnerlich, F., Smits, A. H., Pfaffeneder, T., Jansen, P. W. T. C., Bauer, C., et al. (2013). Dynamic Readers for 5-(Hydroxy)Methylcytosine and Its Oxidized Derivatives. *Cell* 152, 1146–1159. doi:10.1016/j.cell.2013.02.004.

Spruijt, C. G., and Vermeulen, M. (2014). DNA methylation: old dog, new tricks? *Nat. Struct. Mol. Biol.* 21, 949–954. doi:10.1038/nsmb.2910.

Stefanska, B., Suderman, M., Machnes, Z., Bhattacharyya, B., Hallett, M., and Szyf, M. (2013). Transcription onset of genes critical in liver carcinogenesis is epigenetically regulated by methylated DNA-binding protein MBD2. *Carcinogenesis* 34, 2738–2749. doi:10.1093/carcin/bgt273.

Stroud, H., Feng, S., Morey Kinney, S., Pradhan, S., and Jacobsen, S. E. (2011). 5-Hydroxymethylcytosine is associated with enhancers and gene bodies in human embryonic stem cells. *Genome Biol.* 12, R54. doi:10.1186/gb-2011-12-6-r54.

Sunyer, B., Patil, S., Höger, H., and Luber, G. (2007). Barnes maze, a useful task to assess spatial reference memory in the mice. *Protoc. Exch.* doi:10.1038/nprot.2007.390.

Suzuki, M. M., and Bird, A. (2008). DNA methylation landscapes: provocative insights from epigenomics. *Nat. Rev. Genet.* 9, 465–476. doi:10.1038/nrg2341.

Szulwach, K. E., Li, X., Li, Y., Song, C.-X., Wu, H., Dai, Q., et al. (2011). 5-hmC-mediated epigenetic dynamics during postnatal neurodevelopment and aging. *Nat. Neurosci.* 14, 1607–1616. doi:10.1038/nn.2959.

Tahiliani, M., Koh, K. P., Shen, Y., Pastor, W. A., Bandukwala, H., Brudno, Y., et al. (2009). Conversion of 5-methylcytosine to 5-hydroxymethylcytosine in mammalian DNA by MLL partner TET1. *Science* 324, 930–935. doi:10.1126/science.1170116.

Talkowski, M. E., Mullegama, S. V., Rosenfeld, J. A., van Bon, B. W. M., Shen, Y., Repnikova, E. A., et al. (2011). Assessment of 2q23.1 microdeletion syndrome implicates MBD5 as a single causal locus of intellectual disability, epilepsy, and autism spectrum disorder. *Am. J. Hum. Genet.* 89, 551–563. doi:10.1016/j.ajhg.2011.09.011.

Tan, C. P., and Nakielny, S. (2006). Control of the DNA methylation system component MBD2 by protein arginine methylation. *Mol. Cell. Biol.* 26, 7224–7235. doi:10.1128/MCB.00473-06.

Tan, D. W.-M., and Barker, N. (2014). "Intestinal Stem Cells and Their Defining Niche," in *Current Topics in Developmental Biology* (Elsevier), 77–107. Available at: http://linkinghub.elsevier.com/retrieve/pii/B9780124160224000032 [Accessed December 2, 2015].

Tatematsu, K. I., Yamazaki, T., and Ishikawa, F. (2000). MBD2-MBD3 complex binds to hemi-methylated DNA and forms a complex containing DNMT1 at the replication foci in late S phase. *Genes Cells Devoted Mol. Cell. Mech.* 5, 677–688.

Theoharides, T. C., Athanassiou, M., Panagiotidou, S., and Doyle, R. (2015). Dysregulated brain immunity and neurotrophin signaling in Rett syndrome and autism spectrum disorders. *J. Neuroimmunol.* 279, 33–38. doi:10.1016/j.jneuroim.2014.12.003.

Thomson, J. P., Skene, P. J., Selfridge, J., Clouaire, T., Guy, J., Webb, S., et al. (2010). CpG islands influence chromatin structure via the CpG-binding protein Cfp1. *Nature* 464, 1082–1086. doi:10.1038/nature08924.

Torchy, M. P., Hamiche, A., and Klaholz, B. P. (2015). Structure and function insights into the NuRD chromatin remodeling complex. *Cell. Mol. Life Sci. CMLS* 72, 2491–2507. doi:10.1007/s00018-015-1880-8.

Torres-Andrade, R., Moldenhauer, R., Gutierrez-Bertin, N., Soto-Covasich, J., Mancilla-Medina, C., Ehrenfeld, C., et al. (2014). The increase in body weight induced by the lacking of Mecp2 is associated with altered leptin-signalling in the hypothalamus. *Exp. Physiol.* doi:10.1113/expphysiol.2014.079798.

Tou, J. C. L., and Wade, C. E. (2002). Determinants affecting physical activity levels in animal models. *Exp. Biol. Med. Maywood NJ* 227, 587–600.

Tsoi, L. C., Spain, S. L., Knight, J., Ellinghaus, E., Stuart, P. E., Capon, F., et al. (2012). Identification of 15 new psoriasis susceptibility loci highlights the role of innate immunity. *Nat. Genet.* 44, 1341–1348. doi:10.1038/ng.2467.

Turner, J. D., Alt, S. R., Cao, L., Vernocchi, S., Trifonova, S., Battello, N., et al. (2010). Transcriptional control of the glucocorticoid receptor: CpG islands, epigenetics and more. *Biochem. Pharmacol.* 80, 1860–1868. doi:10.1016/j.bcp.2010.06.037.

Unoki, M., Nishidate, T., and Nakamura, Y. (2004). ICBP90, an E2F-1 target, recruits HDAC1 and binds to methyl-CpG through its SRA domain. *Oncogene* 23, 7601–7610. doi:10.1038/sj.onc.1208053.

Wade, P. A., Gegonne, A., Jones, P. L., Ballestar, E., Aubry, F., and Wolffe, A. P. (1999). Mi-2 complex couples DNA methylation to chromatin remodelling and histone deacetylation. *Nat. Genet.* 23, 62–66. doi:10.1038/12664.

Walsh, C. P., Chaillet, J. R., and Bestor, T. H. (1998). Transcription of IAP endogenous retroviruses is constrained by cytosine methylation. *Nat. Genet.* 20, 116–117.

Wang, L., Liu, Y., Han, R., Beier, U. H., Thomas, R. M., Wells, A. D., et al. (2013). Mbd2 promotes foxp3 demethylation and T-regulatory-cell function. *Mol. Cell. Biol.* 33, 4106–4115. doi:10.1128/MCB.00144-13.

Waterfield, M., Khan, I. S., Cortez, J. T., Fan, U., Metzger, T., Greer, A., et al. (2014). The transcriptional regulator Aire coopts the repressive ATF7ip-MBD1 complex for the induction of immunotolerance. *Nat. Immunol.* 15, 258–265. doi:10.1038/ni.2820.

Weaver, I. C. G., Cervoni, N., Champagne, F. A., D'Alessio, A. C., Sharma, S., Seckl, J. R., et al. (2004). Epigenetic programming by maternal behavior. *Nat. Neurosci.* 7, 847–854. doi:10.1038/nn1276.

Weaver, I. C. G., Hellstrom, I. C., Brown, S. E., Andrews, S. D., Dymov, S., Diorio, J., et al. (2014). The methylated-DNA binding protein MBD2 enhances NGFI-A (egr-1)-mediated transcriptional activation of the glucocorticoid receptor. *Philos. Trans. R. Soc. B Biol. Sci.* 369, 20130513–20130513. doi:10.1098/rstb.2013.0513.

Yamada, T., Yang, Y., Hemberg, M., Yoshida, T., Cho, H. Y., Murphy, J. P., et al. (2014). Promoter decommissioning by the NuRD chromatin remodeling complex triggers synaptic connectivity in the mammalian brain. *Neuron* 83, 122–134. doi:10.1016/j.neuron.2014.05.039.

Yang, L., Gilbert, M. L., Zheng, R., and McKnight, G. S. (2014a). Selective Expression of a Dominant-Negative Type Iα PKA Regulatory Subunit in Striatal Medium Spiny Neurons Impairs Gene Expression and Leads to Reduced Feeding and Locomotor Activity. *J. Neurosci.* 34, 4896–4904. doi:10.1523/JNEUROSCI.3460-13.2014.

Yang, M., and Crawley, J. N. (2009). "Simple Behavioral Assessment of Mouse Olfaction," in *Current Protocols in Neuroscience*, eds. J. N. Crawley, C. R. Gerfen, M. A. Rogawski, D. R. Sibley, P. Skolnick, and S. Wray (Hoboken, NJ, USA: John Wiley & Sons, Inc.). Available at: http://doi.wiley.com/10.1002/0471142301.ns0824s48 [Accessed July 3, 2015].

Yang, X., Han, H., De Carvalho, D. D., Lay, F. D., Jones, P. A., and Liang, G. (2014b). Gene body methylation can alter gene expression and is a therapeutic target in cancer. *Cancer Cell* 26, 577–590. doi:10.1016/j.ccr.2014.07.028.

Yi, C.-X., and Tschop, M. H. (2012). Brain-gut-adipose-tissue communication pathways at a glance. *Dis. Model. Mech.* 5, 583–587. doi:10.1242/dmm.009902.

Yildirim, O., Li, R., Hung, J.-H., Chen, P. B., Dong, X., Ee, L.-S., et al. (2011). Mbd3/NURD complex regulates expression of 5-hydroxymethylcytosine marked genes in embryonic stem cells. *Cell* 147, 1498–1510. doi:10.1016/j.cell.2011.11.054.

Yoder, J. A., and Bestor, T. H. (1998). A candidate mammalian DNA methyltransferase related to pmt1p of fission yeast. *Hum. Mol. Genet.* 7, 279–284.

Yoshida, T., Hazan, I., Zhang, J., Ng, S. Y., Naito, T., Snippert, H. J., et al. (2008). The role of the chromatin remodeler Mi-2beta in hematopoietic stem cell self-renewal and multilineage differentiation. *Genes Dev.* 22, 1174–1189. doi:10.1101/gad.1642808.

Zhang, Y., Ng, H. H., Erdjument-Bromage, H., Tempst, P., Bird, A., and Reinberg, D. (1999). Analysis of the NuRD subunits reveals a histone deacetylase core complex and a connection with DNA methylation. *Genes Dev.* 13, 1924–1935.

Zhao, X., Ueba, T., Christie, B. R., Barkho, B., McConnell, M. J., Nakashima, K., et al. (2003). Mice lacking methyl-CpG binding protein 1 have deficits in adult neurogenesis and hippocampal function. *Proc. Natl. Acad. Sci. U. S. A.* 100, 6777–6782. doi:10.1073/pnas.1131928100.

Zhong, J., Yu, Q., Yang, P., Rao, X., He, L., Fang, J., et al. (2014). MBD2 regulates TH17 differentiation and experimental autoimmune encephalomyelitis by controlling the homeostasis of T-bet/Hlx axis. *J. Autoimmun.* doi:10.1016/j.jaut.2014.05.006.

Zhou, X., Jeker, L. T., Fife, B. T., Zhu, S., Anderson, M. S., McManus, M. T., et al. (2008). Selective miRNA disruption in T reg cells leads to uncontrolled autoimmunity. *J. Exp. Med.* 205, 1983–1991. doi:10.1084/jem.20080707.

Zhou, Z., Hong, E. J., Cohen, S., Zhao, W.-N., Ho, H.-Y. H., Schmidt, L., et al. (2006). Brain-specific phosphorylation of MeCP2 regulates activity-dependent Bdnf transcription, dendritic growth, and spine maturation. *Neuron* 52, 255–269. doi:10.1016/j.neuron.2006.09.037.

Zhu, D., Hunter, S. B., Vertino, P. M., and Meir, E. G. V. (2011). Overexpression of MBD2 in Glioblastoma Maintains Epigenetic Silencing and Inhibits the Antiangiogenic Function of the Tumor Suppressor Gene BAI1. *Cancer Res.* 71, 5859–5870. doi:10.1158/0008-5472.CAN-11-1157.

Zhu, Y., Brown, H. N., Zhang, Y., Holford, T. R., and Zheng, T. (2005). Genotypes and haplotypes of the methyl-CpG-binding domain 2 modify breast cancer risk dependent upon menopausal status. *Breast Cancer Res. BCR* 7, R745–752. doi:10.1186/bcr1283.

Zhu, Y., Harrison, D. J., and Bader, S. A. (2004). Genetic and epigenetic analyses of MBD3 in colon and lung cancer. *Br. J. Cancer* 90, 1972–1975. doi:10.1038/sj.bjc.6601776.